Fractionation Strategies to Obtain Multiple Products from the Hydrocarbon Stream of Fatty Acid Pyrolysis

by

Uche Emmanuella Sea-Nduka

A thesis submitted in partial fulfillment of the requirements for the degree of

Master of Science

in

Bioresource and Food Engineering

Department of Agricultural, Food and Nutritional Science
University of Alberta

ABSTRACT

A biorefinery concept defined as the sustainable processing of biomass into a spectrum of products has been proposed to achieve the true sustainability goals of a bio-based economy. Lipid pyrolysis is the thermal decomposition of lipids (triglycerides or fatty acids) into gas, liquid, and solid products. Typically, the complexity of the lipid pyrolytic liquid restricts its direct use for fuel and chemical production. A biorefinery can be established by separating the pyrolytic liquid into fractions to be processed into high-grade products. The aim of this research was to demonstrate a biorefinery concept by developing fractionation strategies for a liquid hydrocarbon feed gotten from the pyrolysis of fatty acids to obtain multiple high-value products such as renewable fuels, solvents, and mid-chain fatty acid compounds.

The first fractionation step done was acid-base extraction using 3 M NaOH to remove the fatty acids present in the feed and 3 M HCl to recover the extracted fatty acids as a separate mixture. The acid-base extraction successfully removed the fatty acids from the feed, creating an acid-free hydrocarbon fraction composed mainly of *n*-alkanes (about 48 %wt) and a fatty acid fraction of about 70 %wt fatty acids.

The second fractionation process explored was distillation. Atmospheric distillation was used to recover *n*-pentane and *n*-hexane solvents from the hydrocarbon fraction. This was done using a 90cm spinning band distillation unit with up to 100 theoretical plates. A naphtha fraction obtained from an initial distillation of the hydrocarbon fraction was also explored as a starting material for recovering the renewable *n*-pentane and *n*-hexane solvents. The effect of reflux ratio on the purity and recovery of the solvent fractions was studied by varying the reflux ratio between 90:1 to 240:1. *n*-Pentane solvent with percentage purity between 70 – 80 % was obtained from all the experiments. The amount of *n*-pentane present in the feed recovered in the *n*-pentane fraction was

between 33 – 43 %wt. For *n*-hexane, the percentage purity was 80 % from all the experiments, and the amount of *n*-hexane in the feed recovered was 21 – 35 %wt for all the distillation runs. For both solvents, the major contaminants were the alkene compounds of the corresponding carbon number. Neither starting material nor reflux ratio influenced the solvents' purity and recovery under the distillation conditions used in this study. Drop-in diesel equivalent cut was obtained as the bottom product of the hydrocarbon fraction distillation and analyzed for conformity to Canadian diesel fuel standards: CAN/CGSB – 3.517-2020. The drop-in diesel equivalent cut met the CAN/CGSB – 3.517-2020 for acid number, kinematic viscosity, cetane number, flashpoint, distillation range and was comparable to the commercial diesel analyzed. On the other hand, the cold flow properties were not comparable to that of the commercially obtained diesel.

Vacuum distillation at 133.3 Pa was used to obtain individual fatty acid cut from the fatty acid extract, using the same spinning band distillation equipment at a reflux ratio of 60:1. Individual fatty acids between C5:0 and C10:0 carbon number was obtained during the distillation process. The purity of the recovered fatty acids ranged between 60 – 80 %, while the recovery was > 60 %wt for all the fatty acids except C10:0. The significant impurities of the fatty acid cuts were higher *n*-alkane compounds and the unsaturated fatty acids of the corresponding carbon number.

This is the first study demonstrating the combined recovery of renewable fuels and solvents together with the valorization of the fatty acids present in the liquid product of the pyrolysis of fatty acids or any other lipid feedstock.

PREFACE

This thesis is an original work by Uche Emmanuella Sea-Nduka. No part of this thesis has been previously published. All experiments in this thesis were discussed and approved by Dr. David C. Bressler and Dr. Justice Asomaning. All experiments were conducted in the Biorefining Conversions and Fermentation lab at the University of Alberta. Dr. Justice Asomaning contributed to the thesis revisions and edits.

ACKNOWLEDGEMENTS

Firstly, I would like to express my gratitude to Dr. David C. Bressler for the opportunity to carry out my Masters' program. Dave has been an excellent tutor and mentor, always available to assist and provide advice on the research, career and life issues in general. I also sincerely thank Dr. Asomaning for his patience, guidance, input, and assistance. This journey was easier under your tutelage (even though we argued half the time). To Dr. Chae, I say a big thank you for your work behind the scenes to ensure that the lab keeps running and for always being there whenever I needed your help. To my committee member Artin Afacan, I really appreciate your assistance, feedback, and suggestions. Thank you for always making time out of your schedule for consultation outside regular meetings. My appreciation goes to the funding partners of this work (Mitacs Accelerate, Forge Hydrocarbnos Inc, NSERC, Bioindustrial Innovation Canada, Agriculture and Agri-Food Canada) without which this research would not have been possible.

To my lab members Samuel, Andres, Amin, Fantahun, Dagem, Ronny, Damaris, Victor, and Alaleh, it was a pleasure to know you and work with you guys these past two half years. The diligence exhibited by you all is inspirational. To Jie, Bingxin, and Bernado, I am blessed to have met you. Thanks for being there to celebrate my highs and lows, for the ongoing assistance in and out of the lab, and for the friendship. To Jingui, you are an indispensable member of Bressler's lab. Your patience, skills, technical expertise, and readiness to help made my work easier.

Finally, to my mother, siblings, and the Livinus family, thank you for the constant motivation. I could not have gotten to the end without your emotional support and unconditional love. To Esther Ijiwade, you are a blessing. Thank you for the continued friendship and the smooth transition into Canada and the University of Alberta. To Chinwe, Deji, Victoria, Yimika, Wande, Oyewole, and Damian, thanks for the emotional support, love, and friendship.

TABLE OF CONTENTS

LIST OF TABLES

LIST OF FIGURES

LIST OF ABBREVIATIONS

µl - microliter

ANOVA - Analysis of Variance

APR - Aqueous Phase Reforming

CGSB - Canadian General Standards Board

cm - centimeter

FAME - Fatty Acid Methyl Ester

FID - Flame Ionization Detector

FTIR - Fourier-Transform Infrared Spectroscopy

g - gram

GC - Gas Chromatograph

HTL - Hydrothermal liquefaction

IEA - International Energy Agency

LLE - Liquid-Liquid Extraction

MCFA - Medium Chain Fatty Acid

mg - milligram

ml - milliliter

MS - Mass Spectroscopy

Rpm - Rotations Per Minute

RRF - Relative Response Factor

SCFA - Short Chain Fatty Acids

VLE - Vapor-Liquid Equilibria

1. INTRODUCTION

1.1. Project background

With the advent of a bio-based economy as a potential solution to sustainability concerns, other pertinent environmental and social issues such as the food versus fuel versus feed debate, deforestation, biodiversity loss, indirect land-use change arose with questions to the 'net' benefit of the bio-based solution. There were also queries around its economic and technological viability. To address these issues, the "biorefinery" concept was introduced (de Jong & Jungmeier, 2015; Gavrilescu, 2014).

The International Energy Agency (IEA) bioenergy task 42 defined a biorefinery as the sustainable processing of biomass into a spectrum of marketable products (Cherubini *et al*., 2010). Like the petroleum refinery, it uses various conversion technologies to produce fuels, chemicals, and other materials, albeit from biomass feedstock, ensuring efficient, sustainable, and maximum biomass utilization. It apportions the environmental and economic burden associated with a bio-based process to different products, reducing a single product's load (Bharathiraja, *et al*., 2016; de Jong & Jungmeier, 2015). Biorefineries can be established by applying different technologies like pyrolysis, fermentation, etc., on biomass such as triglycerides (lipids), sugar, or starchy materials (Cherubini *et al*., 2010).

Lipid pyrolysis is one of the most successful approaches to obtaining products like fuels and chemicals from renewable sources. Lipid feedstocks typically utilised for this process are either composed of triglycerides or fatty acids. Pyrolysis of triglycerides yields oxygenated compounds that are not compatible with present infrastructure (Ferreira *et al.*, 2017; Asomaning *et al.*, 2014). The pyrolysis of free fatty acids into hydrocarbons has been extensively studied and reported by

our group (Asomaning, 2014; Maher *et al*., 2008). A proprietary process, the lipid to hydrocarbon technology is an advanced form of lipid pyrolysis. This is a two-stage thermal process involving the hydrolysis of lipids to convert the acylglycerols into free fatty acids and pyrolysis of the free fatty acids to obtain solid, gas, and liquid products which can separated into drop-in fuels (Asomaning *et al*., 2014).

Traditional pyrolytic liquid is a dark complex mixture with hundreds of compounds, including alkanes, alkenes, aromatics, cyclics, and fatty acids. It has been described as the product with the most potential to replace petroleum in the production of fuels and chemicals (Guo *et al*., 2010; Xiu & Shahbazi, 2012). However, the complexity in composition and properties restricts its use as a direct substitute for fuels and chemicals. Further refining/upgrading of pyrolytic liquid is necessary, but the different groups/compounds in the mixture react differently under various conditions, creating more difficulties in the refining process. This presents a biorefinery opportunity. The lipid pyrolytic liquid can be separated into several fractions to serve as starting materials for further upgrading processes to obtain high-grade products like renewable fuels and chemicals. Fractionation methods such as solvent extraction, centrifugation, liquid chromatography, distillation have been explored for these purposes (Guo *et al*., 2010).

Distillation is a method for separating mixtures based on the difference in the volatility of their components. It is commonly used in the chemical and petroleum industry. Distillation has been utilized to separate pyrolytic liquid to yield fractions that can be upgraded to meet standard fuel requirements and other portions used for chemical production (Li *et al*., 2011; Mancio *et al*., 2018). This method helps separate the volatile compounds present in the pyrolytic liquid that impact its fuel properties. To achieve separation by distillation, the relative volatility between the components must be sufficiently large. A challenge in separating pyrolytic liquid by distillation is

that compounds of different chemical groups have overlapping relative volatilities and boiling points (Gandhi *et al*., 2012).

Another separation technique explored is liquid-liquid extraction (LLE), which is based on a mixture's ability to partition between two immiscible (or partially miscible) solvents in contact with each other (Lebl *et al*., 2019). Liquid-liquid extraction is particularly effective in separating compounds of different polarities. It is also a useful alternative for separating thermal labile compounds like fatty acids present in the pyrolytic liquid. These acids pose a significant restriction in using the pyrolytic liquid as fuels, but they can have important industrial use if separated.

To successfully utilize any lipid pyrolytic liquid, a combination of separation techniques is necessary to produce different product streams that can be upgraded to meet the required market specifications and channeled for various applications. Of particular interest are green (renewable) solvents and chemicals which are widely sought after in the flavor and fragrance industry for a premium price. To that end, this study hypothesized that acid-base extraction and distillation could be applied to a liquid hydrocarbon feed gotten from the pyrolysis of fatty acids to obtain renewable solvents and mid chain fatty acid cuts at similar purity with those commercially obtained.

1.2. Project objectives

This research's general aim was to develop fractionation strategies for a liquid hydrocarbon feed from the pyrolysis of fatty acids to prove the biorefinery concept. The specific objectives were to:

1. Separate the feed into hydrocarbon and fatty acid mixtures by acid-base extraction.
2. Fractionate the hydrocarbon mixture to obtain solvents and fuel cuts using distillation.
3. Analyze the properties of fuel cuts obtained from the hydrocarbon mixture fractionation.
4. Fractionate the fatty acids mixture by distillation to obtain individual acid compounds.

2. LITERATURE REVIEW

2.1. Classification of biorefineries

Biorefineries' classification has been ambiguous due to the wide variety of biomass used, conversion technologies, and products obtained (Gavrilescu, 2014; Maity, 2015). The International Energy Agency (IEA) bioenergy task adopted a comprehensive classification for biorefineries presented in Table 2.1. Biorefineries were classified based on Platform (*intermediate products connecting biorefineries*), Product (the *final consumable product from the biorefinery*), Feedstock, and Conversion process. These criteria are greatly discussed elsewhere (Cherubini *et al*., 2009).

Table 2.1: Classification of biorefineries

Platform	**Product**	**Feedstock**	**Processes (selected)**
1) C5 sugars 2) C6 sugars 3) Oils 4) Biogas 5) Syngas 6) Hydrogen 7) Organic juice 8) Pyrolytic liquid 9) Lignin 10) Electricity and heat	*1) Energy products* *a)* Biodiesel *b)* Bioethanol *c)* Biomethane *d)* Synthetic biofuels *e)* Electricity and heat *2) Material products* a) Food b) Animal feed c) Fertilizer d) Glycerin e) Biomaterials f) Chemicals and building blocks g) Polymer and resins h) Biohydrogen	*1) Dedicated crops* *a)* Oil crops *b)* Sugar crops *c)* Starch crops *d)* Lignocellulosic crops *e)* Grasses *f)* Marine biomass 2) *Residues* a) Lignocellulosic residues b) Oil-based residues c) Organic residues & others	*3. Thermochemical* a) Combustion b) Gasification c) Hydrothermal upgrading d) Pyrolysis e) Supercritical *2) Biochemical* *a)* Fermentation *b)* Anaerobic digestion *c)* Anaerobic conversion *d)* Enzymatic processes *3) Chemical* a) Catalytic processes b) Pulping c) Esterification d) Hydrogenation e) Hydrolysis f) Methanisation g) Steam reforming h) Water electrolysis i) Water gas shift *4) Mechanical* a) Extraction b) Fiber separation c) Mechanical fractionation d) Pressing/ disruption e) Pre-treatment

2.1.1. Feedstock

A biorefinery feedstock refers to the type of biomass utilized in a biorefinery (Cherubini, 2010). Biomass is an organic material that can be converted into food, fuels, materials, and chemicals (Marques *et al*., 2018). These include; herbaceous energy crops like bamboo, switchgrass, miscanthus; woody energy crops such as poplar, willow; oil crops, for example, soybean, jatropha, castor oil; sugar and starchy crops like corn, sugar cane, sorghum; aquatic crops like algae, seaweed; agricultural residues and waste including stalks, leaves, sugarcane bagasse, wheat straw, corn stover, rice hulls; forestry residue which are biomass obtained from forest management operations and households/industrial waste like municipal solid waste, sewage sludge and industrial waste (Maity, 2015; Yaman, 2004).

It has been estimated that feedstock accounts for 40 – 60 % of a biorefinery's operating cost. In the selection of feedstock, the cost, year-round availability, socio-economic/governmental policies, and amenability to technological conversion should be considered as these affect viability of the biorefinery strategy (Ghatak, 2011; Parajuli *et al*., 2015). There is no universal way to group these feedstocks. One classification method divides the feedstocks into three groups: carbohydrates and lignin; triglycerides; and mixed organic residues (Cherubini *et al*., 2010). The structures of the different feedstocks are shown in Figure 2.1.

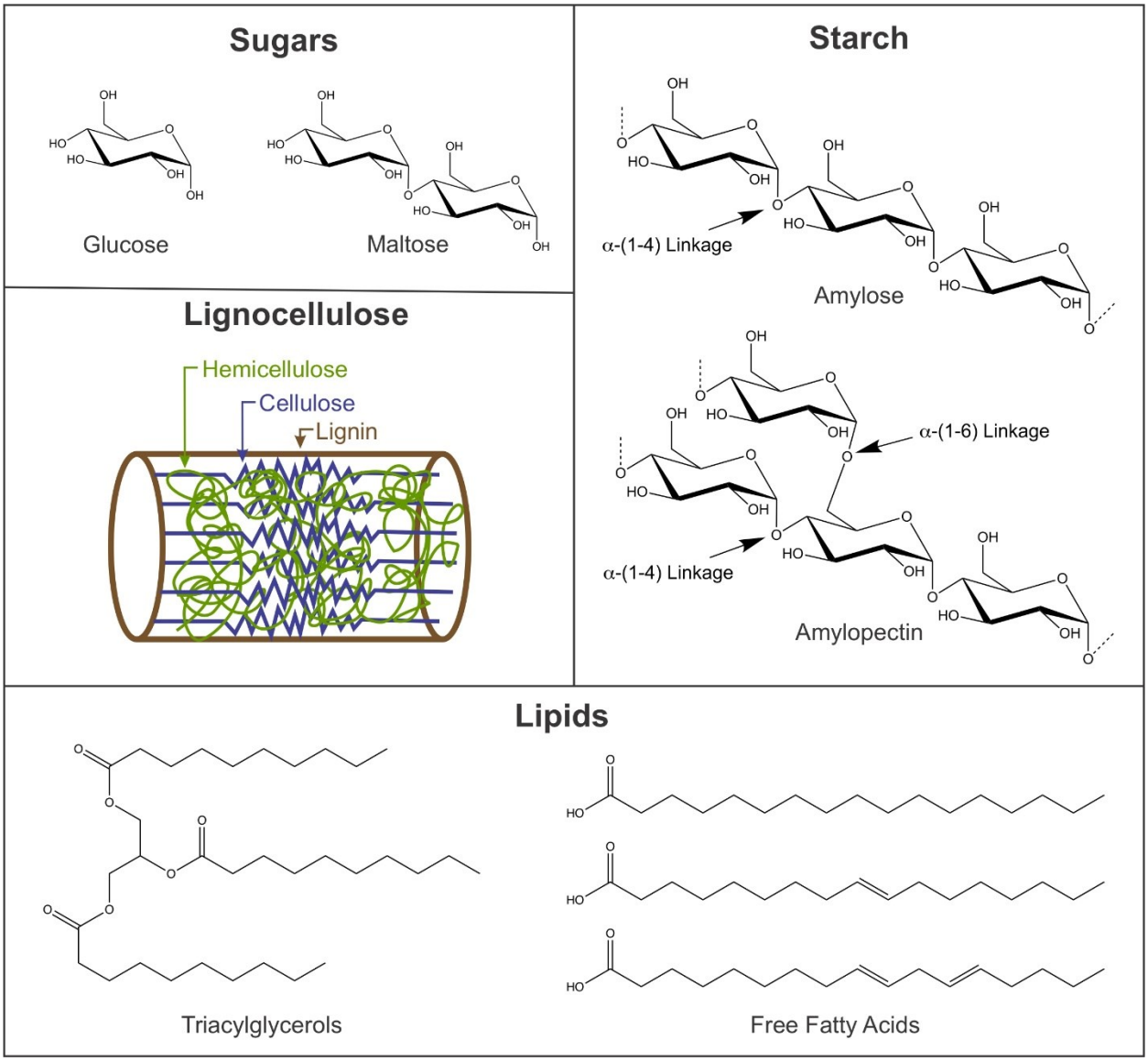

Figure 2.1: Structures of different biomass feedstocks used in a biorefinery.

Carbohydrates are biomolecules made up of carbon, hydrogen, and oxygen. About 75 % of available biomass on earth is carbohydrate in the form of sugar, starch, or cellulose that can be converted into biofuel: *bioethanol* (Mikkola *et al*., 2015). Sugar-based feedstocks like sugar cane contain carbohydrates in simple forms of mono- or disaccharides such as sucrose. Starchy biomass like corn contains complex carbohydrates that are polymers of simple sugars (Cherubini *et al*., 2009). Though these feedstocks are easy to convert into biofuels and chemicals, social

sustainability issues such as competition with food, land, and water use have been raised (Ghatak, 2011). Lignocellulosic materials are the most abundant renewable material on earth. They are relatively cheap biomass that can be sourced from agriculture or forest residues. The main components of lignocellulosic biomass are cellulose, hemicellulose, and lignin (Zhang *et al*., 2008). Cellulose is a 6-carbon sugar polymer, while hemicellulose is a 5-carbon sugar polymer (Fernando *et al*., 2006). Lignin is a 3-D polymer of phenolic compounds. Together, these components form a complex structure that is resistant to biological or chemical degradation, which presents a severe challenge in utilizing lignocellulosic materials in a biorefinery to produce fuels and chemicals despite their abundance. Several efforts are currently being put into the development and scale-up of technologies to combat this challenge (Alzagameem *et al*., 2018; Das & Singh, 2004).

Triglycerides (lipids) are another class of feedstock used in a biorefinery. These are hydrocarbons with three fatty acid chains (typically between 8- 24) and a glycerol backbone, held together by ester bonds (Mikkola *et al*., 2015). These could be sourced from plants or animals. Triglycerides are preferred for biofuel production: *biodiesel* due to their high energy density (Maher & Bressler, 2007), higher carbon-hydrogen ratio, higher caloric heat content, lower sulfur and aromatic compounds, and liquid nature (Bharathiraja *et al*., 2016). Common examples include edible vegetable oil such as canola (Šimáček *et al*., 2009); non-edible vegetable oils (Navarro-Pineda *et al*., 2016); animal fats (Adebanjo *et al*., 2005); waste cooking oils (Alcantara *et al*., 2000; Ma *et al*., 1998), and algal oil (Chisti, 2019; Yen *et al*., 2013). Alongside sugar and starchy feedstocks, edible oils are also termed dedicated crops and have the same social sustainability issues mentioned above like their carbohydrate counterparts (Cherubini, 2010; Ghatak, 2011).

Aquatic biomass is also being explored as a biorefinery feedstock as they address the seasonal availability, land, and water use issues of terrestrial biomass (Ghatak, 2011). They do not require freshwater or arable land to grow and are known to have high proliferation rates. These photosynthetic organisms can be sub-grouped into the unicellular microalgae and the multicellular lower plant- seaweed (also called macroalgae) (Milledge *et al*., 2014). An attractiveness of microalgae is its product versatility. Microalgae has high amounts of lipids and carbohydrates, which can be used to produce different types of biofuels like bioethanol, biobutanol, and biodiesel (Chen *et al*., 2013; Giordano & Wang, 2018).

In contrast to microalgae, seaweeds have low lipid content (2 – 4 % dry weight) but contain high amounts of carbohydrates (40 – 50 % dry weight), which are mostly unique storage polysaccharides like laminarin and fucoidan. These carbohydrates are significantly different from those commonly encountered in other carbohydrate feedstock. They require different processing techniques that are not currently available or explored (Torres *et al*., 2019). In general, the algal biorefinery has not had a lot of commercial success. Utilizing microalgal as a feedstock requires several processing steps involved with high energy demand making it highly uneconomical. The non-fuel applications of macroalgae are highly established and profitable (Milledge *et al*., 2014).

Another type of feedstock worth mentioning is the mixed organic residues. They are a broad group of waste products with various properties. Examples include municipal solid waste, manure, sewage sludge. They are commonly used to produce biogas (Cherubini, 2010).

2.1.2. Conversion technologies

Several processes are adopted to break down the complex structure of biomass and convert it into

valuable products. These processes can be divided into mechanical/physical, chemical, biochemical, and thermochemical, as highlighted in Table 2.1 (Cherubini, 2010; Gavrilescu, 2014).

Thermochemical processes use heat to cause changes in a compound's chemical structure, making new products (Chisti, 2019; Kumar *et al*., 2019; Tanger *et al*., 2013). Gasification is an example of a thermochemical process used for biomass conversion. It is an endothermic reaction in which materials are exposed to high temperatures (800 – 900 °C) and limited air to produce syngas. In a study, cotton stalk was gasified using a bench-scale fixed bed reactor at 900 °C for 90 minutes with an oxygen to biomass ratio of 0.25 to produce hydrogen-rich gas. The produced gas had H_2 and CO concentrations of 45 % and 33 %, respectively. The process had an overall carbon conversion efficiency of 84 % (Hamad *et al*., 2016).

Hydrothermal liquefaction (HTL) and pyrolysis are other thermochemical processes for the conversion of biomass. These reactions are carried out at moderate temperatures in the absence of air to obtain a liquid product. In HTL, water is a vital reactant/catalyst, ensuring that the reaction can proceed to the product formation stage without the biomass drying stage observed in gasification and pyrolysis. HTL is usually carried out at temperatures between 280 – 370 °C and high pressures between 10 – 25 MPa, typically in the presence of a catalyst. An extensive review of the HTL process has been published elsewhere (Toor *et al*., 2011). Using HTL, a 23 % yield of bio-oil from the macroalgae *Enteromorpha prolifera* was reported at a reaction temperature of 300 °C for 30 minutes, with 5 %wt Na_2CO3 as catalyst (Zhou *et al*., 2010).

Pyrolytic reactions are usually carried out at temperatures between 350 – 700 °C. The yield and

properties of the pyrolysis product depend on the conditions of the pyrolysis reaction. Based on the operating conditions, pyrolysis can be categorized into conventional/slow, fast, and flash pyrolysis. These differ based on heating rate, reaction time, and process temperature (Jahirul & Rasul, 2012). Pyrolytic reactions can be catalyzed or uncatalyzed. An uncatalyzed pyrolysis reaction of sugar bagasse using fixed-bed flash pyrolysis at a reaction temperature of 500 °C for 2 minutes at a heating rate of 200 °C /min produced approximately 50 % by mass of bio-oil (Tsai *et al*., 2006). Combustion is a thermochemical process characterized by high temperature and excess air. It is mainly used to convert biomass for heat and power (Cherubini, 2010; Demirbas & Arin, 2002; Demirbas, 2009; Jahirul & Rasul, 2012; Parajuli *et al*., 2015).

Biochemical processes can be defined as the breakdown of biomass into alcohols and other oxygenated compounds through microorganisms' biological activities. Common biochemical processes are anaerobic digestion and fermentation (Balat, 2006). Anaerobic digestion is the decomposition of organic materials by a cocktail of anaerobic microbes chiefly into methane and carbon dioxide. The process occurs in four major steps; *hydrolysis* is when the bonds of the complex molecules of the organic feedstock are broken by water. The resulting compounds are further broken down into smaller compounds like organic acids, alcohols, hydrogen in the *acidogenesis* stage and subsequently into acetate in the *acetogenic* stage. In the last stage: *Methanogenosis*, the acetate and hydrogen produced are used to form methane through the action of methanogenic bacteria (Bajpai, 2020). This process is highly dependent on the pH, temperature, organic loading rate, and hydraulic retention time (Cantrell *et al*., 2008). While the aim of anaerobic digestion is to obtain gaseous fuels (biomethane), fermentation is focused on producing liquid renewable fuels like bioethanol and biobutanol. Fermentation uses living organisms to convert fermentable sugars (preferably hexoses) into these alcohols and consists of hydrolysis,

fermentation, separation (distillation), and dehydration stages (Bajpai, 2020). Where lignocellulosic materials are to be used as the sugar source, a pre-treatment step is required to breakdown the complex structure of the lignocellulosic material, making the sugar accessible for the fermentation steps (Bharathiraja *et al*., 2016; Mohapatra *et al*., 2017).

Chemical processes are those that cause a change in biomass by reacting it with other substances. These are mostly pre-treatment or upgrading steps in a biorefinery process. For example, acid hydrolysis is employed to degrade cellulose and hemicellulose into sugar monomers useful for fermentation (Ghatak, 2011). Transesterification of triglycerides is done with an acid/alkali catalyst under mild temperatures of 50 – 80 °C (323 - 353 K) to produce fatty acid methyl ester (FAME), also known as biodiesel, that can be upgraded to meet transport fuel requirements (Mikkola *et al*., 2015). Other examples of chemical processes include Fischer–Tropsch Synthesis (FTS), steam reforming, methanisation (Cherubini, 2010).

Mechanical processes do not change the biomass's composition but provide size reduction and separation of components such as filtration and cutting (Cherubini, 2010). Mechanical processes are essential in a biorefinery system as the success of other processing types relies on the use of pure and uncontaminated fractions to make desired products (Mikkola *et al*., 2015).

2.2. Lipid (triglycerides) pyrolysis

Despite its attractiveness as biorefinery feedstock, lipids are plagued with the food versus fuel debate. To circumvent this, attention has been turned to lipids from inedible sources and waste feedstock. These alternative sources of lipids also have the added advantage of being less expensive. Amongst the available technologies for lipid conversion, pyrolysis has been identified

as a superior process over other technologies like transesterification because it is compatible with existing infrastructure, relatively cheaper, and creates a liquid product which profile is more similar to transportation fuels (Buzetzki, *et al*., 2011; Jenab *et al*., 2014; Maher & Bressler, 2007).

The pyrolysis of triglycerides is primarily dominated by complex free radical reactions. An initial thermal decomposition step of the oxygenated compounds in the triglycerides is required to produce carboxyl or carbonyl radicals. These radicals undergo several reactions to create different compound groups. The decarboxylation and deketenization of the carboxyl and carbonyl radicals lead to the formation of straight-chain alkanes and alkenes, accompanied by the release of CO_2 or CO. Isomerization of the radicals produce branched compounds. Other reactions undergone by the radicals include Diel – Alders reaction, aromatisation, hydro abstraction, disproportionation, and β-scission. Polymerization and polycondensation yield heavier hydrocarbons (Kubátová *et al*., 2011; Lappi & Alén, 2011; Zarnegar, 2018). A mechanism for the pyrolysis of fatty acids (stearic acids) has been suggested by another author (Maher *et al*., 2008).

Lipid pyrolysis has been extensively studied using triglycerides (Lappi & Alén, 2011; Lima *et al*., 2004; Wiggers *et al*., 2009). The pyrolysis of triglycerides has been reported to yield a high percentage of oxygenated compounds (Kubátová *et al*., 2011). Lipid pyrolysis has also been studied using fatty acids separated from triglycerides by hydrolysis (Asomaning *et al*., 2014; Maher *et al*., 2008). Pyrolysis of lipids has also been studied using catalysts. The thermo-catalytic conversion of lipids enables the pyrolytic reaction to be carried out at lower temperatures and allows for increased selectivity of liquid products that better meet the transport fuel requirements (Asomaning, 2014; Buzetzki *et al*., 2011). These catalyzed reactions can be done in the presence of hydrogen-*hydroprocessing* (Horáček *et al*., 2020; Wang *et al*., 2018) or in the absence of

hydrogen (Alcantara *et al*., 2000; Buzetzki *et al*., 2011; Yu *et al*.,2013).

2.2.1. Lipid pyrolytic liquid

The pyrolytic liquid is from the condensation of vapors formed during a lipid pyrolysis reaction (Jahirul & Rasul, 2012). It is a dark, complex mixture with hundreds of compounds, including alkanes, alkenes, cyclics, aromatics, and acids (Goyal *et al*., 2008; Guo *et al*., 2010; Xiu & Shahbazi, 2012). The compound distribution of the pyrolytic liquid is dependent on the pyrolysis conditions and feedstock used (Mancio *et al*., 2018). Lipid pyrolytic liquid has been described as the product with the most potential to replace petroleum in transport fuels. However, its high carboxylic and olefin content poses a severe limitation as a drop-in fuel due to its potential corrosiveness and instability (Ferreira *et al*., 2017). Strategies adopted to improve the pyrolytic liquid properties include hydrodeoxygenation, catalytic cracking to promote deoxygenation (Lindfors *et al*., 2014). These processes can be applied directly to the lipid feedstock (Harnos *et al*., 2012; Horáček *et al*., 2020; Sari *et al*., 2013). They can also be done using the liquid formed during an initial pyrolysis reaction (Buzetzki *et al*., 2011; Lima *et al*., 2004; Srinivas *et al*., 2000). This approach has been reported to reduce the overall amount of pyrolytic liquid obtainable (Lindfors *et al*., 2014). Another system is the fractionation of pyrolytic liquid using distillation to obtain fractions comparable to petroleum fuels (Mancio *et al*., 2018; Wiggers *et al*., 2009). Fractionation studies of pyrolytic oil from lignocellulosic biomass have shown fractions with improved properties. It also creates multiple product streams that can be utilized or upgraded for different purposes (Li *et al*., 2011). This approach has also been carried out on lipid pyrolytic liquid to achieve these added benefits (Mancio *et al*., 2018).

2.3. Fractionation by distillation

Pyrolytic oil from lignocellulosic biomass has been fractionated using different techniques such as filtration, solvent extraction, centrifugation, liquid chromatography, distillation, condensation (Amen-Chen *et al*., 2001; Guo *et al*., 2010; Lindfors *et al*., 2014). However, for the fractionation of lipid pyrolytic liquid, distillation is the primary separation technique employed. Distillation is a separation technique based on the difference in the thermal properties/ relative volatilities of compounds. Different distillation types investigated include vacuum distillation, steam distillation, reactive distillation, and molecular distillation. Another report gives an exhaustive list of studies that have explored the fractionation of pyrolytic oil by distillation (Mancio *et al*., 2018).

Lipid pyrolytic liquid has been distilled to yield fractions with petroleum fuel-like properties. Pyrolytic oil from the thermal cracking of waste fish oil in a continuous reactor was separated by atmospheric distillation into two fractions: light bio-oil with a final temperature of 220 °C and heavy bio-oil between vapor temperature of 150 – 400 °C to correspond to the boiling range of gasoline and diesel, respectively. The carbon numbers of the compounds in the light bio-oil and heavy bio-oil fractions were also within the limit for gasoline and diesel, respectively. The flashpoint, kinematic viscosity, water, and sulfur content of the heavy bio-oil fraction was better than those of the pyrolytic oil and within the required diesel specification (Wiggers *et al*., 2009). In a different study, the pyrolytic oil from the catalytic cracking of soyabean oil was fractionated by vacuum distillation at 100 Pa into three fractions (green gasoline; < 50 °C; "green diesel" 50 – 150 °C; tar > 150 °C) corresponding to an atmospheric equivalent of < 205 °C; 205 – 307 °C; and > 370 °C respectively. Upon analysis, the properties (heating value, density, and viscosity) of the "green diesel" fraction were within the required specification (Yu *et al*., 2013). In general, from

the studies described, the fuel fraction properties obtained from the distillation of pyrolytic oils are better than the crude pyrolytic oil and are within specifications for transport fuels (Mancio *et al*., 2018).

Distillation has also been used to obtain fractions that can be selectively upgraded to renewable fuels. The liquid product from the pyrolysis of *Nannochloropsis spp* was distilled to yield three fractions (F1: T < 120 °C; F2:120 °C < T < 200 °C; F3: >200 °C). The first two fractions were upgraded by catalytic cracking using a Pd/C catalyst under temperatures of 130 to 250 °C and pressure conditions of 4.1 to 8.3 MPa, respectively. The crude pyrolytic oil was also upgraded for comparison. It was reported that the fuel properties of the upgraded distillates were better than that of the upgraded crude pyrolytic oil. The total acid number of the upgraded distillates was significantly reduced due to deoxygenation. The olefin content was also significantly lower than the upgraded crude pyrolytic oil (Nam *et al*., 2017). Similarly, pyrolytic liquid from rice husk was separated into two fractions using distillation under reduced pressure (∼0.009 MPa). The distillate at 110 °C (383 K) was taken as the "low boiling fraction," and the heavy residues denoted as "high-boiling fraction" was upgraded under supercritical conditions using methanol as solvent and PtNi/MgO catalyst. The heating value, density, and kinematic viscosity reported for the upgraded oil were better than the crude pyrolytic oil and the un-upgraded fraction (Li *et al*., 2011).

2.3.1. Distillation

An overview of the principles of distillation is discussed below.

2.3.1.1. Overview of distillation

Distillation is one of the oldest and predominant methods for separating mixtures in the chemical

and petroleum industry. Compared to other heat processes of separation that require an additional component, distillation utilizes energy solely to achieve separation of mixtures (Steinigeweg & Gmehling, 2005). The distillation process can be summarised in three steps: (1) Generation of a two-phase (liquid-vapor) system, (2) transfer of mass across the interface (3) separation of the two phases (Stichlmair, 2010a).

The principle of separation by distillation is based on a difference in the composition of the liquid and vapor phases of a mixture at equilibrium. This is influenced by the volatility of the components in the mixture. The difference in composition is expressed with the equilibrium ratio (k) which can be derived from Dalton's law and Raoult's law (Luyben, 2013; Stichlmair, 2010a). These are given in Equations (2.1), (2.2) and (2.3), respectively.

$$\text{Dalton's law: } Pi = yi.Pt \tag{2.1}$$

$$\text{Raoult's law: } Pi = \chi i.Pi^{\circ} \text{ or } Pi = \gamma i.\chi i.Pi^{\circ} \tag{2.2}$$

$$\text{Equilibrium ratio (k)} = \frac{yi}{\chi i} = \frac{\gamma i.Pi^{\circ}}{Pt} \tag{2.3}$$

Pi, χi, yi are the partial pressure and mole fraction of *component* '*i'* in the liquid and vapor phase, respectively; Pi^{o} is the vapor pressure of the pure compound of *'i'*; Pt is the mixture's total pressure; γi is the activity coefficient of component *'i'*.

Liquid mixtures to be separated industrially are not always ideal mixtures. Hence, in Raoult's law, γi is used to account for the non-idealities in the liquid phase. It is equal to one in ideal mixtures. In Dalton's law, the pressure *Pi* is replaced with fugacity *f,* and a fugacity coefficient (φ) is used to relate both *P* and *f* (Stichlmair, 2010a).

The relative volatility between two components in a mixture is a ratio of their volatilities and a measure of the ease of separation of the components (Hipple, 2017). It is given in Equation (2.4), where *ya, χa* refers to the molar fraction of the more volatile compound of '*a*' in the vapor and liquid phases, respectively. *yb, χb* are the molar fractions of the less volatile compound '*b*' in the vapor and liquid phases.

$$\text{relative volatility: } \alpha AB = \frac{ya/\chi a}{yb/\chi b} \qquad (2.4)$$

The relative volatility is dependent on the temperature, pressure, and composition of the mixture. In general, the closer the relative volatility between two compounds is to unity (1), the more difficult the separation (Doherty & Knapp, 2004; Nuchteera *et al*., 2020). A list of examples of hydrocarbon mixtures and their relative volatility is given by another author (Rossini, 1953). A difference in the mixture's liquid-vapor composition is necessary for separation by distillation to occur (Doherty & Knapp, 2004; Luyben, 2013; Steinigeweg & Gmehling, 2005). When the liquid-vapor composition of a mixture is the same, an azeotrope is formed, which cannot be separated by ordinary distillation (Lei & Chen, 2013). Knowledge of the Vapor-Liquid Equilibria (VLE) of a mixture is therefore vital for distillation processes (Kiss, 2013).

VLE determination is based on the mixture's thermodynamics, which is governed by mass and energy balance (Stichlmair, 2010a). VLE for mixtures can be calculated using Dalton's and Raoult's law (Stichlmair, 2010a). Data for binary mixtures are commonly represented on a temperature versus composition (*T-χy*) or liquid-vapor (*χy*) VLE diagrams at constant pressure (Luyben, 2013). While there are several data on the VLE of various binary mixtures, experimental data for the VLE of multicomponent mixtures are hard to find. Approaches used for the VLE

calculation of multicomponent mixture involve the use of the equation of states (EOS) like Soave–Redlich–Kwong equation and the Peng–Robinson equation; and the estimation of the activity coefficient using models like Wilson, UNIQUAC, or NRTL models (Steinigeweg & Gmehling, 2005). For a multi-component mixture with *j* components, there are *j – 1* Equations describing the equilibrium relationships of the components. These form the MESH equation (**M**aterial, **E**quilibrium, **S**ummation, and **H**eat balance) necessary for distillation analysis and design. Lately, these rigorous calculations can be done using different process simulators, phasing out the complex shortcut calculation methods like the Fenske-Underwood-Gilliland equations (Kiss, 2013; Steinigeweg & Gmehling, 2005).

In distillation, one separation stage is achieved when VLE is reached. The vapor is condensed to obtain a liquid of a different composition from the initial mixture. In an ideal distillation stage, the more volatile component of a mixture is enriched in the vapor phase at VLE; hence, the distillate is richer in the more volatile component of the mixture (Stichlmair, 2010a). Depending on the relative volatility of the components in the mixture, more than one ideal separation stage might be needed to achieve the desired separation/purity. In practice, columns are used for distillation processes, combining several separation stages into one column where each stage is heated by the vapor from the stage before it (Kiss, 2013; Steinigeweg & Gmehling, 2005; Stichlmair, 2010a). It is common for a distillation process to not achieve an ideal separation stage. Tray efficiency values are used to account for the non-ideality of a distillation separation stage: Therefore, the number of actual separation stages needed for a distillation process is the product of the number of non-ideal stages and the tray efficiency of the system (Kiss, 2013).

During the distillation process, upgoing vapor is stripped of the heavier components by the

downflowing liquid. The down-flowing liquid is a portion of the condensed distillate returned to the column from the condenser above the column; this liquid is termed reflux. The reflux ratio is defined as the ratio between the amount of liquid returned (L0) to the amount of distillate (D) collected as given in Equation (2.5) (Kiss, 2013; Steinigeweg & Gmehling, 2005)

$$\text{Reflux ratio: } = \frac{\text{L0}}{D} \qquad (2.5)$$

Reflux ratio plays a vital role in improving the degree of a separation process (Rose & Long, 1941) and has an inverse relationship with the number of separation stages required for a distillation process (Hipple, 2017). The higher the reflux ratio, the better the separation but, the higher the energy demand (Stichlmair, 2010a). There are two extreme cases of reflux ratio useful for distillation calculations. The first scenario is total reflux (when all the distillate is returned to the column, and there is no distillate collection). Under this condition, the number of separation stages required is at a minimum (Stichlmair, 2010a). This is done to estimate the maximum degree of separation obtainable from a column (Hipple, 2017). The second scenario is when the distillation is done at minimum reflux, corresponding to an infinite number of separation stages (Stichlmair, 2010a). Between these two extremes, the optimum operating conditions for a separation process can be obtained (Carney, 1949).

The distillation column internals have contacting devices promoting rigorous contact between the liquid and vapor phases to increase mass transfer between the phases (Steinigeweg & Gmehling, 2005). There are generally two types of contacting devices - trays and packing. Trays are discreet horizontal plates with openings to support the crossflow of the two phases. There are commonly three types of trays used in distillation column internal: bubble cap trays, sieve trays and valve

trays. Bubble cap trays have a much higher turndown ratio compared to the other tray types. As such, they can operate at very low vapor rates. The drawback to this tray type is the potential for pressure drop. Sieve trays have round holes that create an avenue for rigorous vapor-liquid contact and lower pressure drop. They are cheaper to construct, and their design equations are very reliable, but they can be prone to weeping (Hipple, 2017).

Column packings are solid structures with porosity and higher surface area. Two types of packing designs exist – random packings consisting of a bed of ceramic, metal, or plastic; and structured packing made of ceramic or "parallel corrugated metal sheets with an alternating orientation of subsequent layers" (Hipple, 2017; Stichlmair, 2010b). Packed columns have lower pressure drop than tray columns and can have high efficiencies, especially the structured packings. The drawbacks of packed columns are the need to redistribute the liquid, which tends to gravitate towards the wall, reducing vapor-liquid contacting, and the unreliability of their design equations. In tray columns, it is assumed that one tray is equivalent to one separation stage. For packed columns with continuous contacting devices, a height equivalent of a theoretical plate is estimated where 1 metre of packing is equal to a given number of stages (Hipple, 2017; Steinigeweg & Gmehling, 2005).

Other features that determine a distillation column's efficiency are its pressure drop along the column, liquid holdup in the column, and throughput which can also be described as the liquid-vapor traffic in the column. In general, a low liquid holdup in the column, high column throughput, and low-pressure drop are desired for an efficient column (Carney, 1949). The design of a distillation column/process is the summation of different factors, which include; accurate estimation of the thermodynamic properties of the mixture and its components, the VLE behavior

of the mixture, required separation stage, column structure and dimension, types, and structure of the column internal, energy demand, degree of separation/purity required, condenser and reboiler duty (Hipple, 2017; Stichlmair, 2010b).

2.3.1.2. Spinning band distillation

Columns with mechanical moving parts have been explored to maximize vapor-liquid contact during the distillation process. These columns usually have a spinning center part that diffuses the vapor and liquid into one another by splashing the down-coming liquid away from the column center towards the walls to promote intimate contact between the phases. This is illustrated in Figure 2.2. With a spinning part, commonly a band, the column's flow changes from laminar to turbulent with a greater diffusion coefficient (Carney, 1949). The rotating spiral band can be made of Teflon or metallic material.

Spinning band distillation is especially useful in separation processes requiring a high number of separation stages. It is characterized by low holdup and pressure drop (Kurniawan *et al*., 2019). As such, it is widely utilized in the distillation of essential oils and solvent recycling. An author separated Patchouli, Citronella, and Cajeput essential oils with a B/R Instrument Spinning Band Distillation System Model 36-100 and obtained a citronella alcohol fraction with 88 % purity (Kurniawan *et al*., 2019). Using spinning band distillation, a group recovered previously used acetonitrile which specification matched that of unused HPLC grade acetonitrile (Bellew *et al*., 1981).

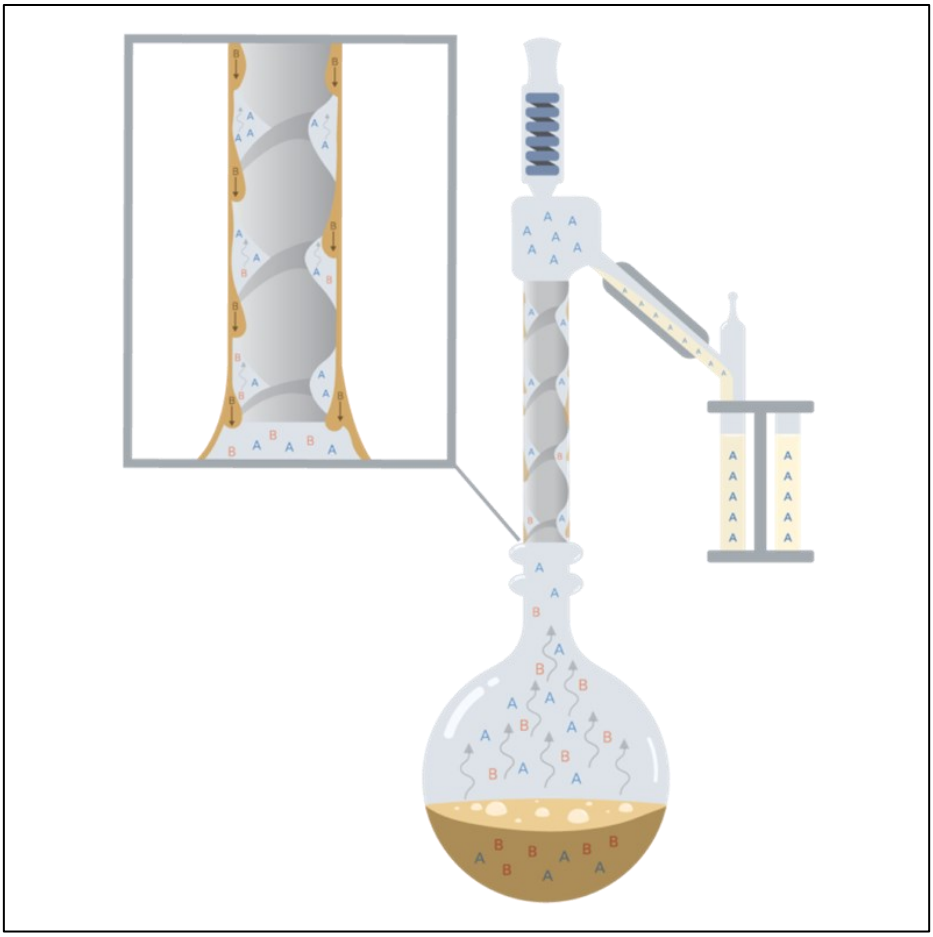

Figure 2.2: Illustration of spinning band distillation. Reproduced with permission from B/R Instrument Corp *(Permission granted: April 26, 2021).*

2.4. Fractionation by liquid-liquid extraction (LLE)

2.4.1. Overview of LLE

LLE separates compounds in a mixture based on their ability to partition between two immiscible (or partially miscible) solvents in contact with each other (Lebl *et al*., 2019). The interaction between the two liquids creates a potential gradient that influences the solute's transfer from one liquid to another. LLE can be achieved using different mechanisms such as pH manipulation to affect solubility, ion-exchange, and reverse osmosis (Iloeje, 2020).

LLE can be characterized based on the interaction between the solvent and the extraction agents into physical, dissociative, and reactive extractions (Schmidt & Strube, 2018; Zhang & Hu, 2013). The steps involved in the LLE process are (1) the addition of an immiscible extractant, (2) the mixing of the resulting mixture (3) separation/partitioning of the phases (Zhang & Hu, 2013). The condition necessary for LLE is the occurrence of a two-phase area between the raffinate and the extract phase (Schmidt & Strube, 2018). Common approaches used to model the thermodynamics of LLE are the Gibbs energy minimization (GEM) and the equilibrium constant (K-value). (Iloeje, 2020). A solute would distribute in different solvents in a partition ratio that remains constant as equilibrium is attained. The ratio of the solute amount in the various solvents is termed the *equilibrium partition ratio* (k). Other important properties of the LLE systems are the *separation factor*, which measures the extractant's sensitivity to the desired solute; the extraction factor is the amount of solute in the extractant and the *distribution coefficient* (Zhang & Hu, 2013). LLE can be carried out in single or multiple stages. Multiple stage extraction can be done either in crosscurrent or countercurrent configurations. Mixing is vital in LLE to create a large phase interface and achieve distribution equilibrium. There are different equipment types available for carrying out LLE; mixer settlers, extraction column, and centrifugal contactors (Iloeje, 2020; Schmidt & Strube, 2018).

Important considerations in selecting liquids for LLE are the *capacity* of the desired compound to distribute between the solvents. The extracting solvents' *selectivity* to extract the desired compound compared to other compounds in the mixture; *low mutual solubility* between the extracting solvent and the raffinate; the difference in *densities* between solvent and raffinate; optimal *interfacial tension* to avoid the formation of emulsions and low *viscosity*. An attractiveness of LLE is that solvents can be recycled (Schmidt & Strube, 2018; Zhang & Hu, 2013).

2.4.2. Applications of LLE to pyrolytic liquid

LLE has been extensively explored to fractionate pyrolytic liquid for characterization purposes and obtain fractions for selective processing (Lindfors *et al*., 2014). For pyrolytic oil from lignocellulosic biomass, an initial fractionation is achieved by adding water to cause a phase separation into water-soluble and water-insoluble fractions (Scholze & Meier, 2001). Pyrolytic oil from rice husk was separated into a water-insoluble fraction containing phenolic compounds from the lignin portion of the biomass; and a water-soluble fraction containing low carboxylic acids and ketones mostly from the cellulose/hemicellulose portion of the biomass. This fraction was subsequently upgraded by reactive distillation (Xu *et al*.,2013).

Pyrolytic oil has also been fractionated using organic solvents of different polarities to obtain acidic, basic, and neutral fractions. Some common organic solvents used are chloroform, methanol, acetone, benzene, tetrahydrofuran, and dichloromethane. Several examples of organic solvent fractionation of pyrolytic liquid are given elsewhere (Fagernäs, 1995). A group developed an organic solvent fractionation scheme for pyrolytic liquid at National Renewable Energy Laboratory (Chum *et al*., 1990).

The organic acids in pyrolytic liquid can be isolated from the mixture by acid-base extraction. This is a dissociative extraction where separation can be done by taking advantage of the fact that carboxylic acid solubility in their neutral state is higher in the organic phase than their charged state with higher solubility in the aqueous phase (Zhang & Hu, 2013). Some authors have utilized this method to isolate organic acid in the pyrolytic liquid. The organic acids in the ethyl soluble fraction of pyrolytic oil were isolated from the mixture into an aqueous phase with 5 % $NaHCO_3$ and recovered by acidification with H_3PO_4 and extraction with ethyl acetate. The solvents were

evaporated to obtain the organic acid mixture (Chum *et al*., 1989). In another study, the acids were removed from the pyrolytic liquid mixture by neutralization using NaOH; this was separated as an aqueous phase from the organic fraction. The acid-containing aqueous phase was acidified to a pH of 1 with HCl and re-extracted with diethyl ether, subsequently evaporated to yield the acid fraction (Beaumont, 2007).

The pyrolytic liquid contains organic acids, including the short-chain fatty acids (Beaumont, 2007) and the mid-chain fatty acids (Asomaning *et al*., 2014). These acids must be removed for pyrolytic liquids to meet the low acid content standard of transport fuels. Given the similarities in the boiling points of the different compounds of both the carboxylic acid and *n*-alkane homologous series, separation by distillation is ineffective. Therefore, another separation method must be adapted. Acid-base extraction has shown promising results for this separation (Gandhi *et al*., 2012). The use of acid-base extraction is also a reasonably common practice seen in the petroleum industry. Naphthenic acids are extracted from crude oil using caustic soda and regenerated by acidification with sulphuric acid for other industrial purposes (Brient *et al*., 2000).

2.5. Fatty acids

Fatty acids are hydrocarbons with the -COOH carboxylic functional group. Depending on the presence and number of double bonds, they can be saturated or mono, or polyunsaturated. Fatty acids with a chain length of 2 – 6 carbon atoms are described as short-chain fatty acids (SCFA), 6 – 12 carbon atoms are described as medium-chain fatty acid (MCFA), and greater than 12 as long-chain fatty acid (Vázquez & Akoh, 2010). Naturally occurring fatty acids have carbon numbers ranging from 4 to 24 with even-numbered chain length (Scrimgeour *et al*., 2020). Natural sources of fatty acids are oils extracted from oilseeds/ oil crops and fats from the rendering industry. Tallow

and lard are the important fat source from the rendering industry. Fatty acids are also obtained from the tall oil of pine wood (Anneken *et al*., 2006).

These compounds have high commercial importance with several applications in multiple industries, including food, personal care, agriculture, medicine, cosmetics, chemicals, lubricants, coating, etc., either directly or as precursors for other chemical compounds (Kenar *et al*., 2017). Acetic acid (C2:0) is a feedstock to produce vinyl acetic monomer, used in the manufacture of vinyl plastics, adhesives, textile finishes, and latex paints. It is also used for acetyl cellulose and acetic anhydride production. Butyric acid (C4:0) is a common flavor additive in the food industry and is also used to produce biobutanol, a renewable fuel (Tajarudin *et al*., 2018). Caproic acid (C6:0) is utilized in the agricultural industry as a growth stimulant and feed additive. It is also important in producing lubricants, fragrance, and paint additive (Chen *et al*., 2017). A table listing the major uses of different carboxylic acids is presented in another report (Anneken *et al*., 2006).

Short chain fatty acids are produced commercially by the hydrocarboxylation of carbon dioxide and the relevant alkene (Gandhi *et al*., 2012). The prevalent method for obtaining the mid chain fatty acids is through the hydrolysis of triglycerols; this is termed fat splitting (Anneken *et al*., 2006; Cermak *et al*., 2012; Chupa *et al*., 2012). Industrially, fat splitting is commonly done using the chemical methods (batch autoclave, Twitchell, or Colgate-Emery) or the enzymatic method (Cermak *et al*., 2012; Gervajio *et al*., 2005). As stated in previous sections, fatty acids are also produced during the pyrolysis of lipids (Asomaning *et al*., 2014; Ferreira *et al*., 2017). Given their industrial importance, there is significant interest in extracting the carboxylic acids formed during the cracking of lipids as a co-product stream, some of which have more market value than fuel, thereby serving as an additional stream of revenue for the biorefinery process (Jones *et al*., 2015).

Some studies have explored this extraction. C2 – C11 carboxylic acids present in the liquid product of soybean/canola oil pyrolysis were extracted using water and 1 M NaOH at different temperatures. It was reported that water was only efficient at removing all the C2 acid and some portion of the C3 – C5 acid; the longer chain acids could not be removed by water due to their increasing insolubility in water. 1 M NaOH yielded better results in extracting the longer chain acids. For both solvents, the temperature did not affect the solvent's extraction efficiency (Gandhi *et al*., 2012). It was demonstrated in a different work that carboxylic acids could be extracted from lipid pyrolytic liquid at sufficient purity required for downstream processing. Acetic acid formed during the pyrolysis of soyabean oil was removed from the pyrolytic liquid with deionized water at multiple stages and distilled from the aqueous mixture containing other short chain fatty acids (C3 – C5). The recovered acetic acid was subsequently used to produce vinyl acetate monomer (Jones *et al*., 2015). Alternatively, amines (trimethylamine and dimethylethanolamine) have also been found to be capable of extracting the short chain fatty acids (C2 – C6) from the pyrolytic liquid of the non-catalytic cracking of soyabean oil (Braegelmann *et al*., 2011).

2.6. Transportation fuels

As the population increases, there is a corresponding increase in transportation fuel demand (Maitlis, 2013). Environmental concerns and fossil fuels have prompted the move for renewable sources of transportation fuel. As discussed in Section 2.1, several options are available to produce renewable transport fuels, albeit, to achieve adoption, these biofuels must be fractionated and upgraded to meet the standard requirements of transport fuels as postulated by the different countries and regions of intended use.

2.7. Organic solvents

Organic solvents are compounds of different homologous hydrocarbon groups and their halogen and nitro derivatives (Sainio, 2015). They are essential for several laboratory and industrial processes (Clarke *et al*., 2018). The compound group of interest for this work is the *n*-alkanes. These are majorly produced by the distillation of crude oil and form a significant constituent of transport fuels. *n*-Pentane and *n*-hexane are the smallest liquid *n*-alkane compounds in petroleum distillate. Asides from being a constituent of gasoline, they are also separated from the gasoline pool and utilized in other applications. *n*-Pentane is mostly used as a laboratory and industrial solvent, while *n*-hexane is a primary solvent for edible oil extraction (Schmidt *et al*., 2014). With the growing environmental concerns, considerable efforts have been put into producing these solvents renewably (Blazeck *et al*., 2013; Xi *et al*., 2016).

A common approach for renewable alkanes production is the aqueous phase reforming (APR) of biomass-derived polyols (Xi *et al*., 2016). A study to produce *n*-pentane and *n*-hexane from sorbitol through a bifunctional reaction pathway. The study reported that the reaction involved the dehydration of sorbitol over a solid acid catalyst (silica-alumina) to produce dehydrated intermediates. The dehydrated intermediate species then migrate to the metallic sites and undergo a hydrogenation reaction. As the process proceeded, a dehydration-hydrogenation cycle was established in the presence of hydrogen, leading to the production of *n*-alkanes like hexane (Huber *et al*., 2004). The selectivity of alkane formed from an aqueous phase reforming process depends on the type of catalyst used, reaction conditions, reactant addition, and reactor type. Many authors have explored these conditions to increase the production of selective higher alkanes, notably hexane from the process (Huber *et al*., 2004; Xi *et al*., 2016). This method involves a cascade of

reactions to convert biomass to polyols (sorbitol), which is then converted to dehydrated intermediates (isosorbides). An attempt was made to directly convert cellulose to hexane with a Ru/C catalyst combined with LiNbMoO6 layered compounds in low concentration phosphoric acid aqueous media. This resulted in a yield of 72 % hexane (Liu *et al*., 2015).

Another approach to producing renewable alkanes is through the Fischer Tropsch synthesis of syngas made from biomass gasification (Huber *et al*., 2004). The Fischer Tropsch synthesis is the catalytic process whereby carbon-monoxide undergoes polymerization and hydrogenation to produce syncrude, a mixture of liquid hydrocarbon (mostly alkanes and alkenes) and water (de Klerk, 2013; Speight, 2020). The equation representing the production of alkanes from Fischer Tropsch synthesis is given in Equation (2.6). The parameters that influence product selectivity have been discussed in another work (de Klerk, 2011). The product distribution is dependent on the probability of chain growth (α), which is a factor of operating temperatures and catalyst type. Catalysts commercially used for Fischer Tropsch synthesis are mostly Fe and Co-based. Ni-based catalysts are prone to fouling, and the high costs of Ru-based catalysts make their commercial use impractical. For all catalyst types, the higher the temperature, the lower the α, the more the shift toward lower weight compounds, predominantly methane (Dry, 2002).

$$\text{Alkanes: } nCO + (2n + 1)H_2 \rightarrow H(CH_2)nH + nH_2O \qquad (2.6)$$

Biosynthetic production of *n*-alkanes in an engineered cellular host through their fatty acids' decarbonylation has also been explored. An oleaginous host, *Yarrowia lipolytica*, was engineered with a lipoxygenase-mediated pathway found in soybeans to cleave linoleic acid and produce pentane with tridecadienoic acid as a by-product. Pentane yield was improved from 1.56 mg/L

pentane to 4.98 mg/L by improving substrate accessibility and overexpressing the lipoxygenase enzyme (Blazeck *et al*., 2013).

In conclusion, significant efforts have been put into obtaining alkane solvents from renewable sources. Lipid pyrolytic liquid contains a significant amount of *n*-alkanes and can be a renewable source of these compounds.

3. METHODOLOGY

3.1. Materials

For this work, the starting material used was the liquid hydrocarbon feed obtained from the pyrolysis of fatty acids. This was supplied by the industrial partner of the project. Prior to being supplied, the heavier ends (boiling points > 320 °C) of the liquid feed were removed. NaOH (98.8 %) was procured from Fisher Scientific Company (Whitby, ON, Canada). HCl, nonadecanoic acid methyl ester (> 99 %), ethyl formate (97 %), *n*-decane (>99 %), and diazomethane (prepared using a Diazald kit) were purchased from Sigma–Aldrich (St. Louis, MO, USA).

3.2. Experimental treatments

3.2.1. Feedstock compositional analysis

The composition of the liquid feed was analyzed using Gas chromatograph (GC) coupled with Mass Spectroscopy (MS) for compounds identification and Flame Ionization Detector (FID) for compound quantification. About 50 µl of the feed sample was transferred into a GC vial and weighed. Nonadecanoic acid methyl ester was added as an internal standard, and its mass was recorded. The sample was derivatized by adding 350 µl diazomethane to the GC vial. This was to convert the fatty acids present in the sample into their methyl ester derivatives for better GC resolution. The instrument used was an Agilent 6890N GC-FID with Agilent 7683B series autosampler and injector. The GC column was an Agilent DB Petro column (100 m × 250 µm × 0.5 µm) purchased from Agilent Technologies (Santa Clara, CA, USA). For the analysis, the injector and detector temperatures were kept constant at 300 °C and 350 °C, respectively. The GC oven temperature program is shown in Table 3.1; the total run time was 115 minutes. Helium was used as the carrier gas at a constant flow rate of 1.7 mL/min. A 20:1 split injection with an injection

volume of 1 µL. Liquid Nitrogen was used for cryogenic cooling. MS identification was conducted on an Agilent GC 6890N coupled to an Agilent 5975B EI/CI MS instrument operated in electron ionization (EI) mode. The column and conditions used in the GC-MS were the same as the GC-FID as described above. The temperature of the GC-MS interface was kept constant at 320 °C.

Table 3.1: GC oven programming for the compositional analysis of the feed.

	Rate (°C/min)	**Temperature (°C)**	**Hold time (min)**	**Run time (min)**
Initial		0	15	15
Ramp 1	1	50	0	65
Ramp 2	2	85	3	85.5
Ramp 3	10	280	10	115

Fourier-transform infrared spectroscopy (FTIR) was also conducted to cross-reference the GC results. A Perkin Elmer Frontier FTIR Spectrometer equipped with a Universal Attenuated Total Reflectance (ATR) Sampling Accessory with diamond prism was used. The background was scanned 16 times before the spectrum of the sample was taken. A drop of the sample was added to the diamond prism and scanned 16 times in the Mid infrared ray (IR) region between 650 – 4000 cm^{-1}.

3.2.2. Fatty acid extraction

The fatty acids present in the feed were extracted by 3 M NaOH solution to de-protonate the acids, making them insoluble in the organic liquid. 3 M NaOH was made by dissolving 120 g of NaOH pellets in 1 liter of distilled water. The feed-NaOH mixing ratio was pre-determined based on the acid-base stoichiometry. A 15 % extra NaOH was added as an allowance for incomplete neutralization. The extraction was carried out in three stages to ascertain complete fatty acid removal from the feed. The feed was weighed before the mixing step, and the mass was recorded.

The mixture was separated by centrifugation using a Beckman Coulter Avanti J-26 XP at 8,000 rpm for 5 minutes. An aqueous-organic layer was formed.

The top organic layer (termed the "hydrocarbon fraction") was decanted, weighed, and recorded. The second extraction was done using this hydrocarbon fraction as the starting material. The hydrocarbon fraction obtained from this second extraction was subsequently used as the starting material for a third extraction. The hydrocarbon fractions recovered from the second and third extractions were also weighed, and the masses were recorded. The hydrocarbon recovery (%wt of starting material) for each extraction stage was calculated using Equation (3.1a), and the overall hydrocarbon recovery was calculated with Equation (3.1b). The hydrocarbon fraction obtained from the acid extraction procedure was used as the feedstock for the distillation experiments described in Section 3.2.4. The bottom aqueous layer from the acid extraction was also collected in a container. This was used in the fatty acid recovery experiment described in Section 3.2.3. All fractions were stored in a refrigerator (Fisher Scientific Isotemp, Model: 50FREEFSA)) at 4 °C before further experiments. The hydrocarbon fractions from the three extraction stages were analyzed by GC FID/MS using the method described in Section 3.2.1 without the derivatization step. The split ratio was increased to 175:1 to avoid column overloading. An FTIR scan of the sample was also done to confirm the total removal of the acids from the sample.

$$\text{Hydrocarbon recovery/extraction stage} = \frac{Mass\ of\ hydrocarbon\ recovered\ from\ extraction\ stage}{Starting\ mass\ of\ material\ for\ extraction\ stage} \times 100 \quad (3.1a)$$

$$\text{Overall hydrocarbon recovery} = \frac{Mass\ of\ hydrocarbon\ recovered\ from\ third\ extraction}{Initial\ mass\ of\ feed} \times 100 \quad (3.1b)$$

3.2.3. Fatty acid recovery

The aqueous layer from Section 3.2.2 was transferred into a separatory funnel and retrieved from the bottom to reduce the amount of hydrocarbon compounds carried over into the fatty acid portion. The fatty acids were recovered by treating the aqueous layer with 3 M HCl to re-protonate the acid ions, making them insoluble in the aqueous phase. The 3 M HCl was prepared by adding 250 ml of 37 % HCl to 750 ml of distilled water. The mixture's initial pH was measured and found to be > 9 (pH meter used: Fisher Scientific AB 15 pH meter). HCl was added to the aqueous layer until a final pH of 1-1.5 was obtained. The mixture was transferred into a separatory funnel. Two layers were formed. The bottom aqueous layer was extracted and discarded, and the top organic layer, which was the fatty acid mixture, was collected, weighed, and the mass recorded. The fatty acid mixture was stored in a refrigerator at 4 °C before its use in the distillation experiments in Section 3.2.6. The fatty acid recovery (%wt of feedstock) was calculated using Equation (3.2). The fatty acid mixture was also analyzed by GC MS/ FID using the method described in Section 3.2.1 with a modified oven temperature program (Table 3.2) to determine the mixture's composition. An FTIR scan of the sample was also taken using the method described in 3.2.1. The process flow diagram for both the acid extraction and acid recovery experiment is given in Figure 3.1.

Table 3.2: GC oven programming for fatty acid compositional analysis.

	Rate (°C/min)	**Temperature (°C)**	**Hold time (min)**	**Run time (min)**
Initial		35	0.1	0.1
Ramp 1	10	320	21.4	50

$$\text{Fatty acid recovery} = \frac{Mass\ of\ fatty\ acid\ mixture\ recovered\ from\ extraction}{Initial\ mass\ of\ feed} \times 100 \qquad (3.2)$$

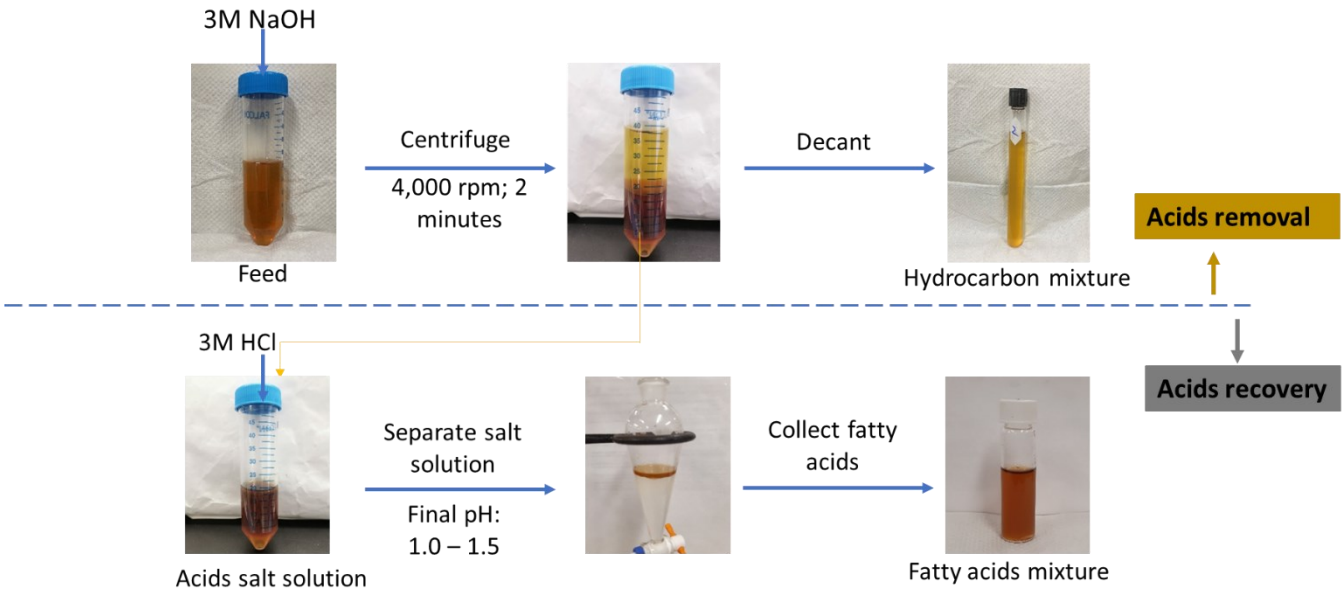

Figure 3.1: Process flow for the organic acid extraction and recovery process of the feed

3.2.4. Distillation of hydrocarbons

3.2.4.1. Determination of the vapor temperature range for the fractions

To determine the appropriate vapor temperature cut points for the solvent fractions of interest, the hydrocarbon fraction obtained from the first stage acid extraction described in Section 3.2.2 was distilled. This fraction was selected as starting material to prevent losses of the compounds of interest associated with the multiple acid extraction stages. The starting material was distilled at atmospheric pressure using a spinning band distillation unit (B/R Instrument M690) with a Teflon band length of 90 cm, spinning at 5000 rpm (speed is based on manufacturer's recommendation for Teflon spinning band). A schematic of the distillation setup is shown in Figure 3.2. About 130 ml of sample was transferred to a pre-weighed round bottom flask, and the sample's mass was recorded. Heating was set at 2 °C/min before boil up and 0.5 °C/min afterward. The heating rate and power percent of the heating mantle were controlled using a temperature controller (J-KEM

Scientific Temperature Controller, Model 210). The coolant temperature was also controlled and adjusted between 0 to 6 °C during the distillation run. The system was allowed to run under total reflux for 120 minutes after boil up to establish the vapor-liquid traffic in the column, before distillate was collected at a reflux ratio of 120:1. This reflux ratio was used based on preliminary distillation runs done to study the distillation profile of the sample). The temperature of the boiling flask and the vapor temperature was recorded. The distillate obtained at specific vapor temperature ranges (Table 3.3a) were collected in as a fraction in a pre-weighed receiver, its volume and mass were recorded. Distillate fractions were collected between the vapor temperature range of 26.5 – 86.0 °C; this was because the compounds of interest were between the C5 and C6 carbon numbers. Each fraction's cut point was kept at the midpoint between the boiling points of 2 corresponding significant compounds present in the hydrocarbon fraction with boiling points within the vapor temperature range of 26.5 – 86.0 °C. A total of eight fractions were collected (Table 3.3a).

3.2.4.2. Distillation of solvents from hydrocarbon fraction

Based on the outcome of the distillation runs done in Section 3.2.4.2, the vapor temperature range was adjusted according to Table 3.3b for fractionating the hydrocarbon sample into solvents and fuels. The number of fractions collected was reduced to five. The vapor temperature range of fractions 2 and 4 was narrowed to increase the purity of the solvent of interest at that fraction, namely: *n*-pentane solvent (fraction 2) and *n*-hexane solvent (fraction 4). The new vapor temperature range for the fractions was used for the rest of the experiments. The distillation was stopped when the vapor temperature reached 160.0 °C. The sample left in the flask (bottoms) with vapor temperature > 160.0 °C was termed the *drop-in diesel equivalent* fraction. The experiments were carried out as stated in Section 3.2.4.1. All the experimental parameters except the reflux

ratio were maintained as in Section 3.2.4.1.

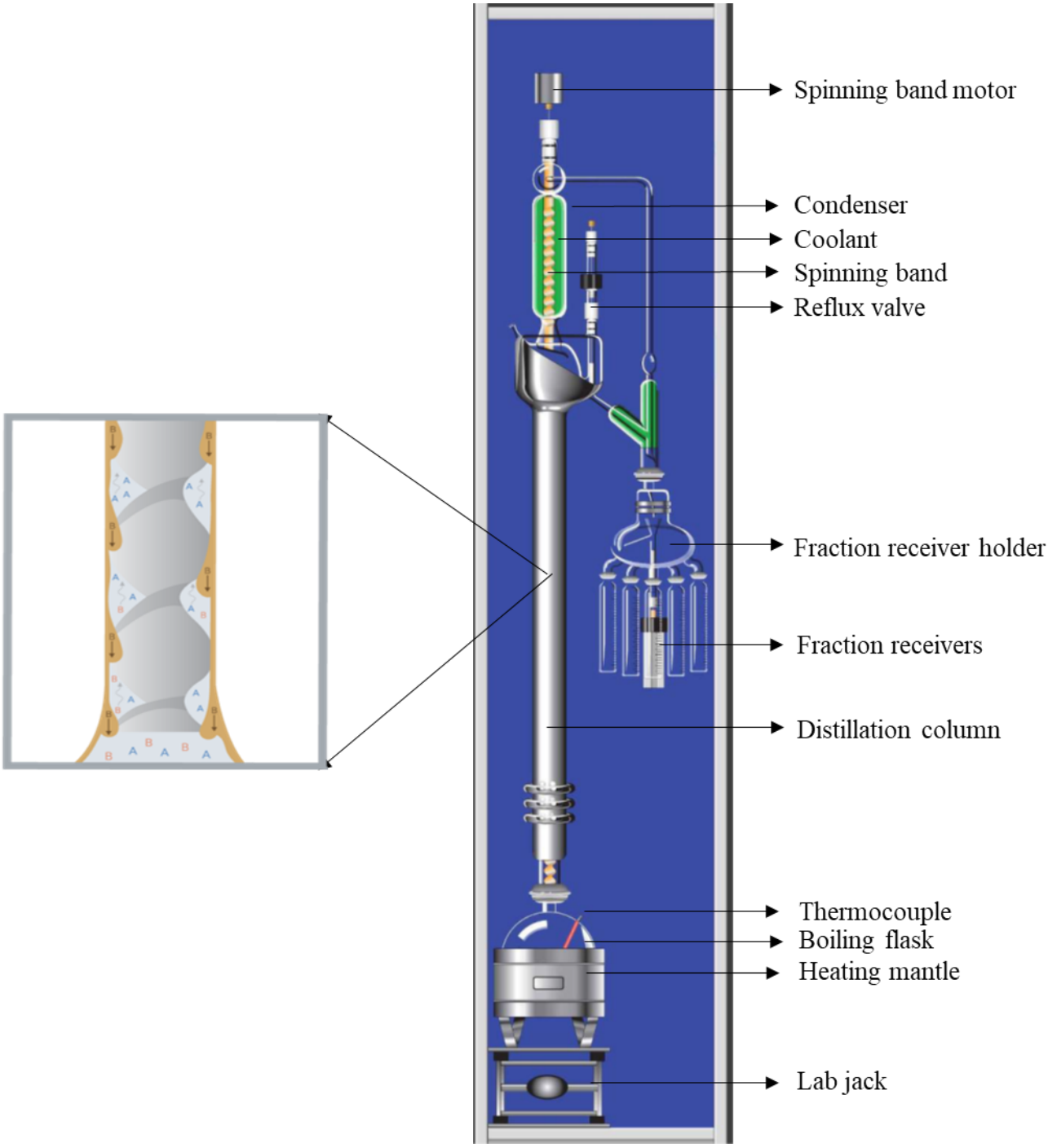

Figure 3.2: Schematic of the distillation experiment setup. Reproduced with permission from B/R Instrument Corp *(Permission granted: April 26, 2021).*

Table 3.3: Initial (a) and adjusted (b) vapor cut points for the hydrocarbon fraction distillation.

(a)

Fraction	Vapor temperature range (°C)
F1	26.5 - 32.0
F2	32.0 - 40.0
F3	40.0 - 54.5
F4	54.5 - 61.5
F5	61.5 - 66.5
F6	66.5 - 69.5
F7	69.5 - 76.0
F8	76.0 - 86.0
Bottom	>86.0

(b)

Fraction	Vapor temperature range (°C)
F1	26.5 - 33.0
F2	33.0 - 34.0
F3	34.0 - 65.0
F4	65.0 - 66.0
F5	66.0 - 160.0
Bottom	>160.0

3.2.4.3. Distillation of solvents from Naphtha

To obtain naphtha for this distillation experiment, the hydrocarbon fraction was distilled at atmospheric pressure using a spinning band distillation unit with a metal band of the length of 45 cm spinning at 2000 rpm (speed is based on manufacturer's recommendation for metal spinning band). Heating was set at 4 °C/min before boil up and 3 °C/min afterward. The system was allowed to run at total reflux for 30 minutes after boil up before distillate was collected at a reflux ratio of 30:1. This low reflux ratio was used as the aim of the distillation was not to achieve a sharp compound cut but to obtain a bulk fraction. Distillate within the vapor range of 26.5 – 160.0 °C was collected in one receiver as a single fraction; this was termed naphtha. The naphtha fraction

was re-distilled under the conditions stated in Section 3.2.4.1 with the adjusted vapor cut range established in Section 3.2.4.2.

3.2.4.4. Effects of reflux ratio on the purity of solvent cut

Three reflux ratios were tested; 90:1, 120:1, 240:1 to study the effect of reflux ratio on the purity of the solvent cuts from the hydrocarbon fraction. These experiments were done under the same distillation conditions in Section 3.2.4.1.

3.2.5. Analysis of hydrocarbon fractions

Distillate fractions obtained from all distillation experiments described in Section 3.2.4 were analyzed using GC-FID and GC-MS. Ethyl formate was used as an internal standard with *n*-decane as the solvent. A solution of 10 ± 2 mg/ml of ethyl formate in *n*-decane was prepared. 1ml of the solution was transferred to a GC vial and weighed. Approximately 50 µl of sample was added to the GC vial, and the mass was recorded. The GC sample mass was obtained as the difference between the GC vial mass before and after sample addition. The GC instrument, column, and parameters used are the same as that in Section 3.2.1, with a modified oven temperature program (Table 3.4).

Table 3.4: GC oven programming for the compositional analysis of the distillate fractions obtained from the distillation experiments.

	Rate (°C/min)	**Temperature (°C)**	**Hold time (min)**	**Run time (min)**
Initial		35	4	4.00
Ramp 1	1.5	57	0	18.67
Ramp 2	3	85	1	29.00
Ramp 3	12	280	4	49.25

The mass of each compound present in the GC sample of each fraction was determined according to Equation (3.3) using the peak area of the compound obtained from the gas chromatograph and a Relative Response Factor (RRF) pre-determined between ethyl formate and each compound group. For the initial hydrocarbon feedstock, compound quantification was limited to compounds before *n*-heptane (C7) as compounds of interest were *n*-pentane (C5) and *n*-hexane (C6). The % amount of a compound present in a fraction was calculated with Equation (3.4); this was used to measure the fraction's purity. The percentage recovery of a compound in the fractions was obtained using Equation (3.5). Total recovery of a compound relative to the initial feedstock was estimated with Equation (3.6).

$$\text{Mass of compound in GC sample} = \frac{GC\ peak\ area\ of\ compound \times Mass\ of\ internal\ standard}{GC\ peak\ area\ of\ internal\ standard \times RRF\ of\ compound} \quad (3.3)$$

$$\%\ \text{purity of solvent fraction} = \frac{Mass\ of\ compound\ in\ GC\ sample\ (equation\ 3)}{Mass\ of\ \ GC\ sample} \times 100 \quad (3.4)$$

$$\%\ \text{recovery of a compound in fraction} = \frac{\%\ amount\ of\ compound\ in\ fraction \times Mass\ of\ fraction}{mass\ of\ compound\ in\ hydrocarbon\ sample} \times 100 \quad (3.5)$$

$$\text{Total recovery (\%)} = \frac{\Sigma(\%\ amount\ of\ compound\ in\ fraction \times Mass\ of\ fraction)}{mass\ of\ compound\ in\ hydrocarbon\ sample} \times 100 \quad (3.6)$$

3.2.6. Distillation of fatty acids

The fatty acid mixture fraction from the acid recovery treatment described in Section 3.2.3 was distilled under vacuum at a pressure of 133.3 Pa, using a B/R spinning band distillation unit with a Teflon band of a length of 90 cm spinning at 5000 rpm (speed is based on manufacturer's

recommendation for Teflon spinning band). The cold trap was filled with dry ice. About 80 ml of sample was transferred to a pre-weighed round bottom flask, the mass of the sample was recorded. Heating was set at 2 °C/min. The heating rate and power percent of the heating mantle were controlled using a J-KEM temperature controller. The temperature of the condenser was also controlled, as seen in Table 3.5. When the bottom flask temperature reached 110 °C (atmospheric equivalent: 295.6 °C), the system was left to run under total reflux for 60 minutes to establish vapor-liquid traffic in the distillation column. Eight fatty acid fractions were collected between the vapor temperature range of 26.5 – 125.0 °C under 133.3 Pa (Table 3.5). An additional five fractions (termed offcuts) were collected between the fatty acid fractions to achieve higher purity of the fatty acid fractions. The distillation was stopped when the pot temperature reached 225.0 °C (atmospheric equivalent: 440.7 °C).

Table 3.5: Vapor cut points for the fatty acids fraction distillation.

Fraction	**Fatty acid**	**Vapor temperature range (atmospheric equivalent temperature (°C))**
F1	-	20.5 – 47.3 (175 – 212)
F2	C5:0	47.3 - 53.9 (212 – 221)
F3	C6:0	61.3 – 66.5 (231 – 238)
F4	C7:0	78.5 – 85.2 (254 – 263)
F5	C8:0	90.5 – 95.8 (270 – 277)
F6	C9:0	99.6 – 106.5 (282 – 291)
F7	C10:0	108.0 – 111.8 (293 – 297)
F8	-	116. 4 – 125.0 (304 – 310)
Bottoms	-	>125.0 (310)

3.2.7. Analysis of fatty acids fractions

The fatty acids fractions obtained from the distillation experiments in Section 3.2.6 were analyzed by GC-FID. A known quantity of methyl nona-decanoate is added to a vial as an internal standard and weighed. About 10 µl of sample was added to the pre-weighed vial, and the mass was recorded. Approximately 300 µl of diazomethane was added to derivatize the fatty acids. The GC method used is as described in Section 3.2.3. Like the analysis of the hydrocarbon fractions in Section 3.2.5, the mass of the fatty acids present in the GC sample of each fraction was determined according to Equation (3.3) above using the peak area of the compound obtained from the gas chromatograph and a relative response factor (RRF) pre-determined between methyl nona-decanoate and each fatty acid. The % amount of a compound present in a fraction was calculated with Equation (3.4); this was used to measure the fraction's purity. The % recovery of the compounds in the fractions was obtained using Equation (3.5). The total recovery of a compound was estimated with Equation (3.6).

3.2.8. Drop-in diesel equivalent properties analysis

The bottom fraction (sample left in the boiling flask after the distillation experiment) from the hydrocarbon fraction's distillations in Section 3.2.4 was termed *drop-in diesel equivalent.* Two samples were obtained by using two vapor temperature cut points: 160.0 °C and 175.0 °C. The fuel properties of the samples were analyzed as follows.

3.2.8.1. Acid number

The acid number of the renewable fuels was estimated according to the ASTM method D974. The sample is dissolved in a titration solution, a mixture of toluene (HPLC grade, Sigma Aldrich),

isopropanol (HPLC grade), and distilled water in the ratio of 100:99:1. The resulting single-phase solution is titrated at room temperature with a base solution made of potassium hydroxide dissolved in isopropanol to an endpoint indicated by the color change of the indicator (p-naphtholbenzein solution) from orange to greenish brown.

3.2.8.2. Flashpoint

Flashpoint was analyzed according to ASTM method D7236. This was done using a Herzoq Pac Optiflash Small Scale instrument. About 2 mL ± 0.1 mL of the sample is introduced into the test cup of the equipment, which is then heated automatically at a constant rate of 2 °C/min ± 0.5 °C/min. An electronic ignited flame is directed through an opening shutter in the test cup lid at specified temperature intervals until the automatic flash detector detects a flash. The temperature at which this occurs is reported as the flashpoint of the sample.

3.2.8.3. Cloud point and Pourpoint

Cloud point and pourpoint were estimated according to ASTM method D2500 and D97, respectively, using a Cloud and Pour Point Bath by Koehler Instrument Company Inc. The temperature of the sample is brought to a specified value, after which it is placed inside the bath filled with methanol and cooled at a specified rate and examined periodically (at intervals of 1 °C for cloud point and 3 °C for pour point). The temperature at which a cloud is first seen at the bottom of the test jar is recorded as the cloud point. For pourpoint, the sample is examined for flow characteristics. The lowest temperature at which no movement is seen when the test jar is placed horizontally is recorded as the pourpoint.

3.2.8.4. Distillation range

The distillation range was analyzed using ASTM method D7345 with OptiPMD Micro Distillation Analyzer by Pac Instruments. 10 ml of the sample is transferred into the distillation flask, placed in the apparatus, and heat is applied to the bottom of the distillation flask. The apparatus measures and records specimen vapor and liquid temperatures and pressure in the distillation flask as the sample gradually distill under atmospheric pressure conditions. After the process, the data is processed, converted to distillation characteristics, and corrected for barometric pressure. Test results are commonly expressed as percent recovered or evaporated versus the corresponding temperature in compliance with industry-recognized standard form and reference method either in a table or graphically, as a plot of the distillation curve.

3.2.8.5. Density

The density of the sample was analyzed according to ASTM method D5002. The equipment used was a Mettler Toledo D5. Approximately 3 mL of sample is introduced into an oscillating U-tube. The oscillating frequency change is used in conjunction with adjustment data to determine the sample's density, relative density, and API gravity.

3.2.8.6. Calculated cetane index

The calculated cetane index was estimated using the Four Variable Equation according to ASTM D4737. The calculated Cetane Index provides a means for estimating the ASTM cetane number of distillate fuels from density and distillation recovery temperature measurements when the result from ASTM Test Method D613 for cetane number is not available. The Four Variable Equation is given by:

$CCI = 45.2 + (0.0892)(T_{10N}) + [0.131 + (0.901)(B)] [T_{50N}] + [0.0523 – (0.420)(B)][T_{90N}] + [0.00049][(T_{10N})^2 - (T_{90N})^2] + (107)(B) + (60)(B)^2$

where:

CCI = Calculated Cetane Index; D = Density at 15 °C, g/mL determined by Test Methods D1298 or D4052; DN = D - 0.85; B = [e(-3.5)(DN)] – 1; T10 = 10 % recovery temperature, °C, determined by Test Method D86 and corrected to standard barometric pressure; T_{10N} = T10 – 215; T50 = 50 % recovery temperature, °C, determined by Test Method D86 and corrected to standard barometric pressure; T_{50N} = T50 – 260; T90 = 90 % recovery temperature, °C, determined by Test Method D86 and corrected to standard barometric pressure, and T_{90N} = T90 – 310

3.2.8.7. Kinematic viscosity

The kinematic viscosity of the samples was analyzed according to the test method ASTM D445. In this method, the time required for a fixed volume of sample to flow under gravity through the capillary of a calibrated viscometer under a reproducible driving head and at a closely controlled and known temperature is measured. The kinematic viscosity (determined value) is the product of the measured flow time and the viscometer's calibration constant.

3.2.9. Data analysis

All reported data (mean ± standard deviation) represent analyses from triplicate samples unless specified otherwise. One–way ANOVA combined with Tukey's test at a 95 % confidence interval was calculated to compare the means on Statgraphics Centurion 18 software, version 18.1.12.

4. RESULTS AND DISCUSSION

4.1. Composition of feedstock

This project aimed at separating a liquid hydrocarbon feed produced from the pyrolysis of fatty acids into different product streams as a biorefinery strategy. Heavier ends (boiling points > 320 °C) were removed from the feed before it was supplied by the project's industrial partner. Upon receipt of the feed, the first task was to determine its composition; this was done using the GC method outlined in Section 3.2.1.

The compounds present in the feed were identified by their retention times and by comparison to the fragmentation pattern of compounds in the mass spectral library of the National Institute of Standards and Testing (NIST) 2011. Only the compounds with quality matches of 90 and above were selected as the identified compounds. In contrast, peaks with a compound match quality of < 90 % were classified as unidentified. The result is presented in Table 4.1. The feed compounds were divided into chemical groups of *n*-alkanes, alkenes, branched alkanes, cycloalkanes, BTEX, other aromatics, and fatty acids. The carbon number of the compounds ranged from C2 – C19. The feed was composed of mostly *n*-alkanes, which made up about 37 % by mass, followed by fatty acids with 13 % by mass. This was similar to the values given in another study (Asomaning *et al*., 2014). The composition of other compound groups is given in Table 4.1. The unidentified compounds accounted for 32 % by mass of the feed.

Table 4.1: Compound distribution of the feed (by %wt) according to carbon number and chemical groups.

Carbon No.	Alkane	Alkenes	Branched alkanes	Cycloalkanes	Cyclo alkenes	BTEX	Other aromatics	Fatty acids	Unidentified
C2	0 ± 0	0 ± 0	0 ± 0	0 ± 0	0 ± 0	0 ± 0	0 ± 0	0.29 ± 0.12	
C3	0 ± 0	0 ± 0	0 ± 0	0 ± 0	0 ± 0	0 ± 0	0 ± 0	0.25 ± 0.13	
C4	0.87 ± 0.11	0.17 ± 0.02	0 ± 0	0 ± 0	0 ± 0	0 ± 0	0 ± 0	0.32 ± 0.04	
C5	2 ± 0.15	0.57 ± 0.24	0.4 ± 0.06	0.33 ± 0.13	0.22 ± 0.02	0 ± 0	0 ± 0	0.78 ± 0.14	
C6	3.04 ± 0.27	1.38 ± 0.09	0.15 ± 0.05	0.55 ± 0.19	0.38 ± 0.08	0.08 ± 0	0 ± 0	1.46 ± 0.22	
C7	3.49 ± 0.41	1.41 ± 0.07	0.07 ± 0.07	0.81 ± 0.1	0.38 ± 0.01	0.48 ± 0.1	0 ± 0	2.17 ± 0.3	
C8	3.55 ± 0.43	1.45 ± 0.08	0.21 ± 0.05	1.44 ± 0.35	0.59 ± 0.15	0.45 ± 0.11	0.27 ± 0.24	2.21 ± 0.27	
C9	2.91 ± 0.37	1.09 ± 0.12	0.2 ± 0.03	0.43 ± 0.06	0.17 ± 0.05	0 ± 0	1.08 ± 0.36	1.93 ± 0.25	
C10	2.45 ± 0.3	0.88 ± 0.12	0 ± 0	0.43 ± 0.06	0 ± 0	0 ± 0	0.99 ± 0.24	1.73 ± 0.17	
C11	2.37 ± 0.29	0.49 ± 0.08	0.15 ± 0.04	0.49 ± 0.09	0 ± 0	0 ± 0	1.57 ± 0.35	0.88 ± 0.07	
C12	2.16 ± 0.25	0.67 ± 0.13	0 ± 0	0 ± 0	0 ± 0	0 ± 0	0.31 ± 0.05	0.62 ± 0.22	
C13	1.82 ± 0.2	0 ± 0	0 ± 0	0 ± 0	0 ± 0	0 ± 0	0 ± 0	0.32 ± 0.02	
C14	1.77 ± 0.19	0 ± 0	0 ± 0	0.58 ± 0.23	0 ± 0	0 ± 0	0 ± 0	0.25 ± 0.02	
C15	3.35 ± 0.22	0 ± 0	0 ± 0	0 ± 0	0 ± 0	0 ± 0	0 ± 0	0 ± 0	
C16	1.3 ± 0.06	0 ± 0	0 ± 0	0 ± 0	0 ± 0	0 ± 0	0 ± 0	0.3 ± 0.08	
C17	5.55 ± 0.29	1.04 ± 0.04	0 ± 0	0.32 ± 0.04	0 ± 0	0 ± 0	0 ± 0	0 ± 0	
C18	0.3 ± 0.06	0 ± 0	0 ± 0	0 ± 0	0 ± 0	0 ± 0	0 ± 0	0.3 ± 0.11	
C19	0.21 ± 0.07	0 ± 0	0 ± 0	0 ± 0	0 ± 0	0 ± 0	0 ± 0	0 ± 0	
Total	**37.14 ± 3.25**	**9.13 ± 0.66**	**1.18 ± 0.14**	**5.38 ± 0.63**	**1.73 ± 0.17**	**1 ± 0.21**	**4.23 ± 0.79**	**13.81 ± 1.64**	**32.15 ± 4.07**

4.2. Fatty acid extraction and recovery

Having determined the percentage of fatty acids present in the feed, the next step was to extract them. Generally, fatty acids impact undesirable properties in lipid pyrolytic liquid, like high freezing point, high acidity (Kubátová *et al*., 2011). As a result, effort is made to remove the acids present in the lipid pyrolytic liquid. While these acids are unwanted in the use of the pyrolytic liquid as renewable fuels, they are valuable compounds with high industrial importance. Therefore, the aim of this extraction exercise was to separate the fatty acids from the other hydrocarbon compounds in the feed and recover them for further experimental procedures. This was done using 3 M NaOH to carry out a three-stage extraction of the acids. Upon addition of NaOH, a two-phase organic-aqueous mixture was formed, and the organic acid-free hydrocarbon mixture was decanted. The total mass of the hydrocarbon mixture recovered was about 74 %wt, 85 %wt, and 86 %wt of the starting mass for the first, second, and third extraction stages, respectively (Table 4.2). The % loss of the compounds of interest (*n*-pentane and *n*-hexane) for each extraction stage is given in Table 4.2. It was observed that the % loss of these compounds increased with an increasing number of extraction stages.

Table 4.2: Recovery (%) of the hydrocarbon fraction and compounds of interest from the three-stage acid extraction process

Extraction stage	First stage	Second stage	Third stage
% Recovery of hydrocarbons	73.8	84.6	86.4
Cumulative % Recovery hydrocarbons	73.8	62.4	54.1
% Recovery n-pentane	88.1	78.5	63.8
% Loss of n-pentane	11.9	21.5	36.2
% Recovery n-hexane	92.6	85.2	72.4
% Loss of n-hexane	7.4	14.8	27.6

Like the feed, the hydrocarbon fractions were mostly composed of *n*-alkanes (Figure 4.1b), with carbon numbers ranging from C4 – C18 (Figure 4.2a). The base wash was successful in removing the acids from the feed (Figure 4.1a). At the end of the extraction process, there was a complete absence of fatty acids in the recovered hydrocarbon fraction. One of the first extraction stage replicates had a residual acid content of about 1 %wt by mass. This explains the small amount of fatty acids shown in Figure 4.1a for this stage. The residual acids in that replicate could be due to crossover from the aqueous phase during decanting. A different study has also attempted to remove the acids in the liquid product from pyrolysis of triglycerides using base extraction. In the study, the acid content was reduced from 22.5 % in the pyrolytic liquid to 10.1 % after the 3-stage extraction using 1 M NaOH at 25°C (Gandhi *et al*., 2012). Another study used amines; trimethylamine (TMA), and dimethylethanolamine (DMEA) for the extraction of the fatty acids present in lipid pyrolytic liquid. It was reported that both amines were able to reduce the fatty acid content of the lipid pyrolysis liquid from an initial content of 22.36 % to 1.57 % with TMA and an undetectable level with DMEA (Braegelmann *et al*., 2011).

The fatty acids were recovered from the aqueous phase of the base extraction by adding 3 M HCl solution until a final pH of 1 – 1.5 was achieved. The pH range of 1 – 1.5 was chosen to ensure that the re-acidification was complete. The total mass of the recovered fatty acids mixture was 9.5 %wt of the feed. As expected, it was composed of mostly fatty acids accounting for about 70 %wt of the mixture (Figure 4.1b), with C6:0 to C10:0 acids being the most dominant (Figure 4.2b). The mixture also contained about 4 %wt of *n*-alkanes. This impacted the separation of the fatty acid mixtures into its individual compound cuts, as discussed in Section 4.5.

(a)

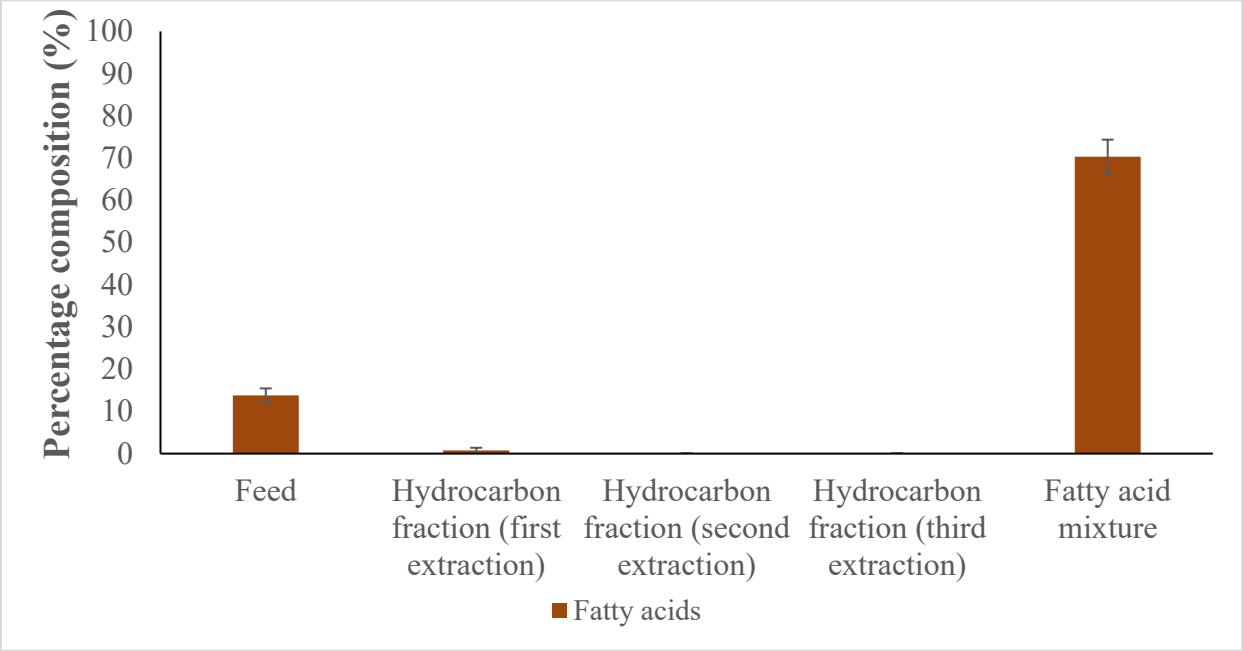

(b)

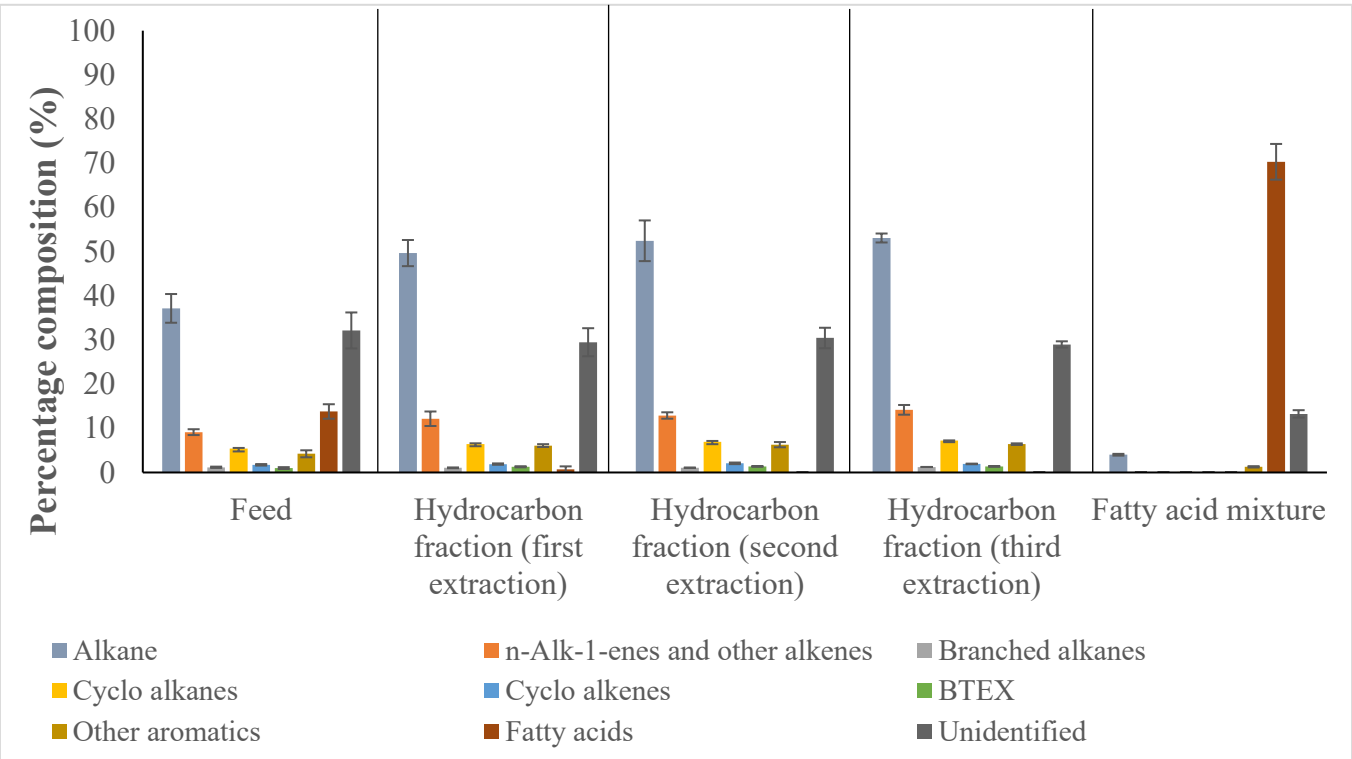

Figure 4.1: Comparison of the compound distribution of the feed, the recovered hydrocarbon fractions from the three-stages of base wash, and the fatty acid fraction. **(a)** shows only fatty acids. **(b)** shows all the identified chemical groups in the mixtures.

(a)

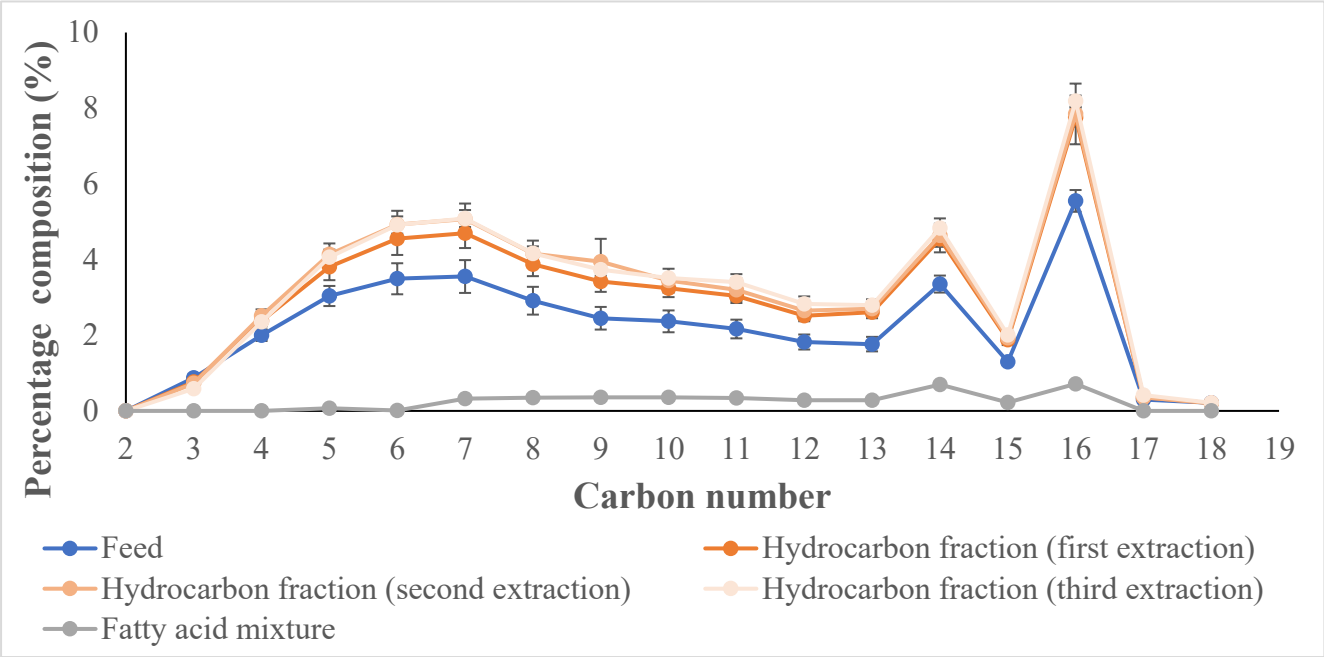

(b)

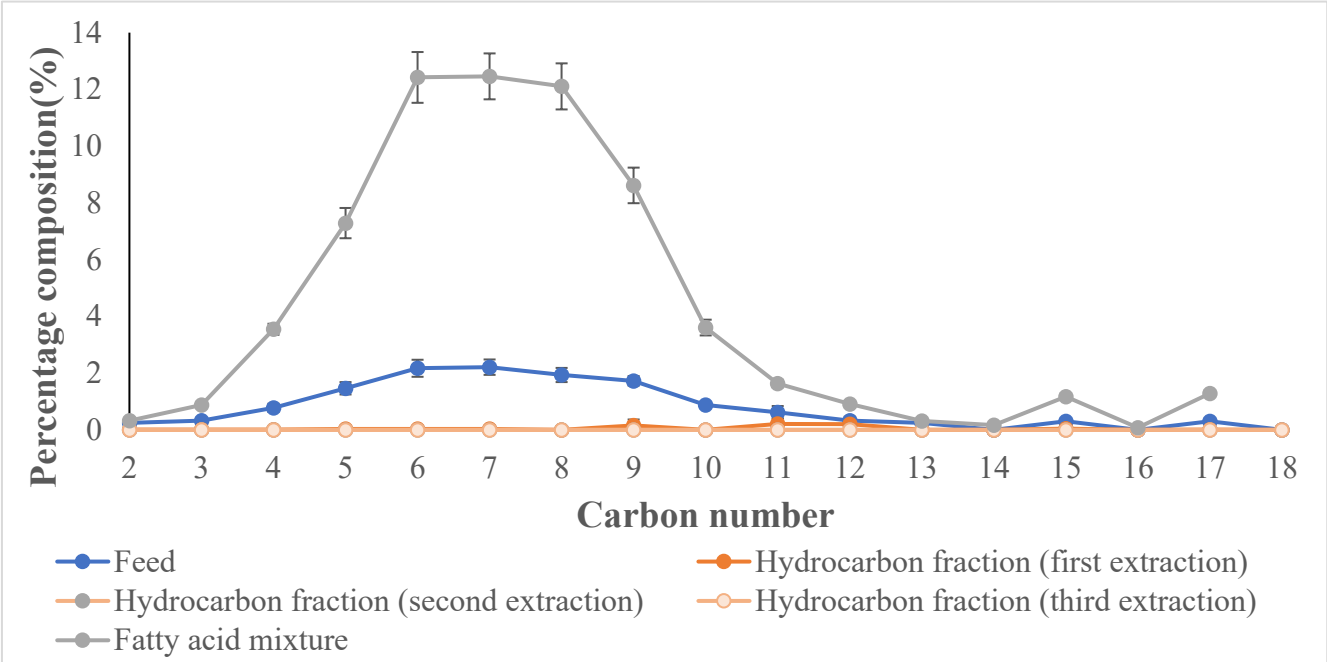

Figure 4.2: *n*-Alkane (**a**) and fatty acids (**b**) chemical groups of the feed, the recovered hydrocarbon fractions from the three-stages of base wash, and the fatty acid fraction as a function of carbon number.

Overall, the composition trend for the *n*-alkane and fatty acid chemical groups were the same for the feed and the recovered fractions (Figure 4.2a and 4.2b). In the *n*-alkane group, there was a steady increase in the percentage of alkanes as the carbon number increased from C3 to C8. A decline in the percentage composition was observed from C8 to C19 except for C15 and C17, where sharp peaks were observed. A similar trend was observed in the fatty acid group with increasing percentage composition from C3:0 to C9:0 followed by a decline in percentage composition from C9:0 to C18:0 except for C16:0 and C18:0 where spikes were observed. The composition trend for the *n*-alkane and fatty acids compounds in hydrocarbon fraction from the three extraction stages mostly mirrored one another.

As a qualitative check, an FTIR analysis was done on the feed and the recovered fraction from the extractions; the spectra are shown in Figure 4.3. The spectra for all mixtures were similar for the most part. The peaks at 1450 cm^{-1} and 2900 cm^{-1} corresponding to C-H scissoring and C-H stretching, respectively, were relatively similar for all mixtures. These indicate the presence of an aliphatic compound in the mixture. However, differences can be observed in the spectra at wavelengths between 1710 – 1720 cm^{-1}, 1415 cm^{-1}, and 1250 - 1270 cm^{-1} corresponding to the C=O stretch, O-H bend, and C-O stretch from the carboxylic acid group, respectively. While these peaks could be noticed in the feed, they are very distinct in the fatty acid mixture but completely absent in the hydrocarbon mixtures from the extraction stages. This further affirms the successful extraction of the fatty acids from the hydrocarbon fraction. A study reported a similar observation for acid extraction from pyrolytic liquid with amines (Braegelmann *et al*., 2011).

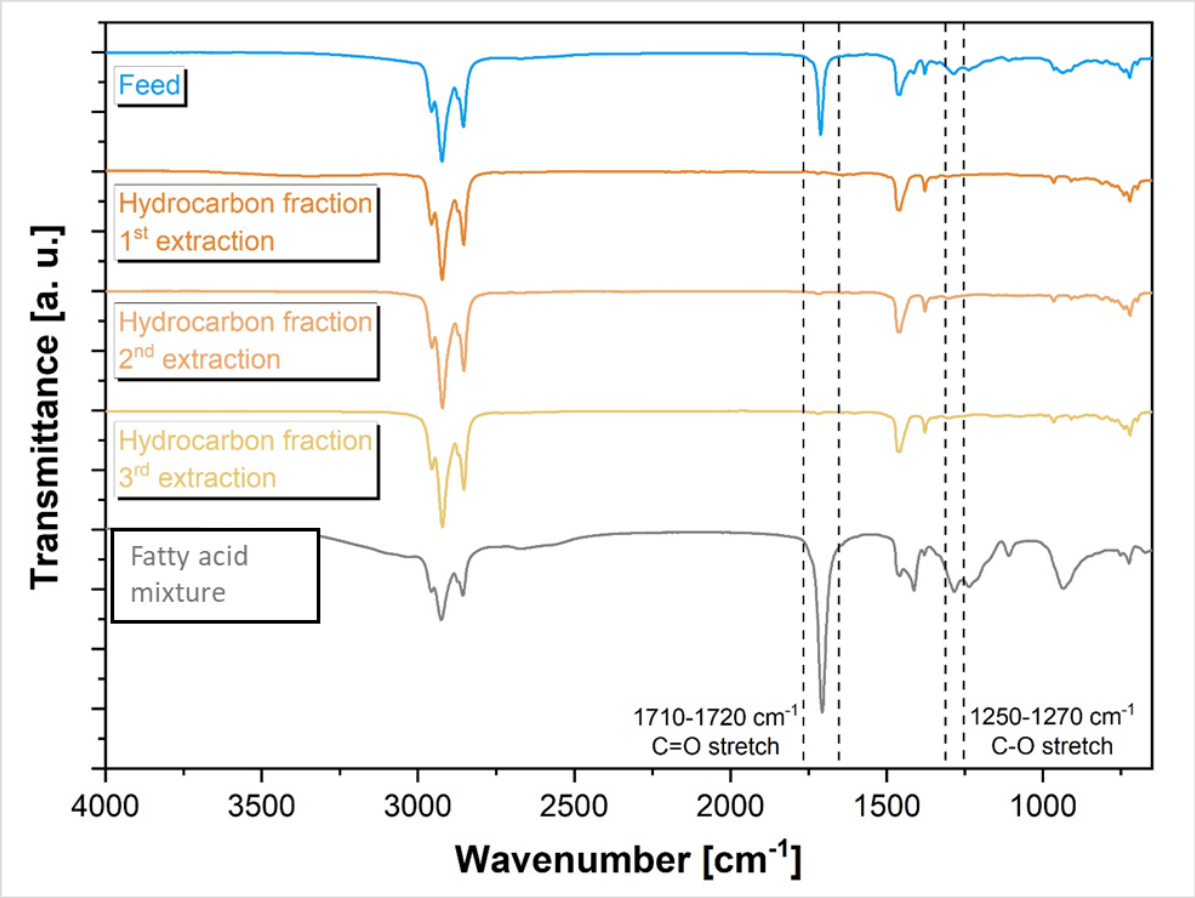

Figure 4.3: FTIR spectrum of the feed, the recovered hydrocarbon fractions from the three-stages of base wash, and the fatty acid fraction.

4.3. Distillation of renewable solvents

After removing the acids from the feed, the next objective was to recover low boiling *n*-alkane solvents and fuel cuts from the de-acidified hydrocarbon fractions. Due to the increasing mass loss observed for the compounds of interest with increasing acid extraction stages (Table 4.2), the distillation of solvents was carried out using the de-acidified hydrocarbon fraction obtained from the first acid extraction stage. The fatty acid profile of this hydrocarbon fraction (Figure 4.2b) also showed that the fatty acid compounds were absent within the vapor temperature range used for the distillation experiments. Therefore, there was no risk of overlapping volatilities and contamination of the solvent distillate by fatty acid compounds.

n-Alkane solvents play an essential role in many industrial/laboratory processes and are mostly petroleum-based. Establishing a renewable source for these organic solvents would be beneficial to these industries from a sustainable standpoint. In particular, the flavor and fragrance industry, have great interest in green (renewable) solvents. The solvents of focus in this work were *n*-pentane and *n*-hexane. Most times, these do not form a part of the petroleum fuel as it is common practice to strip the gasoline pool of compounds from C6 and below before further refining (Eastman & Mears, 2005). These solvents fractions were recovered by distillation using a spinning band column, as discussed in Section 3.2.4.

4.3.1. Determination of the vapor temperature range for the fractions

An initial distillation study was carried out to determine the appropriate vapor temperature cut points necessary to yield the highest purity for the desired solvent fractions (*n*-pentane and *n*-hexane). The hydrocarbon fraction was distilled under atmospheric conditions using a 90 cm Teflon band spinning band distillation unit. The distillates were collected at a reflux ratio of 120:1 between a vapor temperature range of 26.5 – 86.0 °C. The pot and vapor temperature profiles are shown in Figure 4.4. Vapor temperature was constant between 33.0 – 34.0 °C and 65.0 – 66.0 °C labeled A and B in Figure 4.4. From the literature, the boiling points for pure *n*-pentane and *n*-hexane compounds are 36.1 °C and 68.7 °C, respectively (Schmidt *et al*., 2014). Given that the temperature of a system is constant when a compound is boiling off a mixture (Theodore, 2011), it can be concluded that the boiling of these compounds was responsible for the observed constant vapor temperatures.

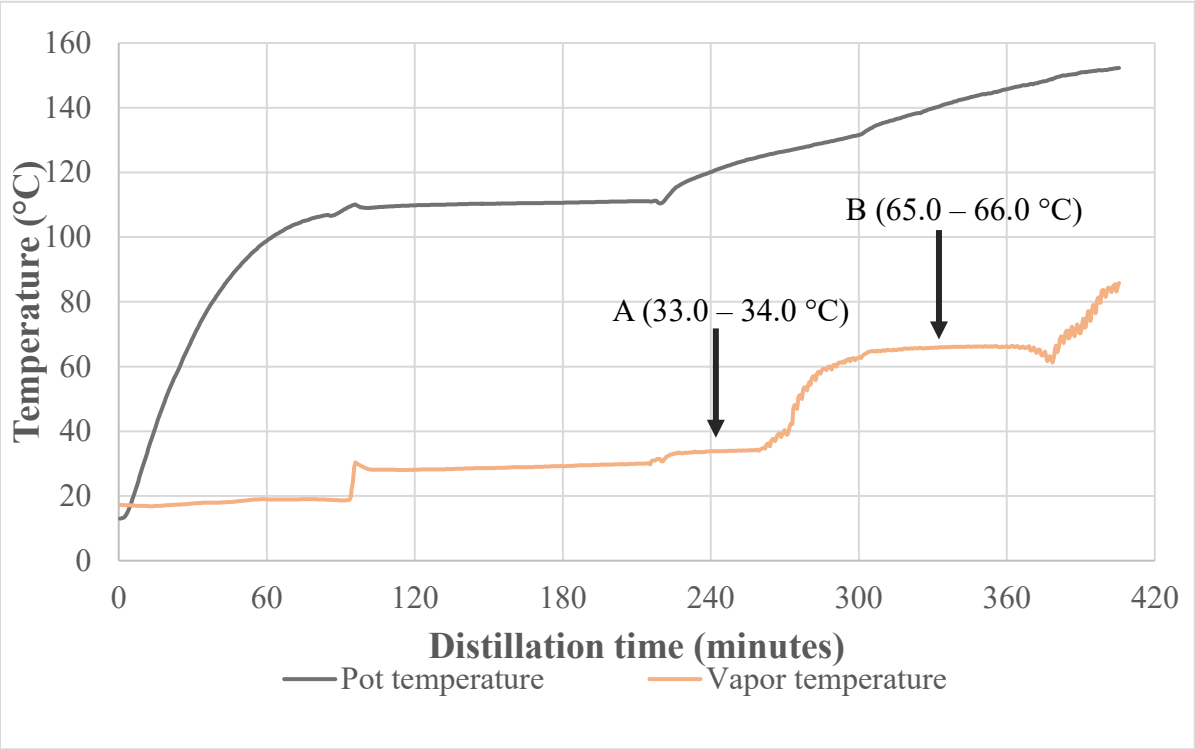

Figure 4.4: Pot and vapor temperature profiles of the atmospheric distillation of the hydrocarbon fraction. Arrows indicate the region of constant vapor temperature.

Eight fractions were collected between the vapor temperature range of 26.5 – 86.0 °C, as indicated in Table 3.3a. The percentage of *n*-pentane and *n*-hexane compounds in each distillate fraction collected was determined upon analysis with GC-FID, and the result is given in Figure 4.5. The second fraction (32.0 – 40.0 °C) was found to contain mostly *n*-pentane, which was about 69 %wt (Figure 4.5a) of the fraction's mass. Likewise, fraction 5 (61.5 – 66.5 °C) contained mostly *n*-hexane, which made up 69 %wt (Figure 4.5b) of the fraction's total mass. The constant vapor temperatures observed in the temperature profiles were found in these fractions; this further validates that the observed constant vapor temperature was due to the *n*-pentane and *n*-hexane solvents' boiling.

Consequently, subsequent distillation experiments were done using the constant vapor temperature range for the *n*-pentane and *n*-hexane fractions. The other fractions' vapor temperature was

adjusted accordingly (Table 3.3b). The parameters of interest were the % purity and % recovery of the solvents. These would be discussed in the following sections.

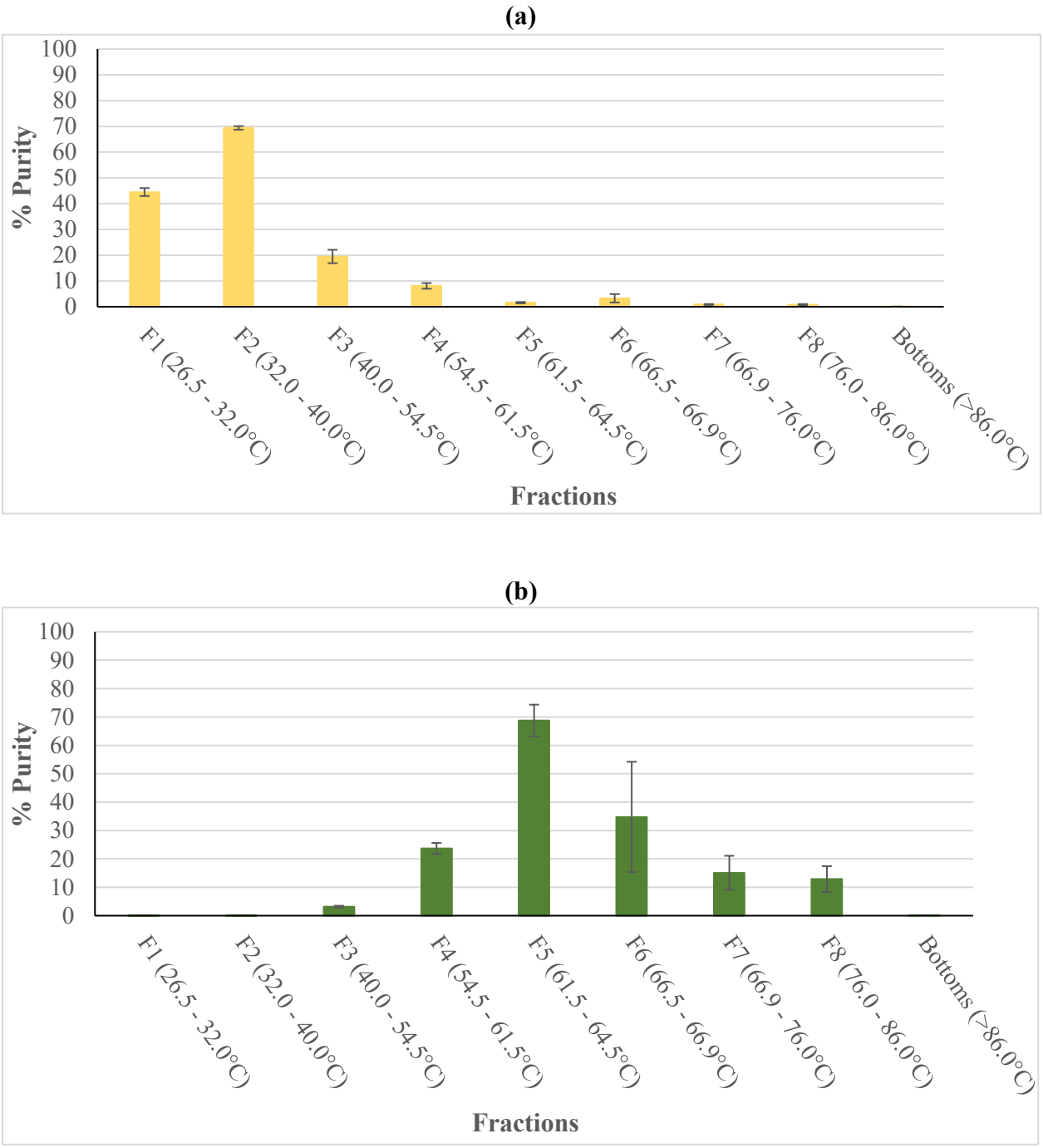

Figure 4.5: Percentage of *n*-pentane (a) and *n*-hexane (b) compounds in the distilled fractions of the hydrocarbon fraction.

4.3.2. Percentage purity of distilled solvents

Having established the vapor temperature cut points for the solvents, different distillation conditions were tested to obtain high purity solvent cuts. The purity of the distilled solvents was calculated as a percentage between the mass of the solvent in its fraction as obtained from the GC-FID analysis and the total mass of sample injected into the GC (Equation 3.4). This would be discussed in the following sections.

4.3.2.1. Effect of starting material

To determine the feedstock suitable to obtain high purity solvent cuts, the distillation experiments were carried out under the conditions described in 3.3.1 using two starting mixtures: the hydrocarbon fraction and a naphtha fraction. The naphtha fraction was obtained by distilling the hydrocarbon fraction using a spinning band distillation unit with a metal band of 45 cm. Equilibration was set for 30 minutes, and the reflux ratio was 30:1. Distillate within the vapor range of 26.5 – 160.0 °C was collected in one receiver as a single fraction. The aim was to reduce the number of compounds in the sample and pre-concentrate the lower boiling compounds in the naphtha sample. This could lead to improved separation of the compounds. The sharpness of separation of a distillation process is influenced by the ratio of the column hold up to the amount of the components present in the mixture (Carney, 1949). Therefore, for a given column with a specific holdup, a sharper separation is observed when there is a higher amount of the compound to be distilled in the mixture. For the same sample volume, the amount of the *n*-pentane and *n*-hexane doubled in the naphtha feedstock (6.5 g and 10.8 g) compared to the hydrocarbon feedstock (3.4 g and 4.9 g), as seen in Table 4.3.

Table 4.3: Comparison of the amount of *n*-pentane and *n*-hexane present in hydrocarbon and naphtha samples.

	Hydrocarbon sample	Naphtha sample
% *n*-pentane in sample	0.035	0.071
% *n*-hexane in sample	0.051	0.118
Volume of sample (ml)	130	130
Mass of sample (g)	98.5	91.5
Amount of *n*-pentane in the sample (g)	3.43	6.46
Amount of *n*-hexane in the sample (g)	4.93	10.83

For both starting samples, there was no difference between the percentage purity of the solvent fractions obtained from the distillation of the hydrocarbon fraction and the naphtha fraction, as seen in Figure 4.6 and 4.7 below. This could be because of a corresponding increase in the mass of the contaminating *n*-alkene compounds (identified in Figure 4.6 and 4.7) alongside the compounds of interest during the initial distillation to obtain the naphtha sample. Other authors have noted that contaminating compounds could be increased alongside the desired compound as distillation rounds increased. In the distillation of plum brandy (Sljivovica), the authors noted that the concentration of methanol, a contaminating compound increased alongside ethanol, the desired compound, as the distillation stages increased from single to double stage (Spaho, 2017).

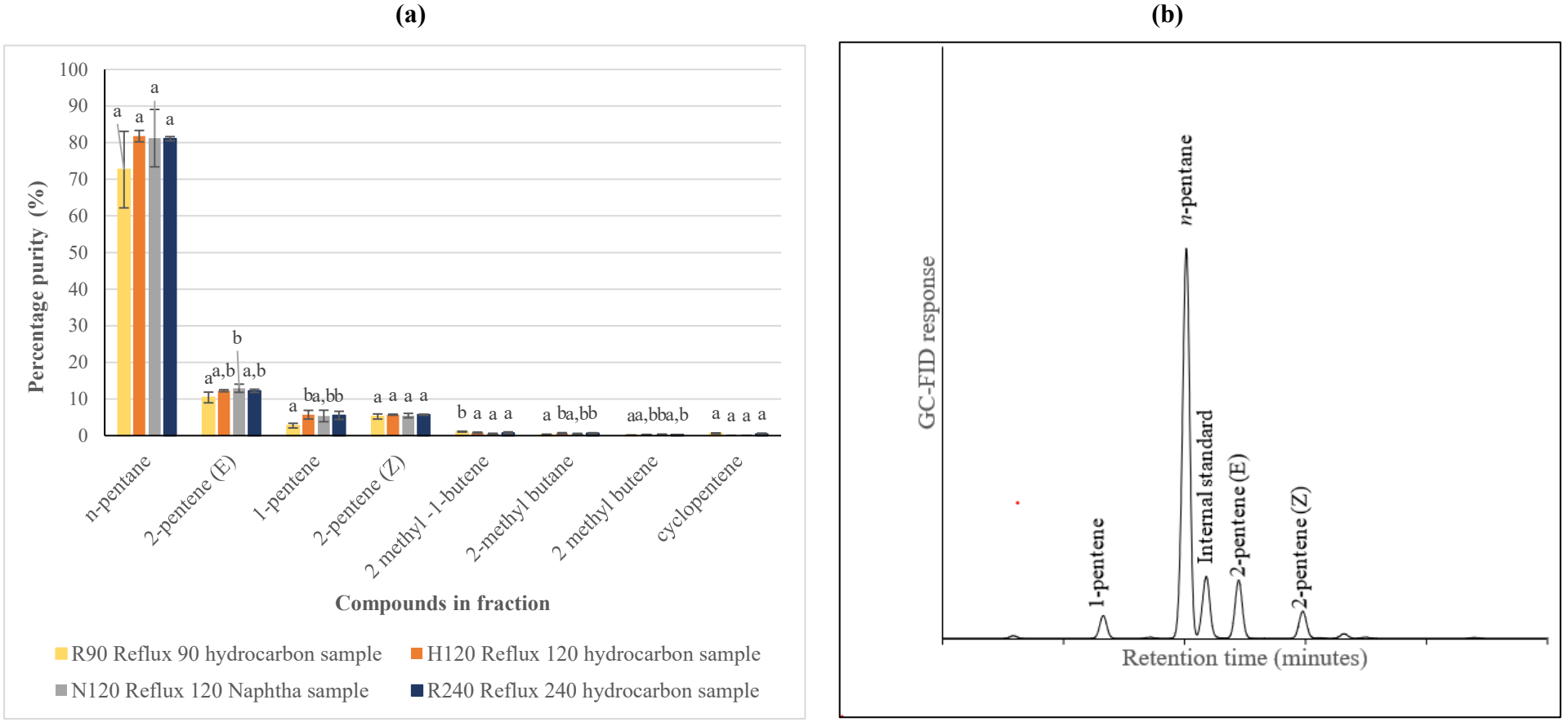

Figure 4.6: Percentage amount of the compounds present in the *n*-pentane fraction (a) from the distillation runs carried out with the hydrocarbon sample at 90:1, 120:1, and 240:1 reflux ratios and the distillation done using the naphtha sample at 120:1 reflux ratio. The GC chromatogram of the *n*-pentane solvent fraction is shown (b). Bars with the same letters are not statistically different at a 95 % confidence interval.

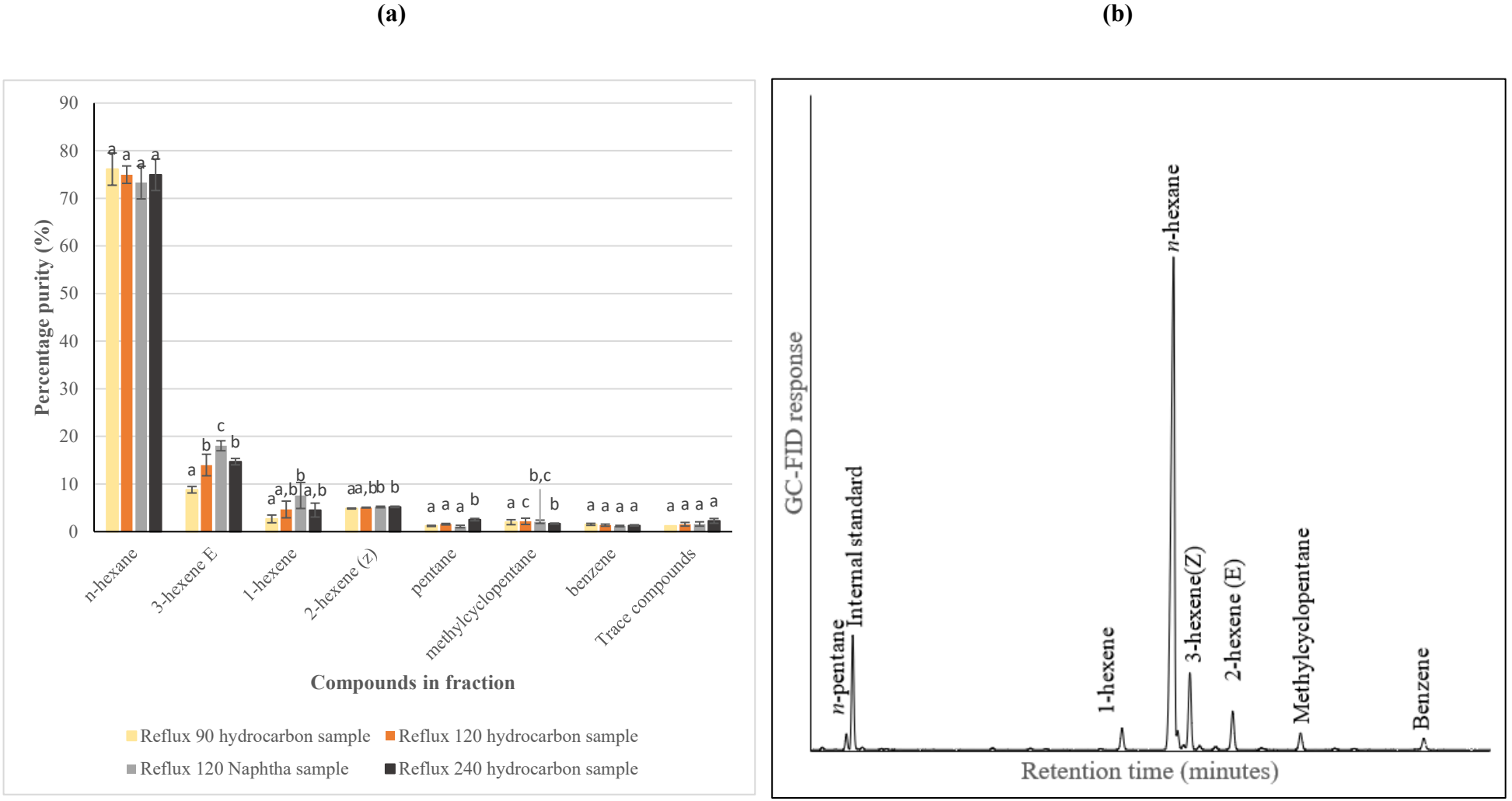

Figure 4.7: Percentage amount of the compounds present in the *n*-hexane fraction (a) from the distillation runs carried out with the hydrocarbon sample at 90:1, 120:1 and 240:1 reflux ratio and the distillation done using the naphtha sample at 120:1 reflux ratio. The GC chromatogram of the *n*-hexane solvent fraction is shown (b). Bars with the same letters are not statistically different at a 95 % confidence interval.

4.3.2.1. Effect of reflux ratio

Having established that the starting feedstock of the distillation experiments did not affect the purity of the solvents obtained, different reflux ratios were explored to determine its effect on solvent purity using the hydrocarbon sample. Reflux ratios of 90:1 and 240:1 were tested. However, there was no statistical difference in the percentage purity of the solvent fractions obtained from the different reflux ratios under the distillation conditions used (Figure 4.6, 4.7, 4.8). An explanation for this observation could be that the reflux ratio's effect on the sharpness of separation is limited in mixtures with low relative volatilities and is more pronounced at lower reflux ratios than higher reflux ratios (Rose & Long, 1941). The percentage purity of solvents at much lower reflux ratios than those explored in this work can be further investigated, as reduced reflux ratio would lead to reduced energy requirement for the distillation process.

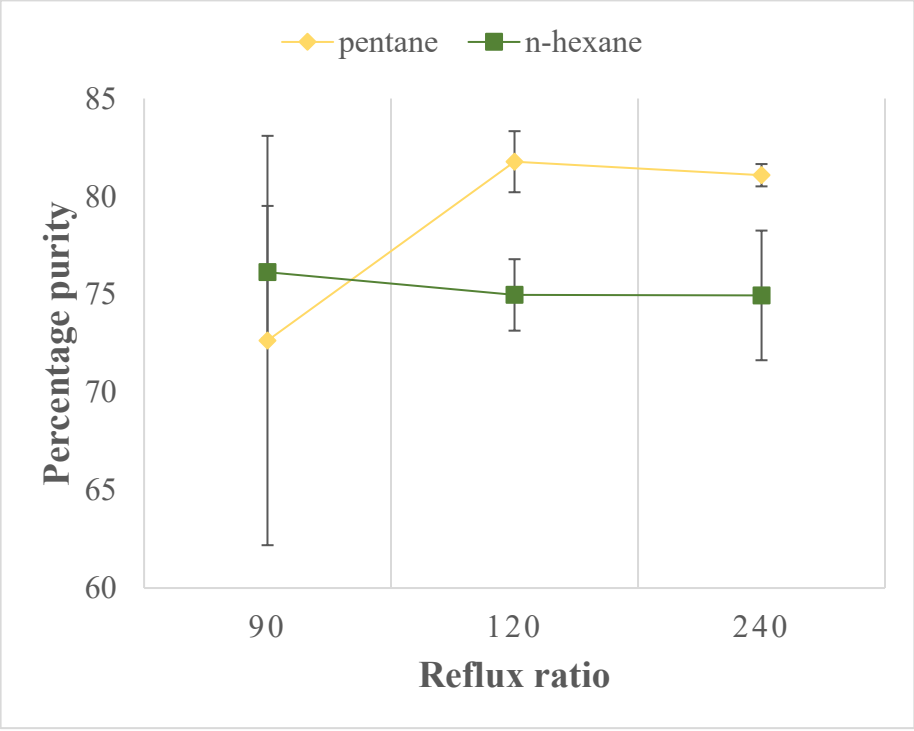

Figure 4.8 Effect of reflux ratio on the percentage purity of *n*-pentane and *n*-hexane compounds obtained from the atmospheric distillation of the hydrocarbon fraction of the feed.

Overall, there was no statistical difference in the percentage purity of the solvent fractions obtained from all distillation runs (Figures 4.6 and 4.7). The significant impurities found in both solvent fractions are shown in Figures 4.6 and 4.7. In the *n*-pentane fraction, the impurities were only C5 compounds of different chemical groups. More impurities were found in the *n*-hexane fraction. These included those shown in Figure 4.7 and other C5 and C6 compounds (Cyclopentene, 3-methyl pentane, Cyclopentane, 2-pentene (E), 2-methyl pentane, 1-pentene, 2-pentene (Z), 2 methyl -1-butene, 2-methyl butane, 2 methyl butene) collectively summed as trace compounds due to their minute amount (<0.5 %wt). A notable impurity in the *n*-hexane fraction was benzene. This could be an indication of the formation of an *n*-hexane-benzene azeotrope. Azeotropes are mixture with constant composition in both the liquid and vapor phases. At such, the recovery of a pure compound from an azeotrope mixture by distillation is practically impossible. The presence of azeotropic compounds increased the difficulty in obtaining pure solvent fractions from the sample.

The percentage purity obtained for the solvent cuts of both *n*-pentane and *n*-hexane compounds was about 70 – 80 % and is lower than the purity of the solvents obtained from the petroleum refining process (up to 99 %). This could be due to the absence of alkene compounds in straight run gasoline mixtures used for distillation of *n*-pentane and *n*-hexane (Jones & Pujadó, 2006; Nolan, 2014). In the solvent cuts obtained from this study, the alkene compounds were observed to be the significant contaminants, accounting for about 15 – 25 %wt of the solvent fractions (Figures 4.6 and 4.7). These compounds are also formed during the pyrolysis process. Separation of the alkane/alkene mixture of low carbon numbers is one of the most challenging separation processes in the chemical industry due to their close relative volatilities (van den Bergh *et al*., 2011; Wang *et al*., 2019). Additional separation methods like adsorption using zeolites or metal-organic frameworks are needed to obtain pure compounds from an alkane/alkene mixture. For

example, the separation of an alkane/alkene mixture of C5 was successfully demonstrated using a combination of metal-organic framework (MIL-96) and zeolites (chabazite) (Maes et al., 2010).

Other works aimed at obtaining *n*-pentane and *n*-hexane solvents from renewable sources yielded results comparable to that presented in this work. A group explored the production of *n*-hexane from cellulose conversion using an Ir-ReOx/SiO2 and HZSM-5 binary catalyst system. A maximum yield of 83 % of *n*-hexane was reported with other branched hexanes, C4, and C5 compounds present as side-product/contaminants (Liu *et al*., 2014). Another group used aqueous phase reforming (APR) to produce alkanes from xylitol with a specific target for *n*-pentane production under different pressure, temperature, and catalyst loading. An *n*-pentane yield of about 89 % was achieved with 2 wt% Ni/HZSM-5 catalyst under reaction conditions of 240 °C and 4 MPa (Jiang *et al*., 2012). When furfural was used as the feedstock in APR for pentane production, a maximum yield of 95.5% was obtained with 14 wt.%Ni/SiO2–Al2O3 at 140 °C and 3 MPa (Xinghua *et al*., 2010).

In general, efforts have been put into obtaining high purity renewable solvents. This is the first work reporting the recovery of *n*-pentane and *n*-hexane solvents and their yield(purity) as a side product from a liquid hydrocarbon stream obtained from the pyrolysis of fatty acids or any other lipid pyrolytic liquids. The several chemical groups formed during lipid pyrolysis adds complexity to the process that could be mitigated by an effective reflux ratio – theoretical plate (column height) combination. The distillation conditions can also be varied to obtain solvents of different compositions as required. This successful demonstration has shown a simple, and effective way of recovering renewable *n*-pentane and *n*-hexane that can be explored during the process of obtaining renewable fuels from other lipid pyrolysis methods.

4.3.3. Percentage recovery of distilled solvents

Another parameter that was investigated was the percentage recovery of the solvents. This was calculated as a percentage between the solvent's mass obtained in each distillate fraction and the solvent's total mass in the sample distilled (Equation 3.5). Of particular interest was the percentage of the *n*-pentane and *n*-hexane solvents recovered in their corresponding fractions. For all distillation experiments, there was no statistical difference in the amount of *n*-pentane and *n*-hexane solvents recovered in their respective fractions (Figure 4.9).

The percentage recovery was between 33 – 43 %wt for *n*-pentane and 21 – 36 %wt for *n*-hexane in their respective fractions. The total recovery of both compounds was lower in the distillation using naphtha sample compared to that carried out using the hydrocarbon sample at the same reflux ratio (Figure 4.9). This can be explained by the cumulative compound loss associated with the distillation run to obtain the naphtha and subsequent distillation run to recover the solvents. Compound loss during distillation is known. Cumulative compound loss was reported when the effect of distillation numbers on the concentration of the volatile compounds in the middle-cut fraction obtained during rakı production was done (Darıcı *et al*., 2019). Figure 4.9 shows that some amounts of *n*-pentane were recovered from all the fractions collected. This further supports the observed *n*-pentane impurity in the *n*-hexane fraction. Overall, the total recovery of *n*-pentane (obtained from all the fractions) was lower due to its higher volatility, leading to more vapor loss than *n*-hexane.

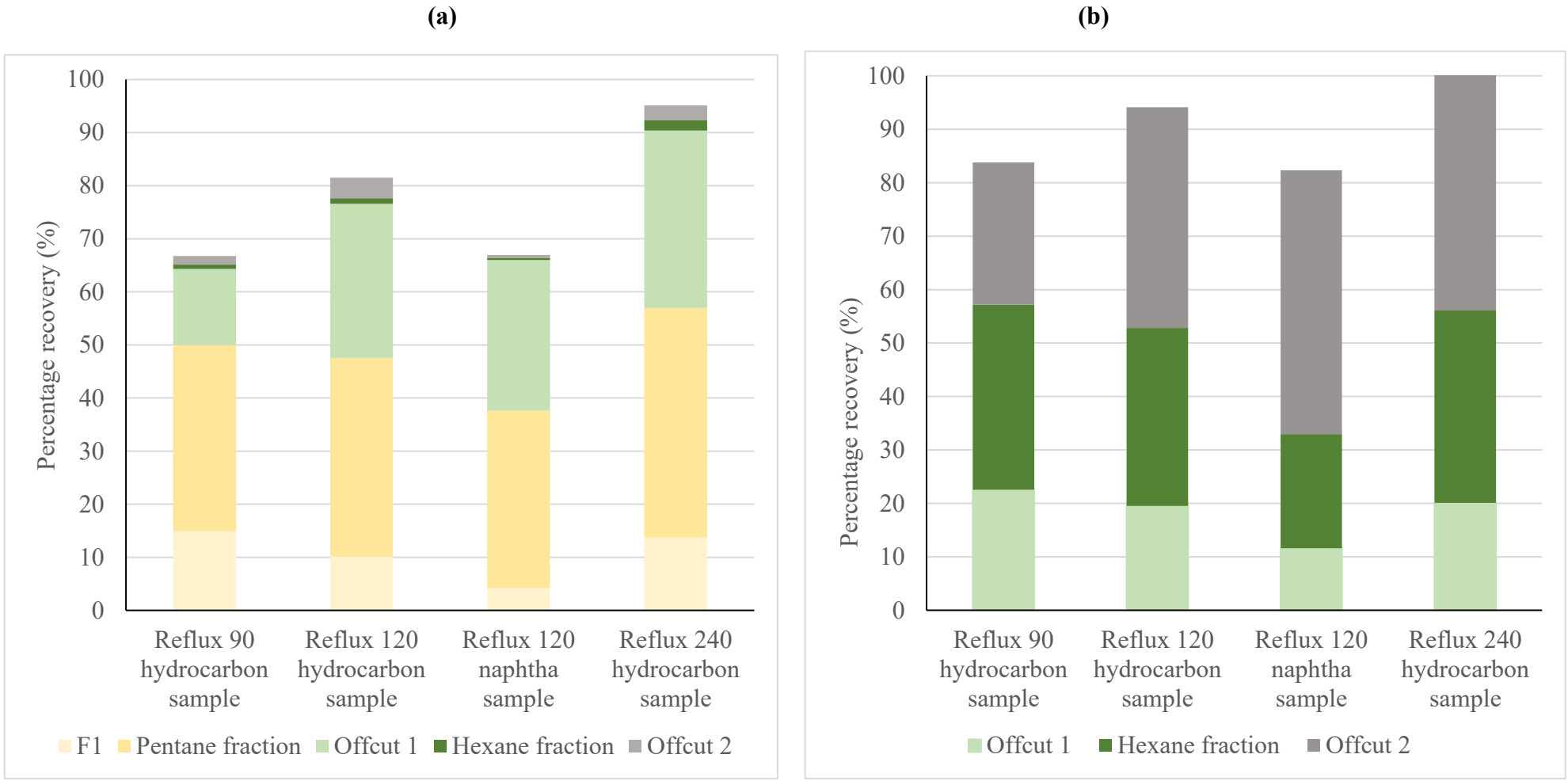

Figure 4.9: Percentage recovery of *n*-pentane (left) and *n*-hexane (right) from the fractions obtained from the distillation runs carried out with the hydrocarbon sample at 120:1 and 240:1 reflux ratio and the distillation done using the naphtha sample at 120:1 reflux ratio.

4.4. Properties of drop-in diesel equivalent cut

The second product stream obtained from the distillation of the hydrocarbon fraction was a drop-in diesel equivalent cut. The fuel properties of this cut are given in Table 4.4. Two vapor temperature start points were used to distill the drop-in diesel equivalent cut: 160.0 °C and 175.0 °C, respectively. This was done to investigate the effect of vapor temperature start point on the drop-in diesel equivalent cut properties and yield. These would be discussed below. The properties of commercial diesel (locally purchased in August 2020 at a gas station in Edmonton), the feed, and the hydrocarbon fraction were also analyzed to determine the effect of fractionation on drop-in diesel equivalent cut properties. These were compared against the Canadian General Standards Board's specification for diesel fuel: CAN/CGSB – 3.517-2020.

Table 4.4: Fuel properties of the drop-in diesel equivalent cuts obtained from the distillation of the hydrocarbon fraction.

Properties	ASTM	Standard requirement (CAN/CGSB-3.517-2020)	Feed	Hydrocarbon fraction	drop-in diesel equivalent (CP:160°C)	drop-in diesel equivalent (CP:175°C)	Commercial diesel
Density (g/ml)	D5002	Not specified	0.79	0.77	0.81	0.82	0.85
Acid number (mg KOH/g)	D974	0.10 (Max)	90.0 ± 3.80	0.02 ± 0.02	0.05 ± 0.02	0.06 ± 0.02	0.03 ± 0.02
Flashpoint (°C)	D7236	40 °C (Min)	-	< 25	72	81	64
Distillation (90% R, °C)	D7345	290.0 – 360.0 °C (Max)	268.9	274.3	286.3	287.4	301.0
cloud point (°C)	D2500	Not specified	-24	-24	-13	-11	-22
Pour point (°C)	D93	Not specified	<-24	<-24	-15	-15	<-24
cetane index	D4737	40.0 (min)	47.6	55.6	56.5	54.6	43.4
Kinematic Viscosity (mm^2/s)	D445	1.3 – 3.6	1.2	1.1	2.0	2.2	2.4

4.4.1. Acid number

The acid number is a vital fuel property that plays a role in the fuel's corrosiveness and cold flow properties (Xu *et al*., 2010). As such, it has very low tolerable limits in fuels (Table 4.4). The fatty acids present in the feed were removed using base extraction. This method successfully removed the acids in the sample. However, the hydrocarbon fraction used for the distillation of the renewable fuels was obtained as the product of the first acid extraction step. This sample had a very small amount of acids present (0.7 %wt), so the fuels obtained from the hydrocarbon fraction had a very low acid number (0.05 and 0.06 mg/KOH). The acid values for the drop-in diesel equivalent cuts were within the CGSB fuels' specification (maximum of 0.1 mg/KOH). Different methods have been studied for the reduction of the acid content of traditional pyrolytic liquids. The use of catalysts during pyrolytic reactions to increase deoxygenation, which would reduce the acid content of the obtainable renewable fuel is widespread in the literature (da Mota *et al*., 2014; Liu *et al*., 2017; Nam *et al*., 2017; Santillan-Jimenez *et al*., 2013). Esterification has also been attempted to reduce the acid content of renewable fuels obtained from the pyrolytic liquid. In a study of the catalytic cracking of soyabean oil using potassium carbonate, the acid number of the distilled diesel fraction was reported to be 36.9 mgKOH/g. This was reduced to 3.2 mgKOH/g upon esterification with methanol (Xu *et al*., 2010). The diesel fraction obtained from the catalytic pyrolysis of acidic waste oil using CaO was reported to have an acid number of 1.95 mgKOH/g; this value was reduced to 0.1 mgKOH/g by washing with 0.375 mol/L NaOH (Long *et al*., 2019). This further demonstrates the capability of base extraction in reducing the acid number of lipid pyrolytic liquid to meet standard requirements.

4.4.2. Other fuel properties

Table 4.4 shows that the values for the flashpoint, cetane number, viscosity, distillation range, and density of the drop-in diesel equivalent cut were comparable to the commercial diesel analyzed and were within the CGSB standard specification. Generally, the renewable fuels' values were mostly higher than those of the feed and hydrocarbon fraction. This is due to removing the acids and lighter boiling compounds from the fuel samples during the distillation process. These compounds are responsible for the low viscosities and boiling points observed in the initial sample. As a result of the change in the sample's chemical composition, these properties are altered (Lima *et al*., 2004; Santos *et al*., 2010). The removal of the volatile compounds from the fuel sample has an opposite effect on the fuels' cold flow properties, as indicated by the cloud point and the pour point. These properties' values were lower in the renewable fuels (pour point: -15 °C) compared to the feed and the hydrocarbon fraction (-24 °C).

Different authors have reported fuel properties values comparable to those in Table 4.4. In one study, the flashpoint and viscosity properties of the distilled bio-diesel fraction of the pyrolytic liquid from animal fat were 71 °C and 1.99 mm^2/s, respectively (Weber *et al*., 2012). Another study reported the densities of the diesel fraction gotten from the pyrolysis of soyabean oil, palm oil, and castor oil, which were reported as 0.84, 0.82, and 0.88 g/ml, respectively (Lima *et al*., 2004). The diesel fraction obtained from beef tallow pyrolytic oil distillation was stated to have a density of 0.82 g/ml and a cetane index of 63.03 (Santos *et al*., 2010).

Generally, the acid-base extraction and distillation methods improved the renewable fuels' properties obtained from the hydrocarbon fraction of the feed. They can be used as a strategy for upgrading the renewable fuel properties to meet the required standards.

4.5. Fractionation of fatty acids fractions

The fatty acid mixture recovered from the acid-base extraction of the feed was distilled to obtain individual acid compound cuts. This was carried out by vacuum distillation at 133.3 Pa using a B/R spinning band distillation unit with a Teflon band of length of 90 cm spinning at 5000 rpm, and the distillate was collected reflux ratio of 60:1 between the vapor temperature range of 26.5 – 121.0 °C. Boiling was observed as soon as the vacuum (133.3 Pa) was applied to the system (atmospheric equivalent of pot temperature at ambient condition was about 175 °C), and some liquid was seen in the ice trap (filled with dry ice). The liquid in the ice trap was analyzed to determine its composition and was found to consist of *n*-alkanes between C8 and C13, 2-methyl phenol, and some amounts of fatty acid compounds (between C3:0 and C8:0). Fatty acids of carbon numbers between C5:0 to C11:0 were the most abundant in the mixture (Figure 4.2); as such, they were the target compounds for recovery. It was also observed that the fatty acid compounds boiled off at a higher atmospheric equivalent temperature than those in the literature (Anneken *et al*., 2006), as seen from the vapor temperature range for the acid cuts given in Table 3.5. Bouts of explosive boiling/bumping, as described in another work (Murray, 1955) was noticed throughout the distillation run. C11:0 fraction was not collected because the distillation runs were done up to a maximum pot temperature of 225 °C under a vacuum of 133.3 Pa. This limit was set to prevent the decomposition of the fatty acids, which has been reported to start from 200 °C (Potts & White, 1953).

A total of thirteen fractions were collected between the set vapor temperature range used for the distillation. The first fraction (F1) contained compounds in the fatty acid mixture that distilled before C5:0 fatty acid. The next six fractions (F2 – F7) contained the target fatty acid compounds (C5:0 - C10:0), as shown in Table 3.5. Five offcut fractions were collected when the vapor

temperature dropped between corresponding fatty acids fractions (an offcut is illustrated in Figure 4.10). The last fraction was (F8) was collected when boil-up was observed towards the end of the distillation run. It was also observed that the coolant temperature influenced the cut collection during the distillation run. Lower coolant temperatures caused freezing of the fatty acid around the instrument's drip tip, disrupting the compound collection. In contrast, higher coolant temperatures could not condense the distillate vapor, causing it to escape to the ice trap where it was collected. To address this, a temperature program was created for the coolant, which was varied between -2 to 15 °C depending on the fraction (fatty acid) being collected. Lower coolant temperatures were used when shorter chain length fatty acids were distilled, and the coolant temperature was gradually increased as the chain length of the fatty acid increased.

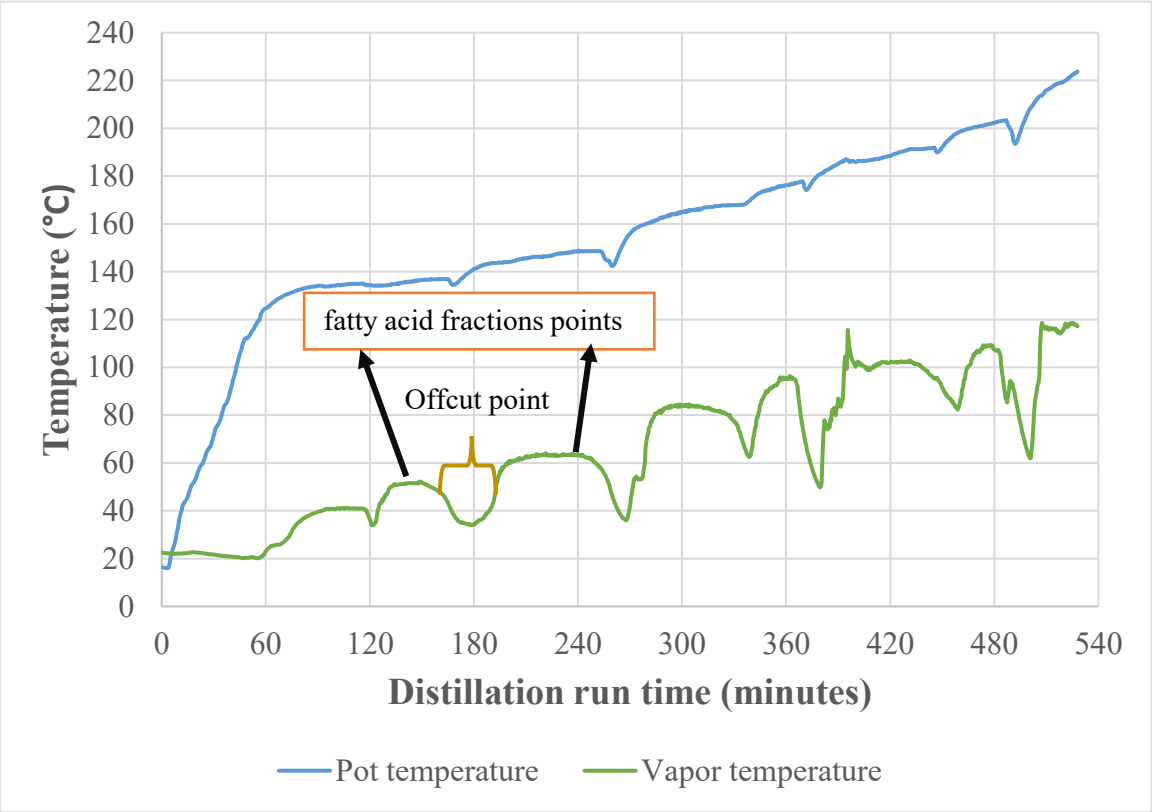

Figure 4.10: Pot and vapor temperature profiles of the fatty acid distillation done under a vacuum of 133.3 Pa.

4.5.1. Percentage purity of the fatty acid fractions

The percentage purity of the fatty acid cuts obtained is shown in Figure 4.11. The fractionated acids' purity was above 60 % for all the fatty acid cuts, with the highest purity obtained for C8:0 at 96 %. In a different study, Cuphea oil was fractionated to obtain C8:0 and C10:0 fractions using a falling film molecular distillation. The maximum percentage purity reported was 98.9 % (Cermak *et al*., 2007). Traditionally, coconut oil and palm kernel oil are the primary sources of short and medium-chain fatty acids. These can be fractionated to obtain very high purity cuts (about 99 %) for specific functions (Gervajio *et al*., 2005).

It is worthy of mention that the fatty acid mixture fractionated in this study contains both odd and even-numbered fatty acids, increasing the complexity of the separation process. Also, from the fatty acid mixture's characterization and as highlighted in Section 4.2 (Figure 4.1), some other compounds produced during the pyrolysis reaction were present in the mixture as impurities, notably *n*-alkanes. This negatively impacted the purity of the fatty acid cuts, given the overlapping volatilities of *n*-alkane compounds and the fatty acid compounds, making their separation by distillation difficult. The major contaminants were the unsaturated fatty acid of the respective carbon number and higher *n*-alkanes (Table 4.5). To obtain a higher purity of the fatty acid cuts, it would be beneficial to have an effective means to completely remove the non-acidic (*n*-alkane) compounds in the fatty acid mixture.

To the author's knowledge, this is the first work reporting the fractionation of a fatty acid mixture obtained as an extractant from pyrolysis of fatty acids (or triglycerides) into individual compound cuts as co-product streams. Given that fatty acids are unwanted in the renewable fuel product obtained from lipid pyrolysis, the extraction and valorization process of the fatty acids demonstrated in this work presents a significant opportunity to upgrade the renewable fuel and improve the feasibility of different lipid pyrolysis technology as the mid-chain fatty acids have high commercial value and broad applicability.

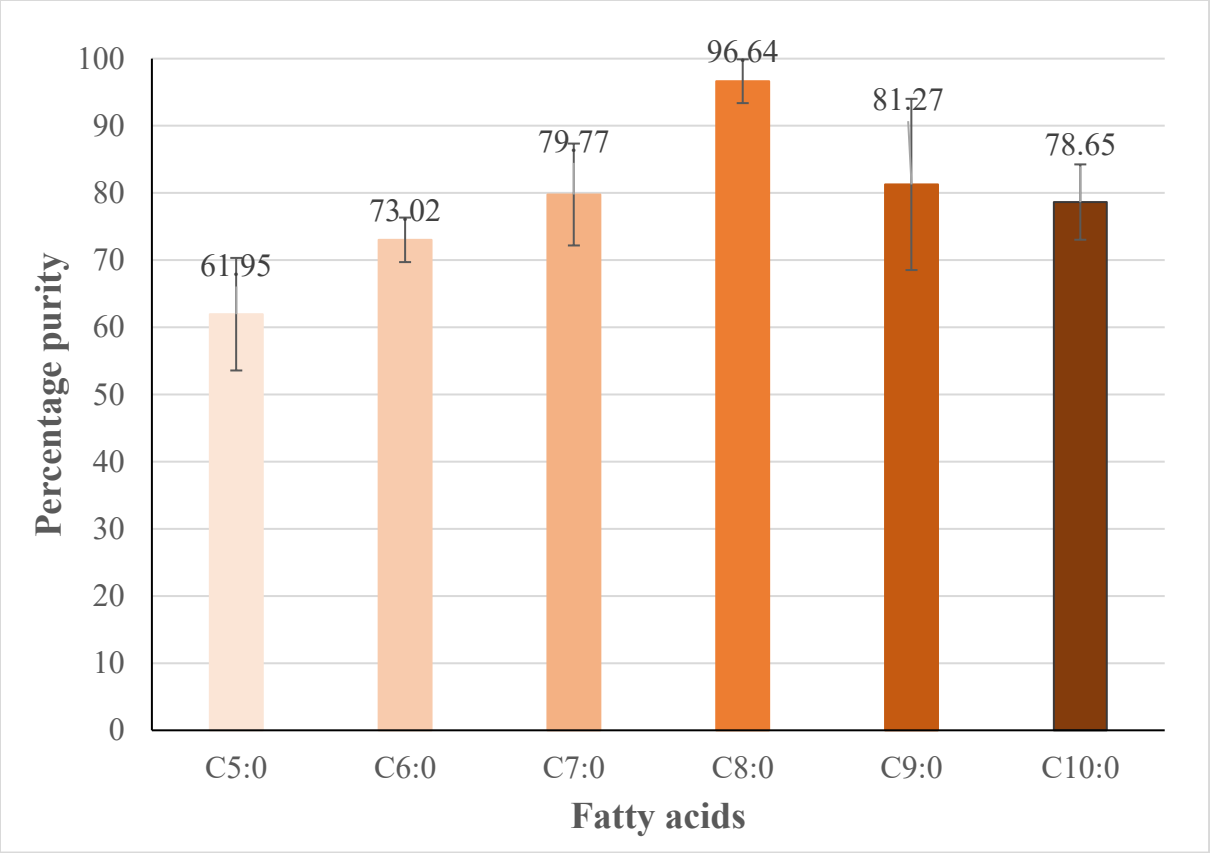

Figure 4.11: Percentage purity of the fatty acid fractions obtained from the vacuum distillation of the fatty acid mixture at 133.3 Pa.

Table 4.5: Major compounds present in the acid fractions obtained from the vacuum distillation of the fatty acid mixture at 133.3 Pa.

Fraction	Compound	Percentage (%)
C5:0 (F2)	Pentanoic acid	61.95 ± 8.38
	Phenol, 2-methyl-	5.09 ± 0.21
	Dodecane	2.54 ± 0.65
	Tridecane	2.33 ± 0.72
	4-Pentenoic acid	1.69 ± 0.26
	Unidentified 1	1.13 ± 0.04
	Total trace compounds	16.39 ± 3.73
C6:0 (F3)	Hexanoic acid	73.02 ± 3.32
	5-Hexenoic acid	3.72 ± 0.47
	Tetradecane	1.66 ± 0.42
	Pentanoic acid	1.32 ± 1.4
	4-Hexenoic acid	0.83 ± 0.26
	Total trace compounds	11.86 ± 2.71
C7:0 (F4)	Heptanoic acid	79.77 ± 7.59
	Pentadecane	2.58 ± 0.45
	Unidentified 2	2.17 ± 0.29
	Octanoic acid	1.4 ± 0.42
	5-Heptenoic acid	1.34 ± 0.18
	Total trace compounds	12.4 ± 1.75
C8:0 (F5)	Octanoic acid	96.64 ± 3.26
	unidentified 3	5.07 ± 0.29
	Heptanoic acid	1.62 ± 0.75
	Benzoic acid	0.93 ± 0.07
	Total trace compounds	10.06 ± 1.49
C9:0 (F6)	Nonanoic acid	81.27 ± 12.75
	Octanoic acid	11.89 ± 16.15
	unidentified 4	3.65 ± 0.52
	Heptadecane	1.53 ± 0.67
	7-Nonenoic acid	1.11 ± 0.33
	Decanoic acid	0.83 ± 0.98
	Total trace compounds	10.13 ± 2.36
C10:0 (F7)	Decanoic acid	78.65 ± 5.61
	unidentified 5	4.9 ± 0.34
	Heptadecane	4.18 ± 0.69
	Nonanoic acid	3.6 ± 1.63
	unidentified 6	1.29 ± 0.11
	unidentified 7	1.07 ± 0.17
	Total trace compounds	10.22 ± 0.77

4.5.2. Percentage recovery of the fatty acid fraction

The percentage recovery of the fatty fractions is shown in Figure 4.12. Offcuts were collected between consecutive fatty acid fractions as indicated to increase the purity of the fatty acids obtained. For all the fatty acids separated, recovery was split between the fatty acid fraction and the offcuts before and after it. Most of the fatty acids were recovered in the appropriate fraction. The percentage recovery for all fatty acids except C10:0 in their respective fractions was between 60 – 85 %wt, with the highest recovery observed for the C7:0 and C9:0 fatty acids. The recovery of C10:0 fatty acid in its fraction was the lowest at about 30 %wt. The C10:0 fatty acid froze at the distillation instrument's drip tip due to a low condenser temperature during the distillation runs. Also, no offcut fraction was collected for the C10:0 fatty acid due to the same reason. As a result, a portion of the C10:0 acid was collected as an additional fraction (F8) at a higher vapor temperature range when the condenser was warm enough for the acid to flow.

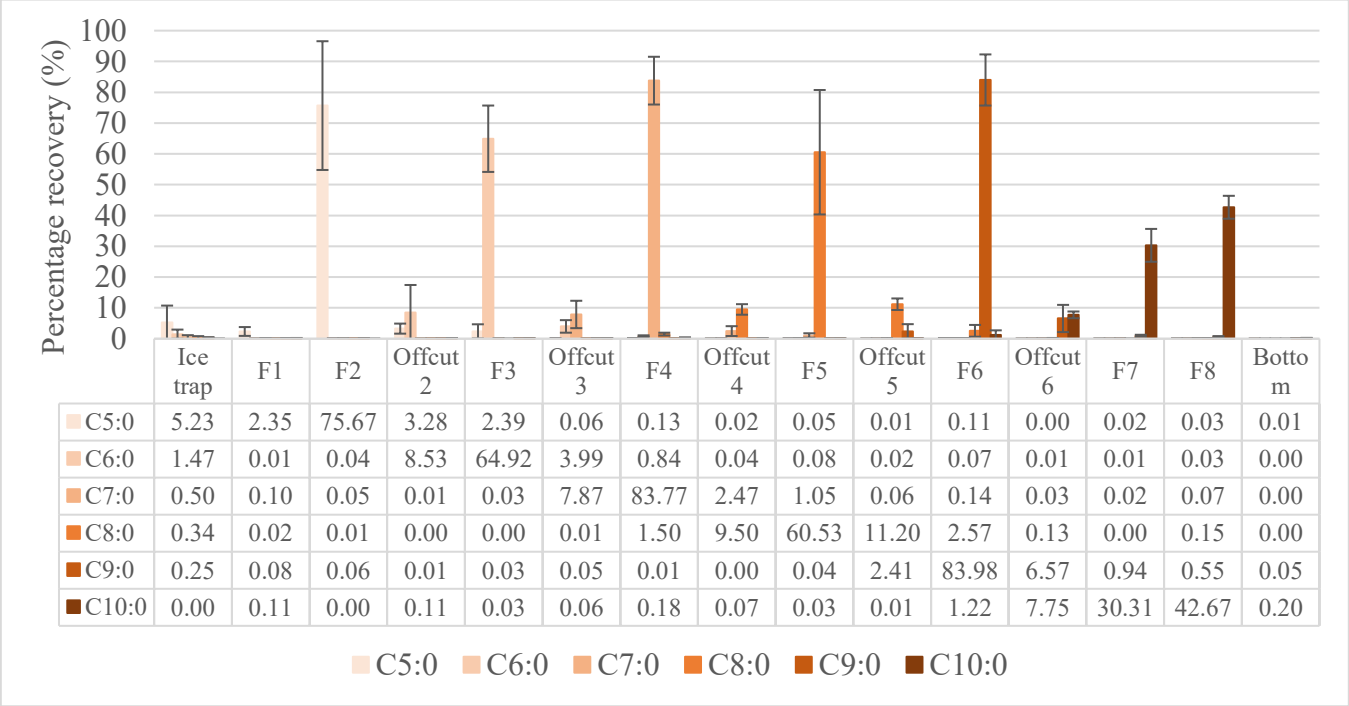

	Ice trap	F1	F2	Offcut 2	F3	Offcut 3	F4	Offcut 4	F5	Offcut 5	F6	Offcut 6	F7	F8	Bottom
C5:0	5.23	2.35	75.67	3.28	2.39	0.06	0.13	0.02	0.05	0.01	0.11	0.00	0.02	0.03	0.01
C6:0	1.47	0.01	0.04	8.53	64.92	3.99	0.84	0.04	0.08	0.02	0.07	0.01	0.01	0.03	0.00
C7:0	0.50	0.10	0.05	0.01	0.03	7.87	83.77	2.47	1.05	0.06	0.14	0.03	0.02	0.07	0.00
C8:0	0.34	0.02	0.01	0.00	0.00	0.01	1.50	9.50	60.53	11.20	2.57	0.13	0.00	0.15	0.00
C9:0	0.25	0.08	0.06	0.01	0.03	0.05	0.01	0.00	0.04	2.41	83.98	6.57	0.94	0.55	0.05
C10:0	0.00	0.11	0.00	0.11	0.03	0.06	0.18	0.07	0.03	0.01	1.22	7.75	30.31	42.67	0.20

Figure 4.12: Percentage recovery of fatty acid compounds in the fractions collected during the vacuum distillation of the fatty acid mixture at 133.3 Pa.

5. CONCLUSIONS

Lipid pyrolytic liquids obtained using either triglyceride or fatty acid feedstock can be a renewable source of fuels and chemicals obtained from petroleum. Like petroleum, it is a complex mixture. To maximize its use, it must be fractionated into different streams that can be further processed to finished products with large commercial applications, thereby establishing the lipid pyrolytic process as a biorefinery. This study explored two fractionation processes to create multiple product streams from the liquid hydrocarbon feed of a fatty acid pyrolysis process.

The first fractionation process was acid-base extraction, using NaOH to remove the fatty acid compounds in the feed through a three-stage extraction process and HCl to recover the extracted fatty acids, creating a hydrocarbon and fatty acid stream from the feed. The acid-base extraction successfully removed the acids present in the feed. The next fractionation process employed was distillation.

Atmospheric distillation was used to obtain renewable solvents (*n*-pentane and *n*-hexane), and fuel cuts from the hydrocarbon fraction and naphtha cut obtained the hydrocarbon fraction. Reflux ratios between 90:1 to 240:1 were used. This study showed that neither feedstock nor reflux ratio influenced the percentage purity and recovery of the solvents under the conditions tested in this study. *n*-Pentane solvent was obtained with a 75 – 85 % purity, and recovery was between 33 – 43 %wt. *n*-Hexane solvent was also fractionated with a purity of 70 – 75 % and recovery of 21 – 36 %wt. This is the first study to report the recovery of *n*-pentane and *n*-hexane solvents from any lipid pyrolysis process, creating another product stream with wide applications. The fuel cuts (drop-in diesel equivalent) obtained from the hydrocarbon fraction were also analyzed to determine their conformity to Canadian fuels specification. Two vapor temperature start points

(160 °C and 175 °C) were tested. As expected, the acid number of the drop-in diesel equivalent cut was below the maximum limit specified. Other fuel properties such as the kinematic viscosity, density, flashpoint, distillation range, and cetane index were within specifications. However, the cold flow properties (cloud point and pour point) of the drop-in diesel equivalent cuts did not meet the Canadian fuel specifications.

For the fatty acid fraction, vacuum distillation at 133.3 Pa was used to separate the mixture into individual compound cuts. C5:0 to C10:0 fatty acid cuts were obtained during the distillation experiment. The percentage purity for all the fatty acid fractions was above 60 %, with C8:0 having the highest purity of 96 %. Percentage recovery was also above 60 %wt for all except C10:0 fractions with percentage recovery of 30 %wt. Like the renewable solvents' recovery, this work is the first to report the fractionation of a fatty acid mixture extracted from any lipid pyrolysis process.

The commercial value and applications of the and mid-chain fatty acids make this recovery process an attractive addition to the traditional lipid pyrolysis process for renewable fuel production, highlighting the valorization of unwanted fatty acids in the lipid pyrolytic liquid. It is also a promising alternative to conventional means of producing fatty acids as both odd and even-numbered fatty acid compounds can be obtained from the liquid pyrolytic liquid compared to natural oils like coconut oil and palm that only contain even numbered fatty acid compounds.

To sum it up, the findings of this work have proven the biorefinery concept and established the viability of fractionating a liquid hydrocarbon stream obtained from the pyrolysis of fatty acids into several product streams. This is of significant economic benefits for other lipid pyrolytic

processes as renewable solvents are highly sought-after industrial products and fatty acids are high-value commodities worth more than fuels on a mass basis. It has also demonstrated the ability to maximize the lipid biomass, especially in the current carbon-constrained world.

5.1. Recommendations

This work has set the stage for subsequent studies to explore the recovery of renewable solvents and fatty acid cuts from traditional lipid pyrolytic liquid obtained from fatty acid or triglyceride feedstock. Some recommendations for future work would be to:

1. Explore adsorption using zeolites or metal organic frameworks to separate the alkene compounds and increase the purity of the solvent cuts.
2. Study the effect of lower reflux ratios on the percentage purity of the renewable solvent cuts.
3. Investigate esterification and solid-phase extraction to increase the purity of the fatty acid cuts.
4. Study the effect of reflux ratio and heating rate on the purity of fatty acid cuts.
5. Evaluate the performance of the solvents and fatty acid cuts in industrial use.

BIBLIOGRAPHY

Adebanjo, A. O., Dalai, A. K., & Bakhshi, N. N. (2005). Production of diesel-like fuel and other value-added chemicals from pyrolysis of animal fat. *Energy & Fuels, 19*(4), 1735-1741.

Alcantara, R., Amores, J., Canoira, L., Fidalgo, E., Franco, M. J., & Navarro, A. (2000). Catalytic production of biodiesel from soy-bean oil, used frying oil and tallow. *Biomass and Biomass energy, 18(6):515-527* doi:https://doi.org/10.1016/S0961-9534(00)00014-3

Alzagameem, A., El Khaldi-Hansen, B., Kamm, B., & Schulze, M. (2018). Lignocellulosic biomass for energy, biofuels, biomaterials, and chemicals. In S. Vaz Jr. (Ed.), *Biomass and green chemistry: Building a renewable pathway* (pp. 95-132). Cham: Springer International Publishing. doi:10.1007/978-3-319-66736-2_5

Anneken, D.J., Both, S., Christoph, R., Fieg, G., Steinberner, U. and Westfechtel, A. (2006). Fatty Acids. *Ullmann's Encyclopedia of Industrial Chemistry, (Ed.)* doi:10.1002/14356007.a10_245.pub2

Asomaning, J. (2014). Thermal cracking of lipids to produce renewable fuels and platform chemicals doi:10.7939/r3v68q Retrieved from https://search.datacite.org/works/10.7939/r3v68q

Asomaning, J., Mussone, P., & Bressler, D. C. (2014). Two-stage thermal conversion of inedible lipid feedstocks to renewable chemicals and fuels. *Bioresource Technology, 158*, 55-62.

Bajpai, P. (2020). Chapter 5 - biomass conversion processes. In P. Bajpai (Ed.), *Biomass to energy conversion technologies* (pp. 41-151) Elsevier.

Balat, M. (2006). Biomass energy and biochemical conversion processing for fuels and chemicals. *Energy Sources, Part A, 28*(6), 517-525.

Beaumont, O. (2007). Flash pyrolysis products from beech wood. *Wood and Fiber Science, 17*(2), 228-239.

Bellew, L., Mangravite, J. A., & Foery, R. F. (1981). Recovery of HPLC-grade acetonitrile by spinning-band distillation. *Journal of Chromatography A, 213*(2), 331-336.

Bharathiraja, B., Chakravarthy, M., Kumar, R. R., Jayamuthunagai, J., & Kumar, R. P. (2016). Integrated biorefinery for bioenergy and platform chemicals. *Platform chemical biorefinery* (pp. 417-435) Elsevier.

Blazeck, J., Liu, L., Knight, R., & Alper, H. S. (2013). Heterologous production of pentane in the oleaginous yeast yarrowia lipolytica. *Journal of Biotechnology, 165*(3-4), 184-194.

Braegelmann, M. P., Azure, A. D., Stahl, D. C., Kubátová, A., Seames, W. S., & Tande, B. M. (2011). Extraction of fatty acids from noncatalytically cracked triacylglycerides using aqueous amines. *Separation Science and Technology, 46*(14), 2167-2173.

Brient, J.A., Wessner, P.J. and Doyle, M.N. (2000). Naphthenic Acids. *Kirk-Othmer Encyclopedia of Chemical Technology*. (Ed.). https://doi.org/10.1002/0471238961.1401160802180905.a01

Buzetzki, E., Sidorová, K., Cvengrošová, Z., & Cvengroš, J. (2011). Effects of oil type on products obtained by cracking of oils and fats. *Fuel Processing Technology, 92*(10), 2041-2047. doi:https://doi.org/10.1016/j.fuproc.2011.06.005

Cantrell, K. B., Ducey, T., Ro, K. S., & Hunt, P. G. (2008). Livestock waste-to-bioenergy generation opportunities. *Bioresource Technology, 99*(17), 7941-7953. doi:https://doi.org/10.1016/j.biortech.2008.02.061

Carney, T. P. (1949). Laboratory fractional distillation. New York: Macmillan.

Cermak, S. C., John, A. L., & Evangelista, R. L. (2007). Enrichment of decanoic acid in cuphea fatty acids by molecular distillation. *Industrial Crops and Products, 26*(1), 93-99. doi:https://doi.org/10.1016/j.indcrop.2007.02.001

Cermak, S. C., Evangelista, R. L., & Kenar, J. A. (2012). Distillation of natural fatty acids and their chemical derivatives. *Distillation-Advances from Modeling to Applications* , 109-142.

Chen, C., Zhao, X., Yen, H., Ho, S., Cheng, C., Lee, D., . . . Chang, J. (2013). Microalgae-based carbohydrates for biofuel production. *Biochemical Engineering Journal, 78*, 1-10. doi:https://doi-org.login.ezproxy.library.ualberta.ca/10.1016/j.bej.2013.03.006

Chen, W., Strik, David P. B. T. B., Buisman, C. J. N., & Kroeze, C. (2017). Production of caproic acid from mixed organic waste: An environmental life cycle perspective. *Environmental Science & Technology, 51*(12), 7159-7168. doi:10.1021/acs.est.6b06220

Cherubini, F., Jungmeier, G., Wellisch, M., Wilke, T., Skiadas, I., Ree, v., R, & Jong, d., E. (2009). Toward a common classification approach for biorefinery systems. *Biofuels Bioproducts and Biorefining, 3*(5), 534-546. doi:10.1002/bbb.172

Cherubini, F. (2010). The biorefinery concept: Using biomass instead of oil for producing energy and chemicals. *Energy Conversion and Management, 51*(7), 1412-1421.

Cherubini, F., Mandl, M., Philips, C., Wellisch, M., Jørgensen, H., Skiadas, I. V., . . . Walsh, P. (2010). IEA bioenergy task 42 on biorefineries: Co-production of fuels, chemicals, power and materials from biomass: IEA bioenergy task 42–Countries report.

Chisti, Y. (2019). In Pandey A., Chang J., Soccol C. R., Lee D. and Chisti Y.(Eds.), *Chapter 1 - introduction to algal fuels* Elsevier. doi:https://doi.org/10.1016/B978-0-444-641922.000019

Chum, H., Black, S. (1990). Process for fractionating fast-pyrolysis oils, and products derved therefrom. US4942269A

Chum, H., Diebold, J., Scahill, J., Johnson, D., Black, S., Schroeder, H., & Kreibich, R. E. (1989). Biomass pyrolysis oil feedstocks for phenolic adhesives. *Adhesives from renewable resources* (pp. 135-151) American Chemical Society. doi:10.1021/bk-1989-0385.ch011 Retrieved from https://doi.org/10.1021/bk-1989-0385.ch011

Chupa, J., Misner, S., Sachdev, A., Wisniewski, P., & Smith, G. A. (2012). Soap, fatty acids, and synthetic detergents. *Handbook of industrial chemistry and biotechnology* (pp. 1431-1471) Springer.

Clarke, C. J., Tu, W., Levers, O., Brohl, A., & Hallett, J. P. (2018). Green and sustainable solvents in chemical processes. *Chemical Reviews, 118*(2), 747-800.

da Mota, S. A. P., Mancio, A. A., Lhamas, D. E. L., de Abreu, D. H., da Silva, M. S., dos Santos, W. G., de Castro, D.A.R., de Oliveira, R.M., Araújo, M.E., Borges, L.E.P. & .Machado, N. T. (2014). Production of green diesel by thermal catalytic cracking of crude palm oil (elaeis guineensis jacq) in a pilot plant. *Journal of Analytical and Applied Pyrolysis, 110*, 1-11.

Darıcı, M., Bergama, D., & Cabaroglu, T. (2019). Effect of triple pot still distillation on the volatile compositions during the rakı production. *Journal of Food Processing and Preservation, 43*(6), e13864.

Das, H., & Singh, S. K. (2004). Useful by-products from cellulosic wastes of agriculture and food Industry—A Critical Appraisal. *Critical Reviews in Food Science and Nutrition*, 44:2, 77-89, DOI: 10.1080/10408690490424630

de Jong, E., & Jungmeier, G. (2015). Biorefinery concepts in comparison to petrochemical refineries. *Industrial biorefineries & white biotechnology* (pp. 3-33) Elsevier.

de Klerk, A. (2011). Fischer–Tropsch Synthesis. *Fischer-Tropsch Refining,* A. de Klerk (Ed.). https://doi-org.login.ezproxy.library.ualberta.ca/10.1002/9783527635603.ch4

de Klerk, A. (2013). Fischer–Tropsch Process. *Kirk-Othmer Encyclopedia of Chemical Technology, (Ed.).* https://doi.org/10.1002/0471238961.fiscdekl.a01

Demirbas, A. (2009). Thermochemical conversion processes. *Biofuels: Green Energy and Technology.* Springer, London. https://doi.org/10.1007/978-1-84882-011-1_6

Demirbas, A., & Arin, G. (2002). An overview of biomass pyrolysis. *Energy Sources, 24*(5), 471-482. doi:10.1080/00908310252889979

Doherty, M.F. and Knapp, J.P. (2004). Distillation, Azeotropic, and Extractive. *Kirk-Othmer Encyclopedia of Chemical Technology.* (Ed.). https://doi.org/10.1002/0471238961.0409192004150805.a01.pub2

Dry, M. E. (2002). High quality diesel via the Fischer–Tropsch process – a review. *Journal of Chemical Technology & Biotechnology, 77*(1), 43-50. doi:https://doi.org/10.1002/jctb.527

Eastman, A. D., & Mears, D. (2005). Hydrocarbons. *Kirk-Othmer Encyclopedia of Chemical Technology, (Ed.).* https://doi.org/10.1002/0471238961.1921182213050118.a01.pub2

Fagernäs, L. (1995). *Chemical and physical characterisation of biomass-based pyrolysis oils: Literature review.* Technical Research Centre of Finland.

Fernando, S., Adhikari, S., Chandrapal, C., & Murali, N. (2006). Biorefineries: Current status, challenges, and future direction. *Energy & Fuels, 20*(4), 1727-1737.

Ferreira, C. C., Costa, E. C., de Castro, D. A. R., Pereira, M. S., Mâncio, A. A., Santos, M. C., Lhamas, D.E.L., da Mota, S.A.P., Leão, A.C., Duvoisin, S., Araújo, M.E., Borges, L.E.P. & Machado, N. T. (2017). Deacidification of organic liquid products by fractional distillation in laboratory and pilot scales. *Journal of Analytical and Applied Pyrolysis, 127*, 468-489.

Gandhi, S., Kadrmas, J., Šťávová, J., Kubátová, A., Muggli, D., Seames, W. S., Sadrameli, S.M. & Tande, B. M. (2012). Extraction of fatty acids from noncatalytically cracked triacylglycerides with water and aqueous sodium hydroxide. *Separation Science and Technology, 47*(1), 66-72.

Gavrilescu, M. (2014). Biorefinery Systems: An Overview. In Gupta V. K., Tuohy M. G., Kubicek C. P., Saddler J. and Xu F.(Eds.), *Bioenergy Research: Advances and Applications*. Elsevier. doi:https://doi-org.login.ezproxy.library.ualberta.ca/10.1016/B978-0-444-59561-4.00014-0

Gervajio, G. C. (2005). Fatty acids and derivatives from coconut oil. In F. Shahidi (Ed.). *Bailey's Industrial Oil and Fat Products.*

Ghatak, H. R. (2011). Biorefineries from the perspective of sustainability: Feedstocks, products, and processes. *Renewable and Sustainable Energy Reviews, 15*(8), 4042-4052. doi:https://doi.org/10.1016/j.rser.2011.07.034

Giordano, M., & Wang, Q. (2018). Microalgae for industrial purposes. In S. Vaz Jr. (Ed.), *Biomass and green chemistry: Building a renewable pathway* (pp. 133-167). Cham: Springer International Publishing. doi:10.1007/978-3-319-66736-2_6 Retrieved from https://doi.org/10.1007/978-3-319-66736-2_6

Goyal, H. B., Seal, D., & Saxena, R. C. (2008). Bio-fuels from thermochemical conversion of renewable resources: A review. *Renewable and Sustainable Energy Reviews,* 12(2), 504 - 517. doi:https://doi.org/10.1016/j.rser.2006.07.014

Guo, X., Wang, S., Guo, Z., Liu, Q., Luo, Z., & Cen, K. (2010). Pyrolysis characteristics of bio-oil fractions separated by molecular distillation. *Applied Energy, 87*(9), 2892-2898. doi:10.1016/j.apenergy.2009.10.004

Guo, Z., Wang, S., Gu, Y., Xu, G., Li, X., & Luo, Z. (2010). Separation characteristics of biomass pyrolysis oil in molecular distillation. *Separation and Purification Technology, 76*(1), 52-57.

Hamad, M. A., Radwan, A. M., Heggo, D. A., & Moustafa, T. (2016). Hydrogen rich gas production from catalytic gasification of biomass. *Renewable Energy, 85*, 1290-1300.

Harnos, S., Onyestyák, G., & Kalló, D. (2012). Hydrocarbons from sunflower oil over partly reduced catalysts. *Reaction Kinetics, Mechanisms and Catalysis, 106*(1), 99-111.

Hipple, J. (2017). Distillation. *Chemical engineering for non-chemical engineers*. John Wiley & Sons, Inc.

Horáček, J., Akhmetzyanova, U., Skuhrovcová, L., Tišler, Z., & de Paz Carmona, H. (2020). Alumina-supported MoNx, MoCx and MoPx catalysts for the hydrotreatment of rapeseed oil. *Applied Catalysis B: Environmental, 263*, 118328. doi:https://doi.org/10.1016/j.apcatb.2019.118328

Huber, G. W., Cortright, R. D., & Dumesic, J. A. (2004). Renewable alkanes by aqueous-phase reforming of biomass-derived oxygenates. *Angewandte Chemie International Edition, 43*(12), 1549-1551.

Iloeje, C. O. (2020). Modeling Liquid–Liquid extraction for critical elements separations: An overview. *Multidisciplinary advances in efficient separation processes* (pp. 335-365) American Chemical Society. doi:10.1021/bk-2020-1348.ch011

Jahirul, M.I.; Rasul, M.G.; Chowdhury, A.A.; Ashwath, N. Biofuels Production through Biomass Pyrolysis —A Technological Review. *Energies* 2012, *5*, 4952-5001. https://doi.org/10.3390/en5124952

Jenab, E., Mussone, P., Nam, G., & Bressler, D. (2014). Production of renewable hydrocarbons from thermal conversion of abietic acid and tall oil fatty acids. *Energy Fuels, 28*(11), 6988-6994. doi:10.1021/ef501746b

Jiang, T., Wang, T., Ma, L., Li, Y., Zhang, Q., & Zhang, X. (2012). Investigation on the xylitol aqueous-phase reforming performance for pentane production over pt/HZSM-5 and ni/HZSM-5 catalysts. *Applied Energy, 90*(1), 51-57. doi:https://doi.org/10.1016/j.apenergy.2011.03.034

Jones, B., Linnen, M., Tande, B., & Seames, W. (2015). The production of vinyl acetate monomer as a co-product from the non-catalytic cracking of soybean oil. *Processes, 3*(3), 619-633.

Jones, D. S., & Pujadó, P. P. (2006). Introduction to crude oil and petroleum processing. In S.A. Treese et al. (eds.). *Handbook of petroleum processing*. Springer Science & Business Media.

Kenar, J. A., Moser, B. R., & List, G. R. (2017). Chapter 2 - naturally occurring fatty acids: Source, chemistry, and Uses. *Fatty acids* (pp. 23-82) AOCS Press. doi:https://doi-org.login.ezproxy.library.ualberta.ca/10.1016/B978-0-12-809521-8.00002-7

Kiss, A. A. (2013). *Advanced distillation technologies* (1. Aufl. ed.). New York: Wiley. Retrieved from http://ebooks.ciando.com/book/index.cfm/bok_id/504304

Kubátová, A., Luo, Y., Šťávová, J., Sadrameli, S. M., Aulich, T., Kozliak, E., & Seames, W. (2011). New path in the thermal cracking of triacylglycerols (canola and soybean oil). *Fuel, 90*(8), 2598-2608. doi:https://doi.org/10.1016/j.fuel.2011.04.022

Kumar, P., Varkolu, M., Mailaram, S., Kunamalla, A., & Maity, S. K. (2019). Biorefinery polyutilization systems: Production of green transportation fuels from biomass. *Polygeneration with polystorage for chemical and energy hubs* (pp. 373-407) Elsevier.

Kurniawan, C., Haryani, S., Kadarwati, S., & Cahyono, E. (2019). (2019). The fractional separation of citronella, cajeput, and patchouli crude oils using spinning band distillation. Paper presented at the *Journal of Physics: Conference Series, 1321*(2) 022038.

Lappi, H., & Alén, R. (2011). Pyrolysis of vegetable oil soaps—Palm, olive, rapeseed and castor oils. *Journal of Analytical and Applied Pyrolysis, 91*(1), 154-158. doi:https://doi.org/10.1016/j.jaap.2011.02.003

Lebl, R., Murray, T., Adamo, A., Cantillo, D., & Kappe, C. O. (2019). Continuous flow synthesis of methyl oximino acetoacetate: Accessing greener purification methods with inline Liquid–Liquid extraction and membrane separation technology. *ACS Sustainable Chemistry & Engineering, 7*(24), 20088-20096. doi:10.1021/acssuschemeng.9b05954

Lei, Z. and Chen, B. (2013). Distillation. *Separation and Purification Technologies in Biorefineries.* https://doi.org/10.1002/9781118493441.ch2

Li, W., Pan, C., Sheng, L., Liu, Z., Chen, P., Lou, H., & Zheng, X. (2011). Upgrading of high-boiling fraction of bio-oil in supercritical methanol. *Bioresource Technology, 102*(19), 9223-9228. doi:https://doi.org/10.1016/j.biortech.2011.07.071

Lima, D. G., Soares, V. C. D., Ribeiro, E. B., Carvalho, D. A., Cardoso, É C. V., Rassi, F. C., Mundim, K.C., Rubim, J.C. & Suarez, P. A. Z. (2004). Diesel-like fuel obtained by

pyrolysis of vegetable oils. *Journal of Analytical and Applied Pyrolysis.*71(2), 987 - 996 doi:https://doi.org/10.1016/j.jaap.2003.12.008

Lindfors, C., Kuoppala, E., Oasmaa, A., Solantausta, Y., & Arpiainen, V. (2014). Fractionation of bio-oil. *Energy & Fuels, 28*(9), 5785-5791.

Liu, S., Zhang, Y., Fan, L., Zhou, N., Tian, G., Zhu, X., Cheng, Y., Wang, Y., Liu, Y. & Chen, P. (2017). Bio-oil production from sequential two-step catalytic fast microwave-assisted biomass pyrolysis. *Fuel, 196*, 261-268.

Liu, S., Tamura, M., Nakagawa, Y., & Tomishige, K. (2014). One-pot conversion of cellulose into n-hexane over the ir-ReO x/SiO2 catalyst combined with HZSM-5. *ACS Sustainable Chemistry & Engineering, 2*(7), 1819-1827.

Liu, Y., Chen, L., Wang, T., Zhang, X., Long, J., Zhang, Q., & Ma, L. (2015). High yield of renewable hexanes by direct hydrolysis–hydrodeoxygenation of cellulose in an aqueous phase catalytic system. *RSC Advances, 5*(15), 11649-11657.

Long, F., Li, F., Zhai, Q., Wang, F., & Xu, J. (2019). Thermochemical conversion of waste acidic oil into hydrocarbon products over basic composite catalysts. *Journal of Cleaner Production, 234*, 105-112.

Luyben, W. L. (2013). Fundamentals of vapor–liquid equilibrium (VLE). *Distillation design and control using AspenTM simulation.* (Second ed.). John Wiley & Sons, Inc.

Ma, F., Clements, L. D., & Hanna, M. A. (1998). The effects of catalyst, free fatty acids, and water on transesterification of beef tallow. *Transactions of the ASAE, 41*(5), 1261.

Maes, M., Alaerts, L., Vermoortele, F., Ameloot, R., Couck, S., Finsy, V., Denayer, J.F.M., & De Vos, D.E. (2020). Separation of C5-Hydrocarbons on Microporous Materials: Complementary Performance of MOFs and Zeolites. Journal of the American Chemical Society 2010 132 (7), 2284-2292. DOI: 10.1021/ja9088378

Maher, K. D., & Bressler, D. C. (2007). Pyrolysis of triglyceride materials for the production of renewable fuels and chemicals. *Bioresource Technology, 98*(12), 2351-2368.

Maher, K. D., Kirkwood, K. M., Gray, M. R., & Bressler, D. C. (2008). Pyrolytic decarboxylation and cracking of stearic acid. *Industrial & Engineering Chemistry Research, 47*(15), 5328-5336.

Maitlis, P.M. (2013). What is Fischer–Tropsch? In Maitlis P.M. & de Klerk A. (Eds). *Greener Fischer-Tropsch Processes for Fuels and Feedstocks*.

Maity, S. K. (2015). Opportunities, recent trends and challenges of integrated biorefinery: Part I. *Renewable and Sustainable Energy Reviews, 43*, 1427-1445.

Mancio, A. A., da Mota, S. A. P., Ferreira, C. C., Carvalho, T. U. S., Neto, O. S., Zamian, J. R., Araújo, M.E., Borges, L.E.P. & and Machado, N. T. (2018). Separation and characterization of biofuels in the jet fuel and diesel fuel ranges by fractional distillation of organic liquid products. *Fuel, 215*, 212-225. doi:10.1016/j.fuel.2017.11.029

Marques, S., Moreno, A. D., Ballesteros, M., & Gírio, F. (2018). Starch biomass for biofuels, biomaterials, and chemicals. In S. Vaz Jr. (Ed.), *Biomass and green chemistry: Building a renewable pathway* (pp. 69-94). Cham: Springer International Publishing. doi:10.1007/978-

3-319-66736-2_4 Retrieved from https://doi.org/10.1007/978-3-319-66736-2_4

Mikkola, J., Sklavounos, E., King, A. W., & Virtanen, P. (2015). The biorefinery and green chemistry. *Ionic Liquids in the Biorefinery Concept: Challenges and Perspectives*, 2015, pp. 1-37 DOI: 10.1039/9781782622598-00001eISBN: 978-1-78262-259-8

Milledge, J. J., Smith, B., Dyer, P. W., & Harvey, P. (2014). Macroalgae-derived biofuel: A review of methods of energy extraction from seaweed biomass. *Energies, 7*(11), 7194-7222.

Mohapatra, S., Mishra, C., Behera, S. S., & Thatoi, H. (2017). Application of pretreatment, fermentation and molecular techniques for enhancing bioethanol production from grass biomass – A review. *Renewable and Sustainable Energy Reviews,* 78, 1007-1032. doi:https://doi-org.login.ezproxy.library.ualberta.ca/10.1016/j.rser.2017.05.026

Murray, K. E. (1955). Low pressure fractional distillation and its use in the investigation of lipids. *Progress in the Chemistry of Fats and other Lipids,* 3, 243 - 246. doi:https://doi-org.login.ezproxy.library.ualberta.ca/10.1016/0079-6832(55)90009-4 "

Nam, H., Kim, C., Capareda, S. C., & Adhikari, S. (2017). Catalytic upgrading of fractionated microalgae bio-oil (nannochloropsis oculata) using a noble metal (pd/C) catalyst. *Algal Research.* 24(A), 188 - 198 doi:https://doi.org/10.1016/j.algal.2017.03.021

Navarro-Pineda, F. S., Baz-Rodríguez, S. A., Handler, R., & Sacramento-Rivero, J. C. (2016). Advances on the processing of jatropha curcas towards a whole-crop biorefinery. *Renewable and Sustainable Energy Reviews.* 54, 247 - 269.

doi:https://doi.org/10.1016/j.rser.2015.10.009

Nolan Dennis, P. (2014). Physical properties of hydrocarbons and petrochemicals. *Handbook of fire and explosion protection engineering principles* (3rd Edition ed., pp. 1-2) Elsevier.

Nuchteera, I., Thirasak, P., Chavagorn, M., Thanyalak, C., & Kitipat, S. (2020). Cyclopentane purification from multicomponent azeotropic mixtures. *Computer Aided Chemical Engineering, 48*, 277-282.

Parajuli, R., Dalgaard, T., Jørgensen, U., Adamsen, A. P. S., Knudsen, M. T., Birkved, M., Gylling, M. & Schjørring, J. K. (2015). Biorefining in the prevailing energy and materials crisis: A review of sustainable pathways for biorefinery value chains and sustainability assessment methodologies. *Renewable and Sustainable Energy Reviews, 43*, 244-263.

Potts, R. H., & White, F. B. (1953). Fractional distillation of fatty acids. *Journal of the American Oil Chemists' Society, 30*(2), 49-53.

Rose, A., & Long, H. H. (1941). Calculation of the effect of reflux ratio in batch fractionation. *Industrial & Engineering Chemistry, 33*(5), 684-687. doi:10.1021/ie50377a034

Rossini, F. D. 1. (1953). Hydrocarbons from petroleum : The fractionation, analysis, isolation, purification, and properties of petroleum hydrocarbons ;an account of the work of the american petroleum institute research project 6. New York (State): Reinhold, 1953. Retrieved from https://hdl.handle.net/2027/mdp.39015065257076

Sainio, M. A. (2015). Chapter 7 - neurotoxicity of solvents. *Handbook of Clinical Neurology.* 131, 93 - 110. doi:https://doi.org/10.1016/B978-0-444-62627-1.00007-X

Santillan-Jimenez, E., Morgan, T., Lacny, J., Mohapatra, S., & Crocker, M. (2013). Catalytic deoxygenation of triglycerides and fatty acids to hydrocarbons over carbon-supported nickel. *Fuel, 103*, 1010-1017.

Santos, A. L. F., Martins, D. U., Iha, O. K., Ribeiro, R. A. M., Quirino, R. L., & Suarez, P. A. Z. (2010). Agro-industrial residues as low-price feedstock for diesel-like fuel production by thermal cracking. *Bioresource Technology.* 101(15), 6157 - 6162.

Sari, E., DiMaggio, C., Kim, M., Salley, S. O., & Ng, K. Y. S. (2013). Catalytic conversion of brown grease to green diesel via decarboxylation over activated carbon supported palladium catalyst. *Industrial & Engineering Chemistry Research, 52*(33), 11527-11536.

Schmidt, A., & Strube, J. (2018). Application and fundamentals of Liquid–Liquid extraction processes: Purification of biologicals, botanicals, and strategic metals. *Kirk-Othmer Encyclopedia of Chemical Technology*, John Wiley & Sons, Inc (Ed.). doi:https://doi-org.login.ezproxy.library.ualberta.ca/10.1002/0471238961.koe00041

Schmidt, R., Griesbaum, K., Behr, A., Biedenkapp, D., Voges, H., Garbe, D., Paetz, C., Collin, G., Mayer, D. & Höke, H. (2014). Hydrocarbons. *Ullmann's Encyclopedia of Industrial Chemistry, (Ed.).* doi:https://doi.org/10.1002/14356007.a13_227.pub3

Scholze, B., & Meier, D. (2001). Characterization of the water-insoluble fraction from pyrolysis oil (pyrolytic lignin). part I. PY–GC/MS, FTIR, and functional groups. *Journal of Analytical and Applied Pyrolysis, 60*(1), 41-54. doi:https://doi.org/10.1016/S0165-2370(00)00110-8

Šimáček, P., Kubička, D., Šebor, G., & Pospíšil, M. (2009). Hydroprocessed rapeseed oil as a

source of hydrocarbon-based biodiesel. *Fuel.* 88(3), 456 - 460 doi:https://doi.org/10.1016/j.fuel.2008.10.022

Spaho, N. (2017). Distillation techniques in the fruit spirits production. *Distillation-Innovative Applications and Modeling,* Marisa Fernandes Mendes, IntechOpen, DOI: 10.5772/66774. Available from: https://www.intechopen.com/books/distillation-innovative-applications-and-modeling/distillation-techniques-in-the-fruit-spirits-production

Speight, J. (2020). Fischer-tropsch process. *Handbook of gasification technology* (pp. 381-425) doi:https://doi-org.login.ezproxy.library.ualberta.ca/10.1002/9781118773970.ch12

Srinivas, S. T., Dalai, A. K., & Bakhshi, N. N. (2000). Thermal and catalytic upgrading of a biomass-derived oil in a dual reaction system. *The Canadian Journal of Chemical Engineering, 78*(2), 343-354.

Steinigeweg, S. and Gmehling, J. (2005). Distillation. In Afonso, C.A.M. and Crespo, J.G. (Eds). *Green Separation Processes.* https://doi.org/10.1002/3527606602.ch3b

Stichlmair, J. (2010). Distillation, 1. Fundamentals. *Ullmann's Encyclopedia of Industrial Chemistry,* (Ed.). https://doi.org/10.1002/14356007.b03_04.pub2

Stichlmair, J. (2010). Distillation, 2. Equipment. *Ullmann's Encyclopedia of Industrial Chemistry*, (Ed.). https://doi.org/10.1002/14356007.o08_o01

Tajarudin, H. A., Zacharof, M., Ratanapongleka, K., Williams, P. M., & Lovitt, R. W. (2018). Intensive production of carboxylic acids using C. butyricum in a membrane bioreactor (MBR). *Fermentation, 4*(4), 81.

Tanger, P., Field, J. L., Jahn, C. E., Defoort, M. W., & Leach, J. E. (2013). Biomass for thermochemical conversion: Targets and challenges. *Frontiers in Plant Science, 4*, 218. doi:10.3389/fpls.2013.00218

Toor, S. S., Rosendahl, L., & Rudolf, A. (2011). Hydrothermal liquefaction of biomass: A review of subcritical water technologies. *Energy, 36*(5), 2328-2342. doi:https://doi.org/10.1016/j.energy.2011.03.013

Torres, M. D., Kraan, S., & Domínguez, H. (2019). Seaweed biorefinery. *Reviews in Environmental Science and Bio/Technology, 18*(2), 335-388.

Tsai, W. T., Lee, M. K., & Chang, Y. M. (2006). Fast pyrolysis of rice straw, sugarcane bagasse and coconut shell in an induction-heating reactor. *Journal of Analytical and Applied Pyrolysis, 76*(1), 230-237.

van den Bergh, J., Gücüyener, C., Pidko, E. A., Hensen, E. J. M., Gascon, J., & Kapteijn, F. (2011). Understanding the anomalous alkane selectivity of ZIF-7 in the separation of light alkane/alkene mixtures. *Chemistry – A European Journal, 17*(32), 8832-8840. doi:https://doi.org/10.1002/chem.201100958

Wang, F., Xu, J., Jiang, J., Liu, P., Li, F., Ye, J., & Zhou, M. (2018). Hydrotreatment of vegetable oil for green diesel over activated carbon supported molybdenum carbide catalyst. *Fuel, 216*, 738-746. doi:https://doi.org/10.1016/j.fuel.2017.12.059

Wang, Y., Peh, S. B., & Zhao, D. (2019). Alternatives to cryogenic distillation: Advanced porous materials in adsorptive light olefin/paraffin separations. *Small, 15*(25), 1900058.

doi:https://doi.org/10.1002/smll.201900058

Weber, B., Stadlbauer, E. A., Stengl, S., Hossain, M., Frank, A., Steffens, D., Schlich, E. & Schilling, G. (2012). Production of hydrocarbons from fatty acids and animal fat in the presence of water and sodium carbonate: Reactor performance and fuel properties. *Fuel, 94*, 262-269. doi:https://doi-org.login.ezproxy.library.ualberta.ca/10.1016/j.fuel.2011.08.040

Wiggers, V. R., Meier, H. F., Wisniewski, A., Chivanga Barros, A. A., & Wolf Maciel, M. R. (2009). Biofuels from continuous fast pyrolysis of soybean oil: A pilot plant study. *Bioresource Technology, 100*(24), 6570-6577. doi:https://doi.org/10.1016/j.biortech.2009.07.059

Wiggers, V. R., Wisniewski, A., Madureira, L. A. S., Barros, A. A. C., & Meier, H. F. (2009). Biofuels from waste fish oil pyrolysis: Continuous production in a pilot plant. *Fuel, 88*(11), 2135-2141. doi:https://doi.org/10.1016/j.fuel.2009.02.006

Xi, J., Xia, Q., Shao, Y., Ding, D., Yang, P., Liu, X., . . . Wang, Y. (2016). Production of hexane from sorbitol in aqueous medium over pt/NbOPO4 catalyst. *Applied Catalysis B:Environmental, 181 (699 - 706)*doi:https://doi.org/10.1016/j.apcatb.2015.08.052

Xinghua, Z., Tiejun, W., Longlong, M., & Chuangzhi, W. (2010). Aqueous-phase catalytic process for production of pentane from furfural over nickel-based catalysts. *Fuel, 89*(10), 2697-2702. doi:https://doi.org/10.1016/j.fuel.2010.05.043

Xiu, S., & Shahbazi, A. (2012). Bio-oil production and upgrading research: A review. *Renewable and Sustainable Energy Reviews, 16*(7), 4406-4414. doi:10.1016/j.rser.2012.04.028

Xu, J., Jiang, J., Sun, Y., & Chen, J. (2010). Production of hydrocarbon fuels from pyrolysis of soybean oils using a basic catalyst. *Bioresource Technology, 101*(24), 9803-9806.

Xu, J., Jiang, J., Zhang, T., & Dai, W. (2013). Biofuel production from catalytic cracking of triglyceride materials followed by an esterification reaction in a scale-up reactor. *Energy & Fuels, 27*(1), 255-261.

Yaman, S. (2004). Pyrolysis of biomass to produce fuels and chemical feedstocks. *Energy Conversion and Management, 45*(5), 651-671. doi:10.1016/S0196-8904(03)00177-8

Yen, H., Hu, I. -., Chen, C., Ho, S., Lee, D., & Chang, J. (2013). Microalgae-based biorefinery – from biofuels to natural products. *Bioresource Technology.* 135, 166 - 174.

Yu, F., Gao, L., Wang, W., Zhang, G., & Ji, J. (2013). Bio-fuel production from the catalytic pyrolysis of soybean oil over me-al-MCM-41 (Me=La, ni or fe) mesoporous materials. *Journal of Analytical and Applied Pyrolysis, 104*, 325-329.

Zarnegar, S. (2018). A review on catalytic-pyrolysis of coal and biomass for value-added fuel and chemicals. *Energy Sources, Part A: Recovery, Utilization, and Environmental Effects, 40*(12), 1427-1433. doi:10.1080/15567036.2018.1472680

Zhang, J. and Hu, B. (2013). Liquid-Liquid Extraction (LLE). In Ramaswamy, S., Huang, H.J., & Ramarao, B.V. (Eds). *Separation and Purification Technologies in Biorefineries*

Zhang, Y. P. (2008). Reviving the carbohydrate economy via multi-product lignocellulose biorefineries. *Journal of Industrial Microbiology & Biotechnology, 35*(5), 367-375.

Zhou, D., Zhang, L., Zhang, S., Fu, H., & Chen, J. (2010). Hydrothermal liquefaction of macroalgae enteromorpha prolifera to bio-oil. *Energy Fuels, 24*(7), 4054-4061. doi:10.1021/ef100151h